ASYMMETRIC SYNTHESIS OF CHIRAL CAMPHOR FUSED PYRIDINE TYPE NOVEL ORGANOCATALYSTS

A THESIS SUBMITTED TO
THE GRADUATE SCHOOL OF NATURAL AND APPLIED SCIENCES
OF
THE MIDDLE EAST TECHNICAL UNIVERSITY

BY

MURAT KÜÇÜKDİŞLİ

IN PARTIAL FULFILLMENT OF THE REQUIREMENTS
FOR
THE DEGREE OF MASTER OF SCIENCE
IN
CHEMISTRY

JULY 2009

Approval of the thesis:

ASYMMETRIC SYNTHESIS OF CHIRAL CAMPHOR FUSED PYRIDINE TYPE NOVEL ORGANOCATALYSTS

submitted by **MURAT KÜÇÜKDİŞLİ** in partial fulfillment of the requirements for the degree of **Master of Science in Chemistry Department, Middle East Technical University** by,

Prof. Dr. Canan Özgen _____
Dean, Graduate School of **Natural and Applied Sciences**

Prof. Dr. Ahmet M. Önal _____
Head of Department, **Chemistry**

Prof. Dr. Cihangir Tanyeli _____
Supervisor, **Chemistry Dept., METU**

Examining Committee Members:

Prof. Dr. Metin Balcı _____
Chemistry Dept., METU

Prof. Dr. Cihangir Tanyeli _____
Chemistry Dept., METU

Prof. Dr. Özdemir Doğan _____
Chemistry Dept., METU

Prof. Dr. Metin Zora _____
Chemistry Dept., METU

Assoc. Prof. Dr. Adnan Bulut _____
Chemistry Dept., Kırıkkale University

Date: 17.07.2009

I hereby declare that all information in this document has been obtained and presented in accordance with academic rules and ethical conduct. I also declare that, as required by these rules and conduct, I have fully cited and referenced all material and results that are not original to this work.

Name, Last name : Murat Küçükdişli

Signature :

ABSTRACT

ASYMMETRIC SYNTHESIS OF CHIRAL CAMPHOR FUSED PYRIDINE TYPE NOVEL ORGANOCATALYSTS

Küçükdişli, Murat

M.S., Department of Chemistry

Supervisor: Prof. Dr. Cihangir Tanyeli

July 2009, 84 pages

Chiral pyridines as organocatalysts have been used in asymmetric organic synthesis in recent years. The asymmetric synthesis of camphor fused pyridine type novel organocatalysts were perfomed starting from cheap and easily available natural (+)-camphor. Using camphor fused pyridine skeleton, six organocatalysts **29**,, **32**, **33**, **38**, **40**, and **41**were successfully synthesized. The first four nucleophilic and Lewis base catalysts **29**, **32**, and **33** are different P-oxides and P,N-dioxides which were tested in allylation of aldehydes via allyltrichlorosilane. *L*-proline amide **38** and *D*-proline amide **40** can be named as secondary amine catalyst. They were tested in direct aldol reaction between acetone and aromatic aldehydes in aqueous medium. Final group of catalyst is hydrogen bonding type catalyst which is thiourea based **41**.

Key words: Organocatalyst, *P,N*-dioxide, aldol, allylation, thiourea

ÖZ

KİRAL KAMFOR İÇERİKLİ PİRİDİN TİPİ
YENİ ORGANOKATALİZÖRLERİN ASİMETRİK SENTEZİ

Küçükdişli, Murat
Yüksek Lisans, Kimya Bölümü
Tez Yöneticisi: Prof. Dr. Cihangir Tanyeli

Temmuz 2009, 84 sayfa

Son yıllarda organokatalizör olarak kiral piridinler kullanılmaktadır. Ucuz ve kolay bulunan doğal (+)-kamfordan başlanarak kamfor içerikli piridin tipi yeni organokatalizörlerin asimetrik sentezi yapılmıştır. Kamfor temelli piridin iskeleti kullanılarak yedi adet organokatalizörler **29**,, **32**, **33**, **38**, **40**, ve **41** başarılı bir şekilde sentezlenmiştir. İlk dört nükleofilik ve Lewis baz katalizörleri **29**, **32**, ve **33**, aliltriklorosilanla aldehitlerin alilasyonunda denenen değişik *P*-oksitler ve *P,N*-dioksitlerdir. *L*-proline amit **38** ve *D*-proline amit **40**, ikincil amin katalizörleri olarak isimlendirilebilir. Bunlar, sulu ortamda aseton ve aromatik aldehitlerin arasındaki aldol tepkimelerinde test edildi. Son katalizör grubu, tiyoüre temelli **41** hidrojen bağı türü katalizörlerdir.

Anahtar kelimeler: Organokatalizör, *P,N*-dioksit, aldol, tiyoüre

To my dear family

ACKNOWLEDGEMENTS

I would like to express my sincere thanks to my supervisor Prof. Dr. Cihangir Tanyeli for his guidance, support and patience throughout this study.

I would also thank to Murat Işık for his encouragement, interesting scientific discussions and his friendship.

I would like to give special thanks to Merve Çayir for her support, understanding and unlimited tolerance everytime.

Very special thanks to Yunus Emre Türkmen, Osman Candaş Dağdaş and Osman Mahmut Eryurt for their kind friendship.

I wish also thank to Emre Yusuf Yazıcıoğlu for his patience while answering my endless questions.

I would like to thank to Seda and Zehra for the NMR spectra.

I would also thank to TÜBİTAK for scholarship.

Finally I want to thank to my lab mates from D-251, D-254 and D-255 for their friendship.

TABLE OF CONTENTS

LIST OF TABLES

TABLES

LIST OF FIGURES

FIGURES

LIST OF SCHEMES

SCHEMES

LIST OF ABBREVIATIONS

DCE: 1,2-dichloroethane

DCM: Dichloromethane

DCC: Dicyclohexylcarboxydiimide

DIPEA: Diisopropylethylamine

DMAP: Dimethylaminopyridine

DMF: *N,N'*-Dimethylformamide

KHDMS: Potassium hexamethyldisilazide

MCPBA: *m*-chloroperbenzoic acid

PTSA: *p*-toluenesulfonamide

TFA: Trifluoroacetic acid

TFAA: Trifluoroacetic anhydride

THF: Tetrahydrofurane

PTC: Phase transfer catalysis

CPTC: Chiral phase transfer catalysis

CHAPTER 1

INTRODUCTION

1.1. Importance of asymmetric synthesis

Asymmetric synthesis has become challenging topic of research for chemists in both industry and the academic world over the past few decades. This topic is not only a open research area for scientists but also a highly fertile field for the development of technologies for the production of high-value pharmaceuticals and agrochemicals [1]. The important difference in physiologic properties for enantiomers is now well known in the scientific community.

In living organism, all the enzymes, DNA, RNA, receptors, etc. contain only one chiral form. Therefore, their interactions have diastereomeric character although all the physical properties of enantiomers are the same. Hence, different effects of enantiomers like different taste, smell, pharmacological effect, etc. have been observed upon their interactions with a human body [2]. This is the ultimate reason why asymmetric synthesis has become a substantial area.

When looking from pharmaceutical aspect, asymmetric synthesis is more vital. More than half of all useful drugs appear to exist in enantiomeric forms and generally, one of these enantiomers is much more effective than its mirror image enantiomer, exhibiting a better fit to its receptor. For instance, the *S* enantiomer of methacholine, a parasymphathomimetic drug, is over 250 times more potent than the *R* enantiomer. Penicillamine [3], ketamine [4] and thalidomide [5] can be given as known examples to chiral drugs whose enantiomers show different pharmacological effects (Figure 1). Furthermore, the more active enantiomer at any receptor type, may be less active at another type. The *S* enantiomer of

carvedilol (Figure 1) is a potent beta receptor blocker, while the *R* enantiomer is 100-fold weaker at the beta receptor. However, both enantiomers are approximately equipotent as alpha receptor blockers [6].

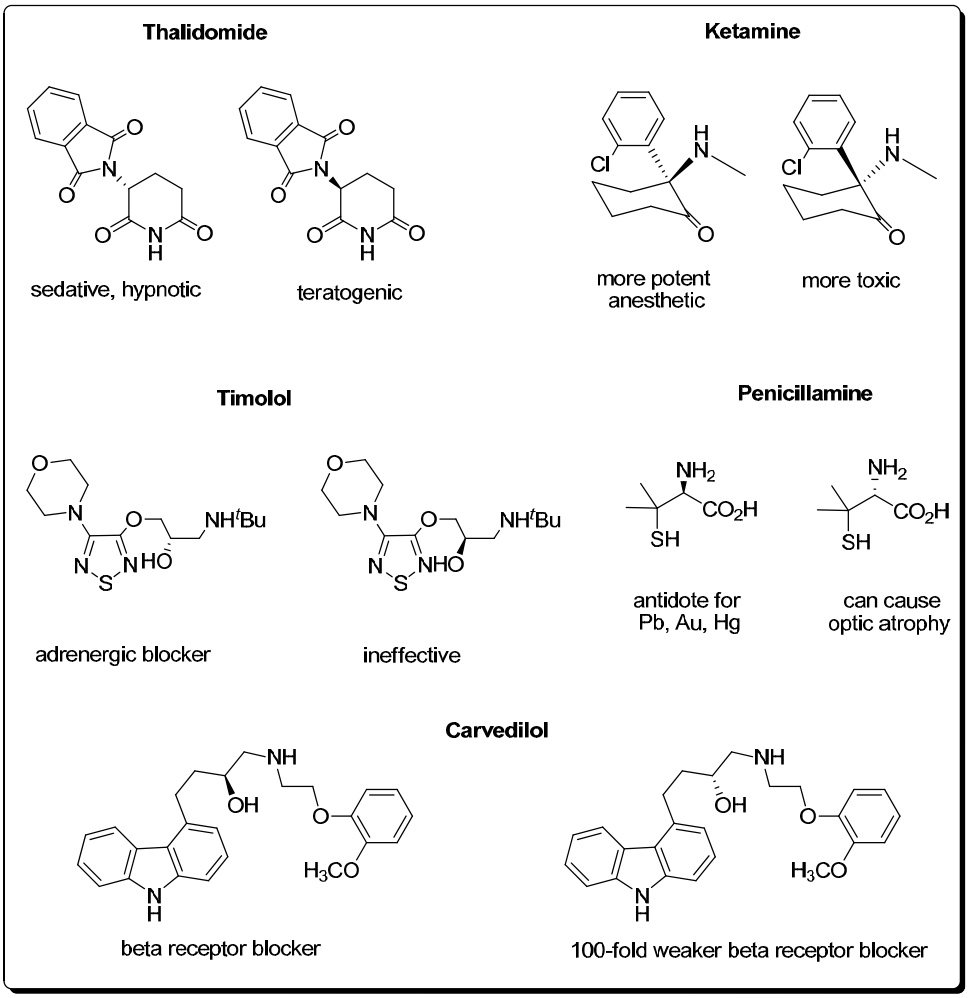

Figure 1. The structures and pharmacological effects of the enantiomers of some biologically active chiral molecules

1.2. History of asymmetric organocatalysis

The use of chiral organocatalysts in asymmetric synthesis has been attractive from 2000 up to today. Before understanding of this new concept, organocatalysis, only enzymes and synthetic chiral metal complexes are used in the asymmetric synthesis [7]. The common definition of organacatalysis is that the acceleration of an chemical reaction by using catalytic amount of pure organic compounds which does not contain any metal [8]. The first organocatalyst is an achiral molecule, acetaldehyde. Justus von Liebig's was the first chemist who synthesize oxamide from dicyan and water in 1871 (Scheme 1) [9].

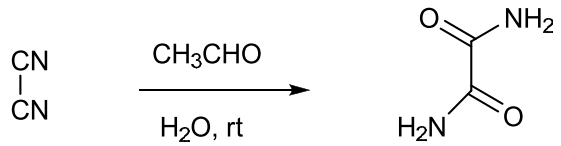

Scheme 1. von Liebig's oxamide synthesis

After this investigation of Liebig, transition from achiral to asymmetric organocatalytic reaction took a long time. In 1960, Pracejus reported that methyl phenyl ketene could be converted to (-)-α-phenyl methylpropionate in 74% ee by using *O*-acetylquinine **1** as catalyst [10] (Scheme 2).

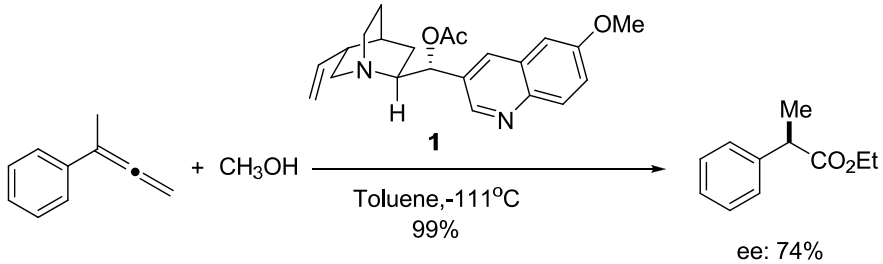

Scheme 2. Pracejus' ester synthesis from phenyl methyl ketene

From this finding, cinchona based organocatalysts has started to use in other types of asymmetric reactions. The first Michael addition of *β*-keto esters to acrolein was done by Bergson and Langstrom and 2-(hydroxymethyl)- quinuclidine (Figure 2) was used as catalyst [11].

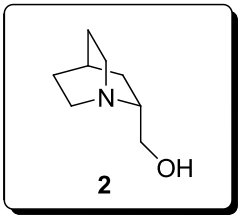

Figure 2. 2-(hdyroxymethyl)-quinuclidine

Wynberg and collaborators performed important experiments about the use of cinchona alkaloids as chiral catalyst nucleophilic and Lewis-base catalysts [12], and illustrated this type of alkaloid to be a versatile catalyst, promoting a variety of 1,2- and 1,4-additions of a wide range of nucleophiles to carbonyl compounds. In these early studies, it is important that it was often observed that natural cinchona alkaloids were greater efficiency, in terms of both catalytic activity and stereoselectivity, in order to modify cinchona alkaloids derived from modification of the C-9 hydroxyl group. To rationalize this phenomenon, Wynberg stated that the natural cinchona alkaloids were bifunctional catalysts utilizing both the tertiary amine and hydroxyl group to activate and orient the nucleophile and electrophile, respectively, thus achieving optimum asymmetric catalysis [12].

Another important event in the history of asymmetric organocatalytic reaction was the discovery of efficient *L*-proline-mediated asymmetric Robinson annulation reported during the early 1970s. The so-called Hajos-Parrish-Eder-Sauer-Wiechert reaction (an intramolecular aldol reaction) allowed access to some of the key intermediates for the synthesis of natural products (Scheme 3) [13,14], and offered a practical and enantioselective route to the Wieland-Miescher ketone [15].

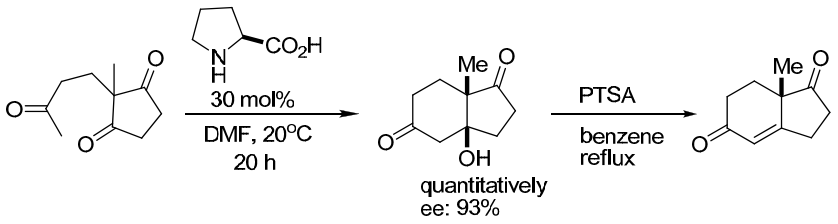

Scheme 3. The *L*-proline-mediated Robinson annulation

During this period a number of reactions that carried on *via* ion-pairing mechanisms were discovered. Additionally, Lipton and *co*workers reported that chiral diketopiperazine **3** (Figure 3) was used in asymmetric synthesis of α-amino nitriles from substituted imines with excellent enantiomeric excess [16].

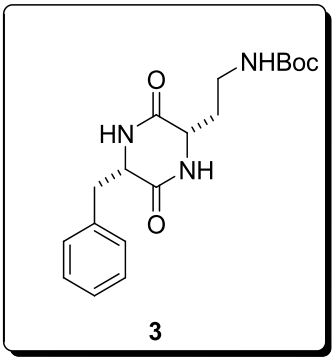

Figure 3. Chiral diketopiperazine

The advent of efficient phase-transfer reactions dates back to the mid-1980s. Substituted 2-phenyl-1-indanone systems **4** were alkylated with a very good enantioselectivity (up to 94%) in the presence of catalytic amounts of substituted *N*-benzylcinchoninium halides **5** by Dolling (Scheme 4) [17].

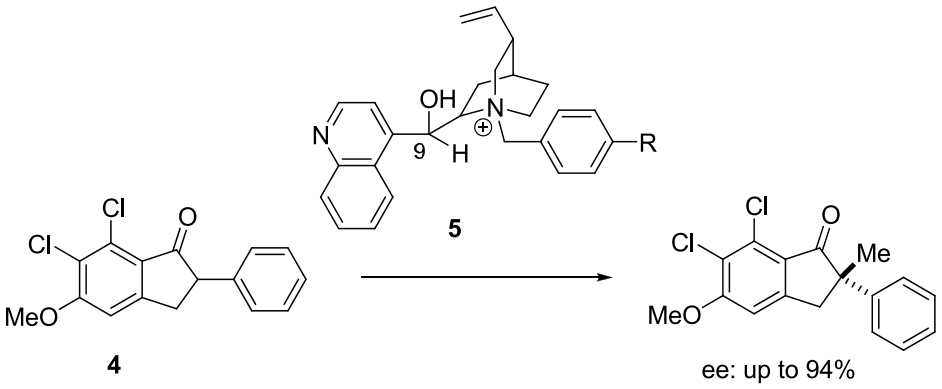

Scheme 4. Asymmetric alkylation reaction

Today, when one thinks about asymmetric organocatalysis, the first comes to mind is *L*-proline. As mentioned before, the first use of *L*-proline as an organocatalyst was in Hajos-Parrish-Eder-Sauer-Wiechert reaction. The general mechanism of this reaction and a reasonable transition-state was not revealed for decades despite the fact that the reaction has been performed on an industrial scale since its invention thirty years prior.

Reinvestigation of the proline as a organocatalyst by List and Barbas during the late 1990s also opened a new era for a number of related transformations such as the enantioselective intermolecular cross-aldol reactions, as well as Mannich, Michael and Diels-Alder type transformations [18], and multistep (domino) reactions [19]. An example of multistep reaction is given in scheme 5. Here in this three-component reaction, (*S*)-proline was used as catalyst in the reaction between cyclohexanone, benzaldehyde and compound **6** which is also known as Meldrum's acid.

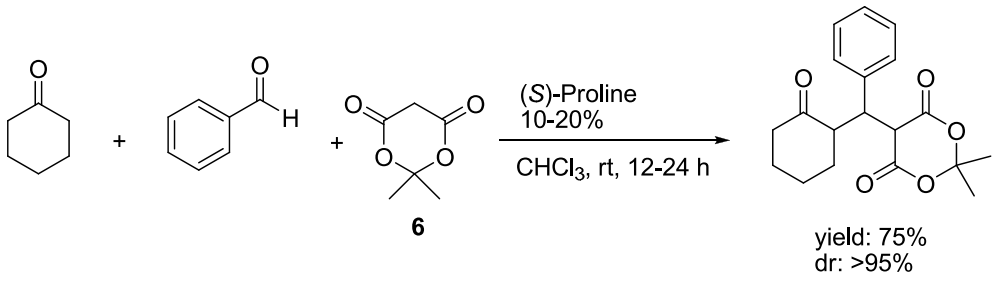

Scheme 5. Proline-catalyzed three-component asymmetric reaction

Before understanding of the importance of organocatalysis, Nicolaou and Sorenson in 1996, reported that there has been two classes of efficient asymmetric catalysts: enzymes and synthetic metal complexes [7]. However, today, this view has changed with reinvestigation of organocatalysts, as a new class of powerful asymmetric catalysts (Figure 4) [20]. After the creation of new term "organocatalysis" by MacMillan in 2000, organocatalytic reaction has become a highlight topic.

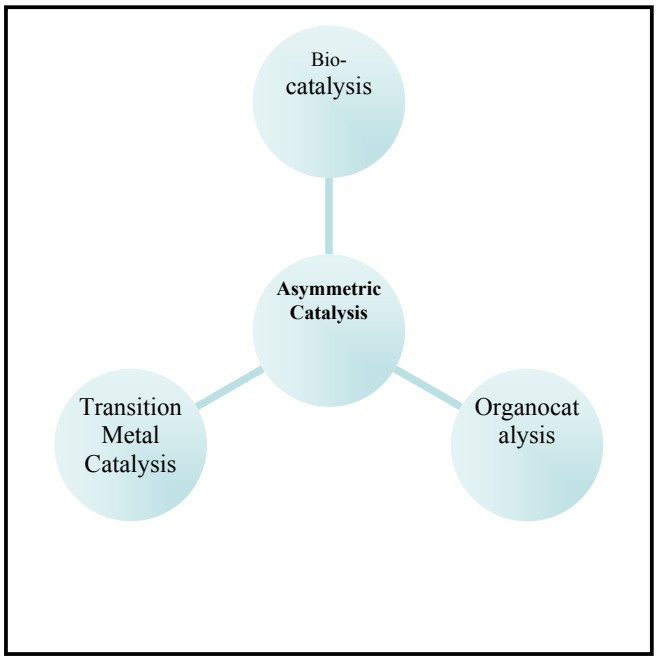

Figure 4. Three pillars of asymmetric catalysis

1.3. Classification of asymmetric organocatalysis

After the creation of this new term, scientists have proposed some classification of organocatalysts in order to get better understanding about how they works. The most common classification is based on interaction between catalyst and substrate. According to Berkessel and Gröger, organacatalysts are divided into two groups namely covalent catalysis and non-covalent catalysis (Figure 5) [18]

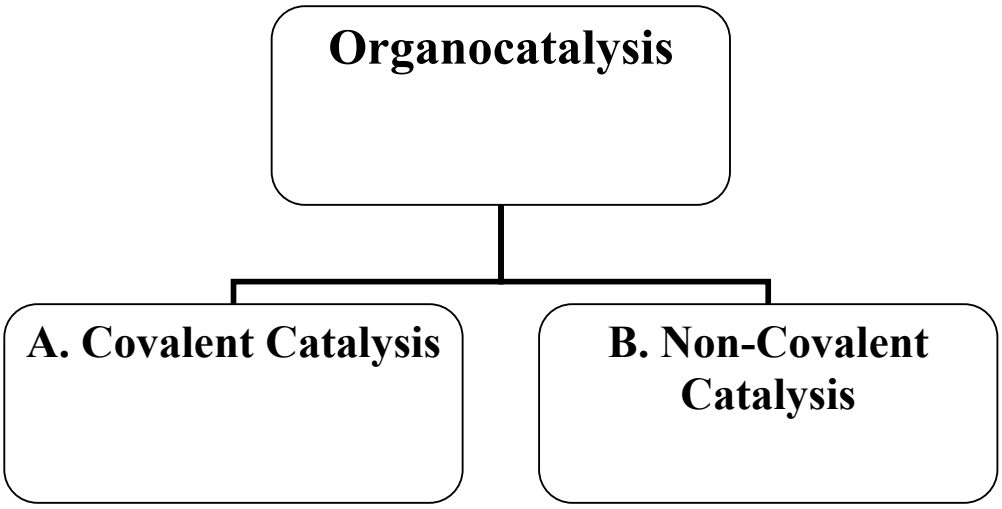

Figure 5. General mechanistic consideration of organocatalysis

In the first group, covalent bond formation is formed between catalyst and substrate. The formation of covalent substrate-catalyst adducts might occur, by a single step Lewis acid and Lewis base interaction or by multi-step reactions such as the formation of enamines from aldehydes and secondary amines. In non-covalent catalysis, non-covalent interaction such as hydrogen bond or ion pairs involves in the mechanism instead of covalent bond formation. In many instances non-covalent catalysis relies on the formation of hydrogen-bonded adducts between substrate and catalyst or on protonation/deprotonation processes. Organic phase-transfer catalysts (PTC) can also be grouped as ‘‘non-covalent catalysis’’. However, it has a different

mechanism because PTC promotes reactivity not only by altering the chemical properties of the reactants but also involves a transport phenomenon [18].

Another classification of organocatalysts is reported by Seayad and List in 2005 [20]. This grouping is based on the acidic or basic type of the catalytic cycle. Lewis base, Lewis acid, Brønsted base, and Brønsted acid are four catalytic cycles (Figure 6). They proposed that Lewis base catalyst (B:) starts the catalytic cycle via nucleophilic addition to the substrate (S). The resulting complex undergoes a reaction and then releases the product (P) and the catalyst for further turnover. Lewis acid catalysts (A) activate nucleophilic substrates (S:) in a similar manner. Brønsted base and acid catalytic cycles are initiated via a (partial) deprotonation or protonation, respectively. [20]

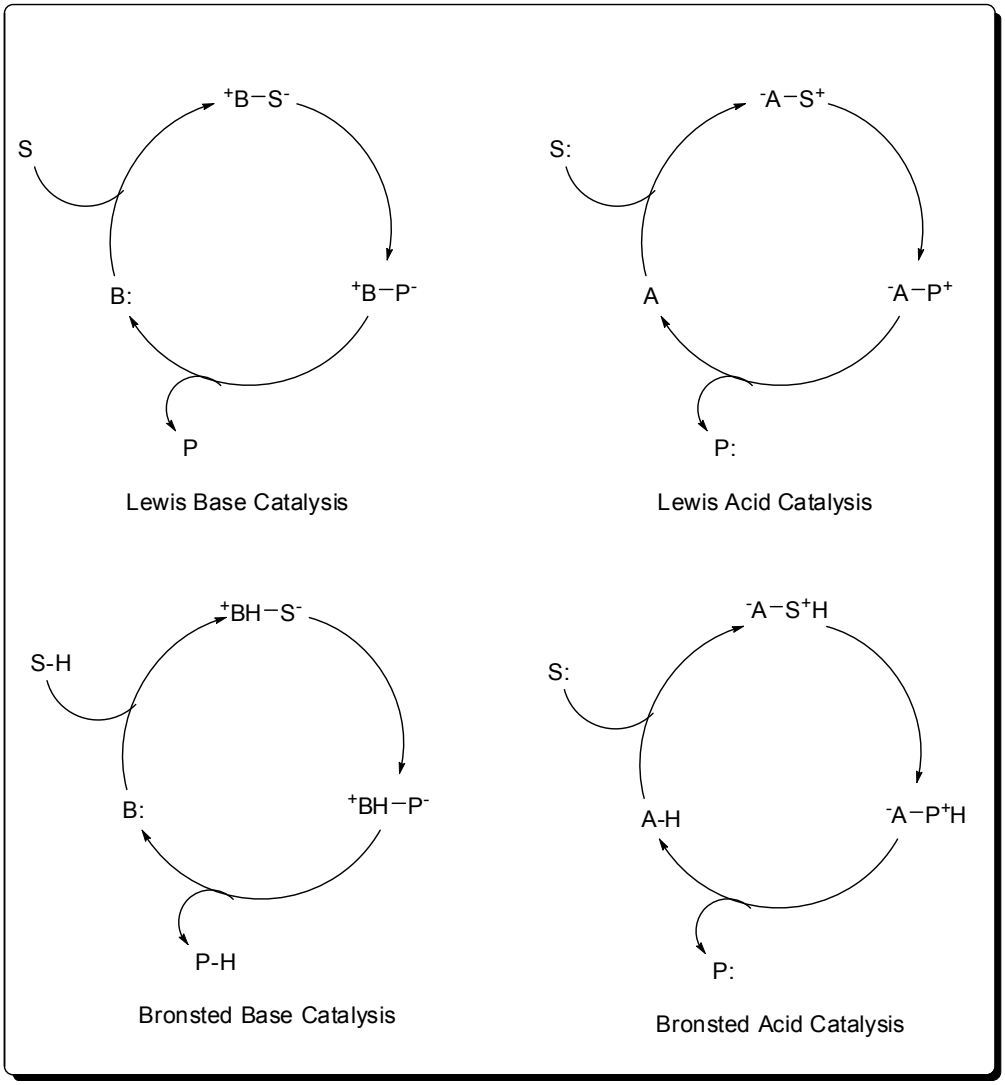

Figure 6. Catalytic cycles of organocatalysis

Other classification is based on transition state and it is more specific from previous works. Gaunt and *co*workers reported that five different modes of catalysis are investigated to detail the scope of organocatalysis and how it can be applied to the synthesis of pharmaceutically relevant molecules. Classification is based on the type of transition state [21]. These five modes of catalysis are:

- Secondary amine catalysis via enamines
- Secondary amine catalysis via iminium ions
- Phase-transfer catalysis

- Nucleophilic catalysis and Brønsted base catalysis
- H-bonding catalysis

Although the type of classification looks very specific, it covers most of organocatalysis. Therefore, each type of catalysis is discussed in detail including specific reaction from literature and working principles of catalysts.

1.3.1. Secondary amine catalysis *via* enamine formation

Enamine catalysis involves enamine intermediate that is generated from substrate and a catalyst containing secondary amine unit, then deprotonation of an iminium ion. The formed enamine reacts with various electrophiles or undergoes pericyclic reactions.

As mentioned before, the first example of asymmetric enamine catalysis is the Hajos-Parrish-Eder-Sauer-Wiechert reaction, an intramolecular aldol reaction catalyzed by proline (Scheme 3) [13, 14]. Although this reaction used in natural product and steroid synthesis, the extensive potential of the Hajos-Parrish-Eder-Sauer-Wiechert reaction had not been explored, due to its ambiguous mechanism. Although the mechanism was studied in 1980s, proposed mechanisms did not explain the nonlinear effect in asymmetric aldol reactions. The proposed mechanism is shown in Scheme 6 [21]. Proline, first, generates iminium ion, then the iminium ion transforms into enolate which can react with an electrophile. Finally, proline removes from adduct and continues its catalytic cycle.

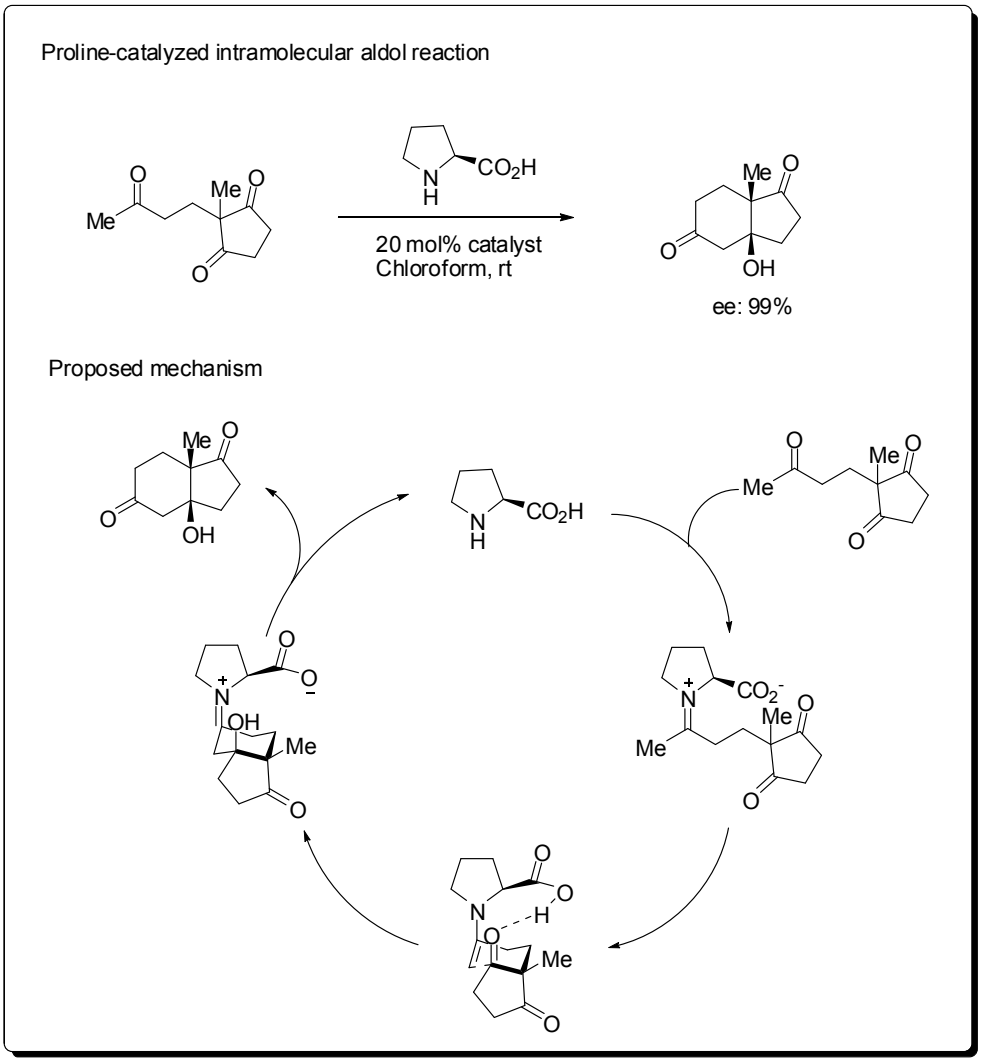

Scheme 6. Proline-catalyzed intramolecular aldol reaction

Enamine catalysis is also used in intermolecular nucleophilic addition to an electrophile. When the electrophile is an carbonyl, it is called as aldol reaction. Imines can be used as electrophile in Mannich reaction. Enamine catalysis is not only used in aldol and mannich type reaction, it is also used in oxygenation [23], amination [24], chlorination [25] and fluorination [26] of the "*α*" position of aldehydes. These reactions are summarized in Scheme 7.

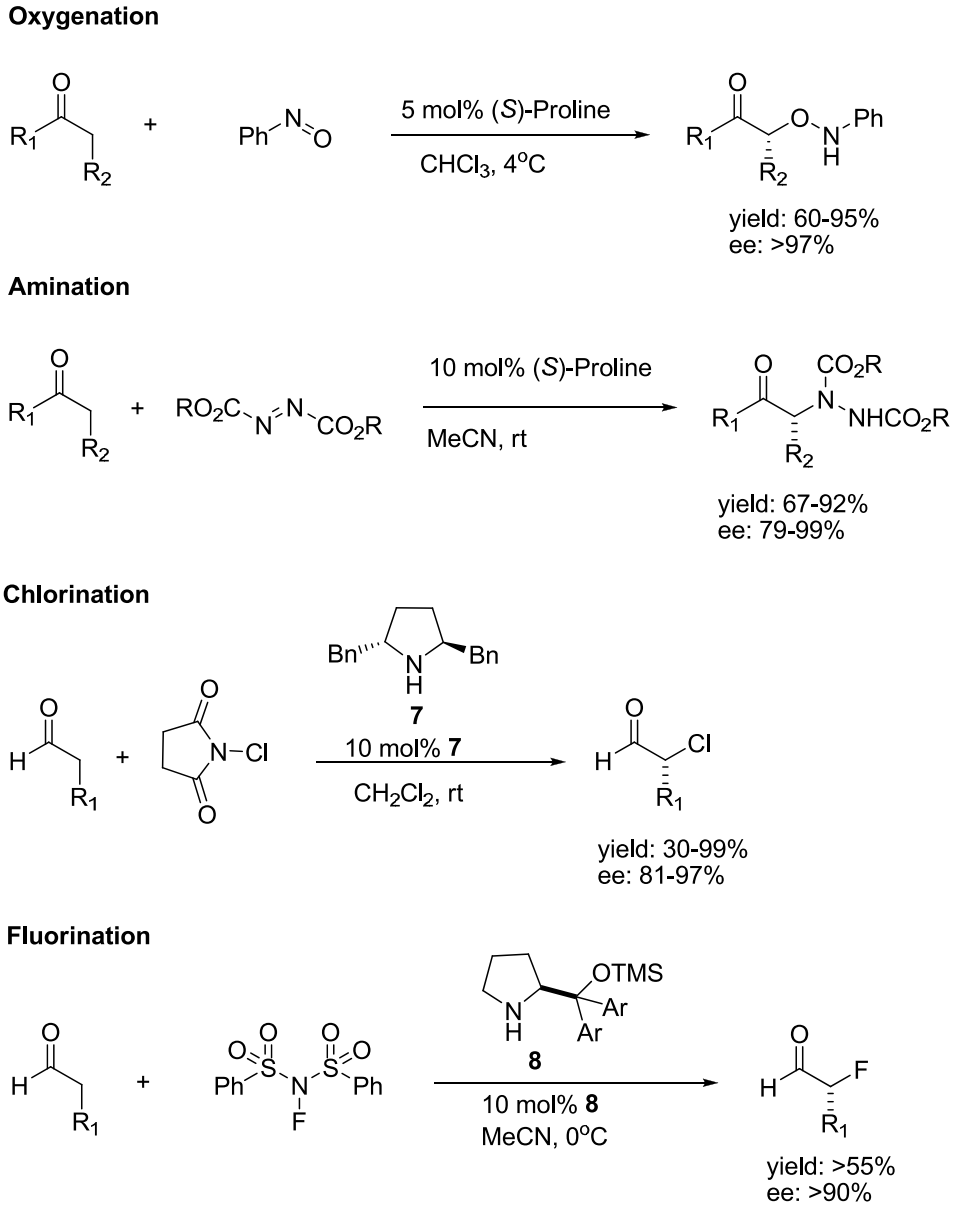

Scheme 7. Enamine catalysis reactions

1.3.2. Secondary amine catalysis *via* iminium Ion

A secondary amine can also catalyzed some asymmetric reactions by forming iminium ion from a carbonyl compound. Generation of iminium lowers

the LUMO energy of the system. Decreasing LUMO energy increases the acidity of α-hydrogen and activates carbonyl carbon [20]. The first use of secondary amine catalysis via iminium ion was reported during the late 1990s by MacMillan and *co*workers [27]. The function of iminium simulated that of Lewis acids. In other words, iminium catalysis provides an organocatalytic alternative to conventional Lewis acid catalysis (Figure 7) [21].

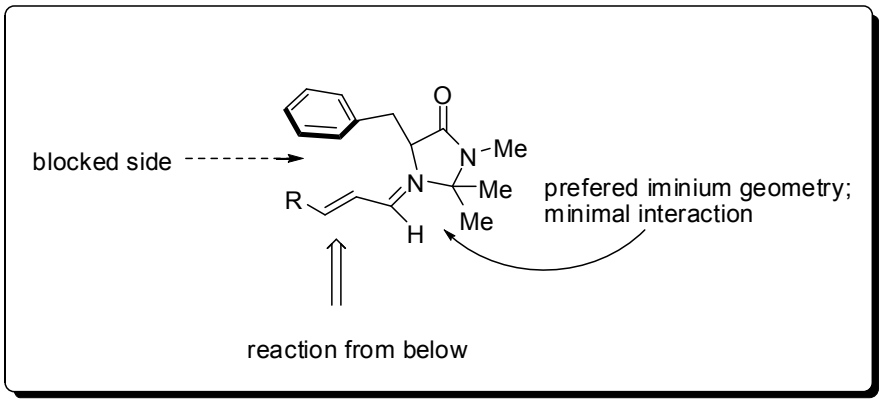

Figure 7. Stereoconrol elements in the iminium ion

Iminium catalysis is generally used in asymmetric cycloaddition [27], cyclopropination [28], epoxidation [29], conjugate addition to enals [30], and cascade reactions [31]. In scheme 8, asymmetric Diels-Alder reaction is shown that was done by MacMillan and his *co*workers [27]. The catalyst **9** is also known as MacMillan imidazolidinone. It should be noted that this work was also a milestone in asymmetric organocatalysis such as proline.

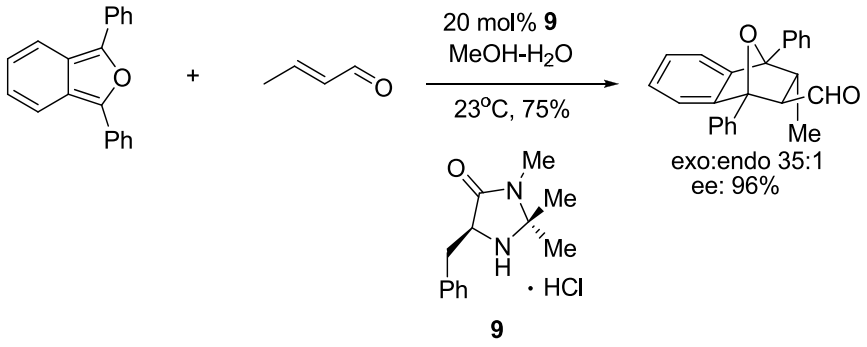

Scheme 8. Enantioselective Diels-Alder reaction

1.3.3. Phase-transfer catalysis

Despite a wide application area of phase-transfer catalysis (PTC) in organic transformations, only recently have significant advances in chiral phase-transfer catalysis (CPTC) been made.

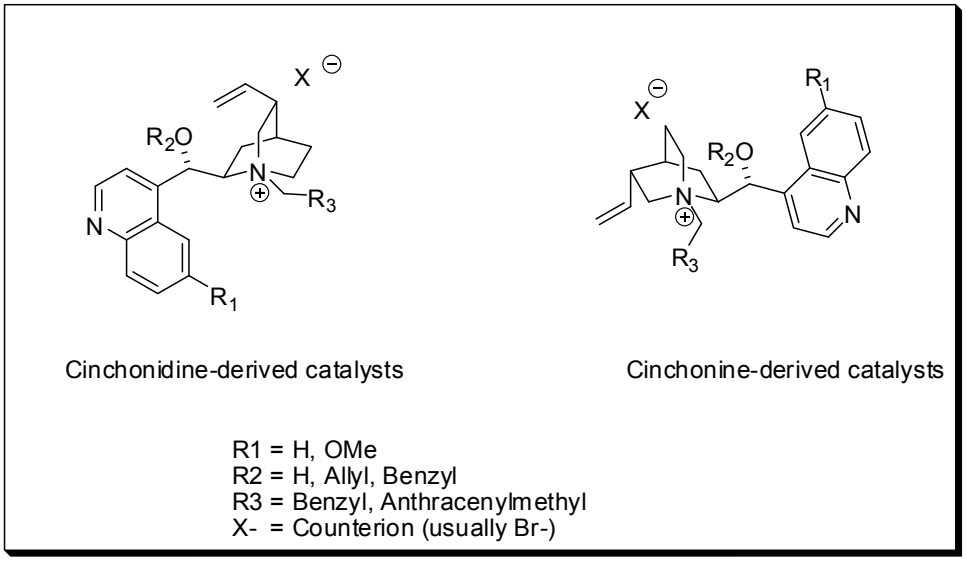

Figure 8. Cinchona-derived chiral phase transfer catalysts

The cinchona alkaloids, that are commercially available and can be transformed to active quaternary ammonium salt catalysts in one or two steps, have served as the primary source of effective chiral phase-transfer catalysts (Figure 8) [32]. The use of cinchona-derived catalysts for the asymmetric epoxidation of chalcones and quinones dates back to 1976 by Wynberg in 1976. The results are high in chemical yields but modest in enantioselectivities [33]. In 1997, Lygo and *co*workers reported that using NaOCl as the oxidant and an *O*-benzylated *N*-anthracenylmethyl cinchona-derived catalyst **10** increase the enantioselectivity for the epoxidation of chalcones [34]. In order to increase selectivity, *O*-benzylated *N*-anthracenylmethyl catalyst under solid-liquid PTC conditions and KOCl as the oxidant was used in 1999 by Corey (Scheme 9) [35].

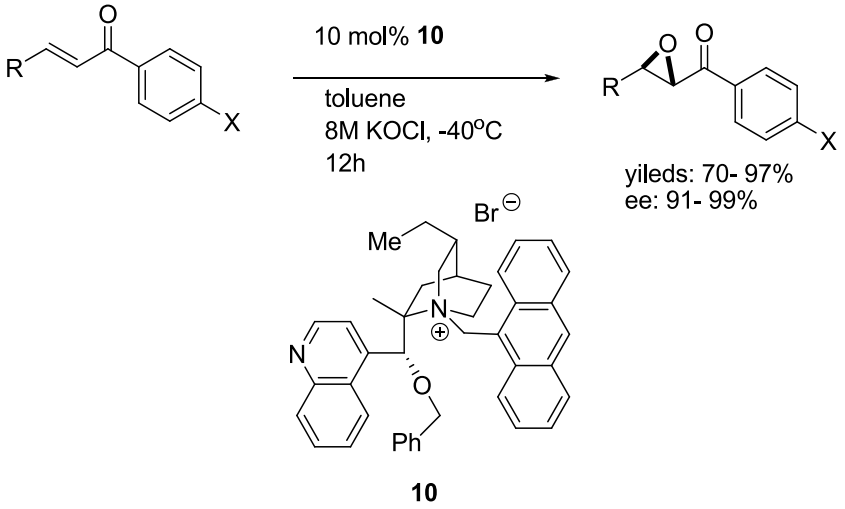

Scheme 9. Enantioselective epoxidation of reaction

The modified cinchona catalysts have dominated and revolutionalized the development of the CPTC field. They have demonstrated the possibility of achieving highly enantioselective transformations under phase-transfer conditions for a variety of C-C, C-O and C-N bond-forming reactions. Additionally, highly enantioselective Michael [36], Mannich [37], and aziridination [38] reactions have also been developed under CPTC conditions. It is evident from the considerable development of CPTC methods in the recent years that more synthetically useful

transformations will continue to be applied and investigated under phase-transfer conditions.

1.3.4. Nucleophilic and Brønsted base catalysis

Nucleophilic catalysts play important role in the development of new synthetic methods [39]. Most common nucleophilic catalysts are cinchona alkaloids. They act as bases to deprotonate substrates, and form contact ion pairs between the anion and protonated cinchona alkaloids. The electrostatic interaction between opposite charges, create a chiral environment around the anion and the chiral information will be transferred to the product (Figure 9) [21].

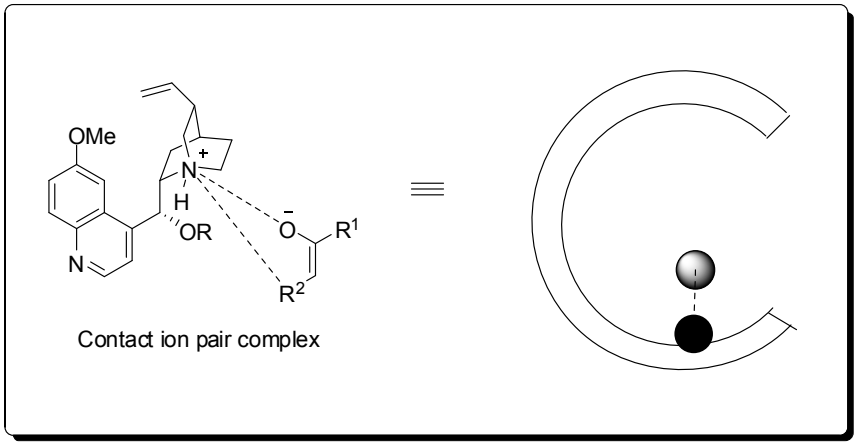

Figure 9. Cinchona alkaloids as catalysts for reactions through chiral contact ion pairs

Cinchona alkaloids can also catalyze the Morita-Baylis-Hillman reaction. Cinchona alkaloid derived organocatalyst **11** can also catalyze this reaction with excellent enantioselectivity (Scheme 10) [40].

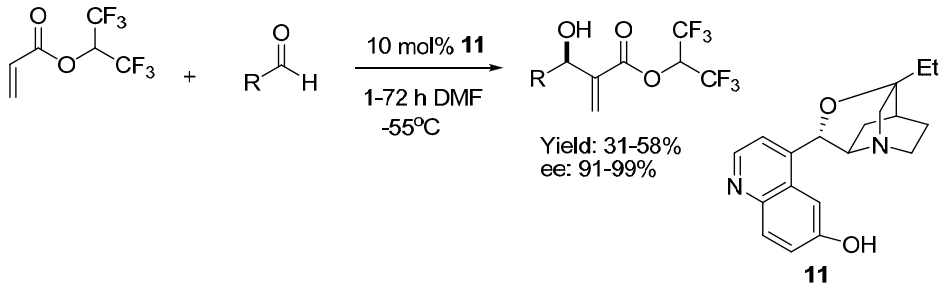

Scheme 10. Cinchona alkaloid-catalysed Baylis–Hillman reaction

Despite the fact that few tertiary amines catalyze the Baylis–Hillman reaction with a acceptable enantioselectivity, the cinchona derivatives can catalyze this transformation with both aldehydes and tosylimines (Scheme 11) [41]. The disadvantage of this method is that one enantiomer will be synthesized because of being one possible enantiomer of quinine-derived catalyst.

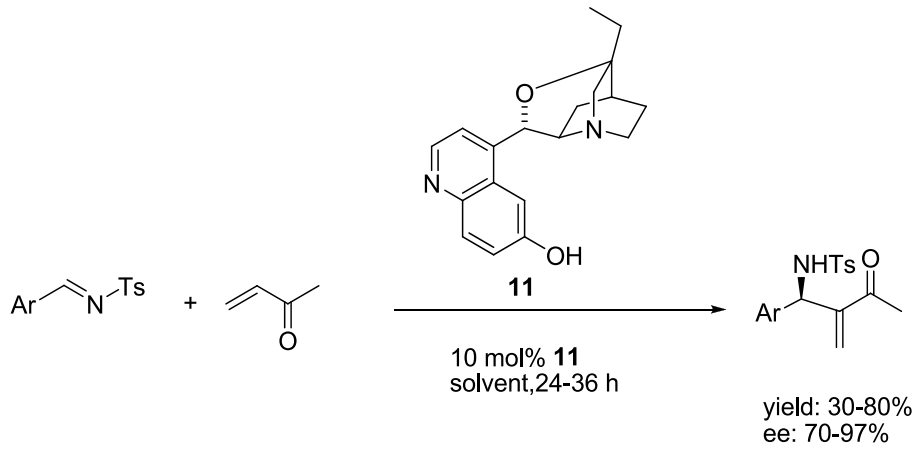

Scheme11. Cinchona-catalyzed Baylis-Hillman reaction of tosylimines

Another interesting area of nucleophilic organocatalysts is the nucleophilic carbene catalysts. Rovis and *co*workers reported that a chiral carbene catalyst **12** induces excellent enantioselectivity in asymmetric intramolecular Stetter reaction

over a broad range of cyclic products in good yields and enantiomeric excesses (Scheme 12) [42].

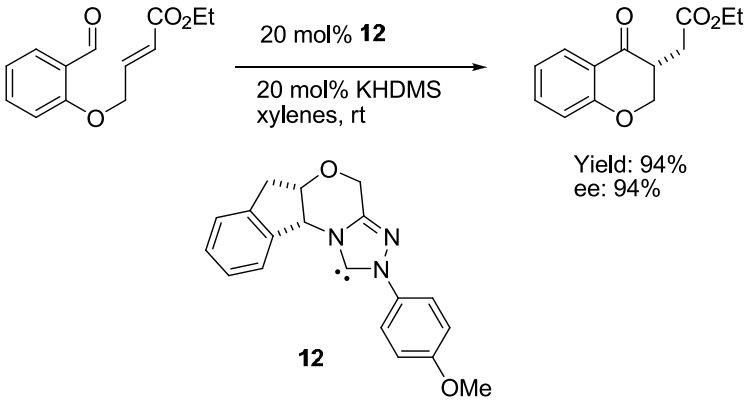

Scheme 12. Catalytic enantioselective intramolecular Stetter reaction

1.3.5. Hydrogen bonding catalysis

The hydrogen bonding catalysis has received insignificant attention even if hydrogen bonding catalysts have known for a long time [43, 44]. Similar to Lewis acid activation, hydrogen bonding catalysis activates electrophiles with H-bonding. Instead of using metals to coordinate the lone pair of a carbonyl, this type of catalysts bind to substrates via formation of hydrogen bonding to activate the substrate and transfer the chiral information into electrophiles [21].

One of the H-bonding catalysts is chiral diol derivatives. Hydrogen atom, attached to hydroxyl unit activates carbonyl compounds *via* H-bonding. The most common example is Taddol **13**. It catalyzes hetero-Diels Alder reactions to form dihydropyranones **14** in high yields and enantiomeric excesses (Scheme 13) [45].

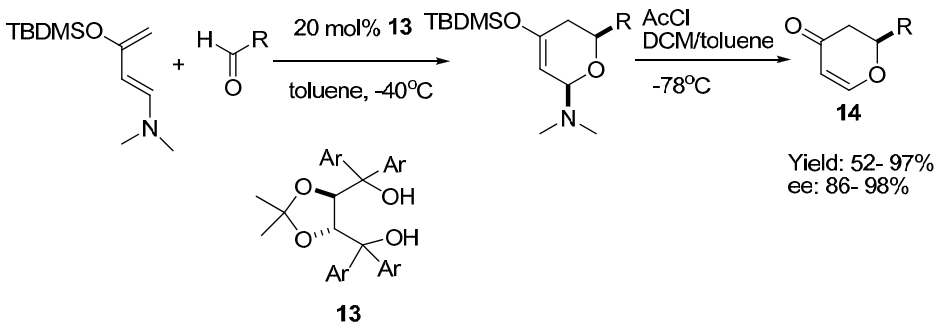

Scheme 13. Enantioselective cycloaddition

Binol derivative **15** catalyzed Baylis-Hillman reaction of an aldehyde or imine. This can be seemed as a useful solution to the existing problem of an enantioselective Baylis-Hillman reaction (Scheme 14) [46, 47].

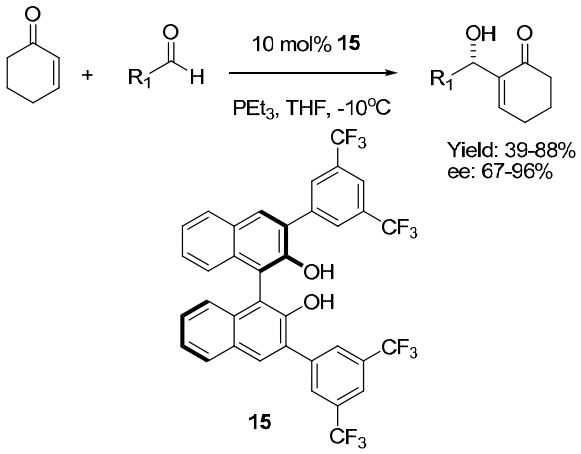

Scheme 14. Enantioselective Baylis-Hillman reaction

Another type of H-bonding catalyst is chiral thiourea derived organocatalyst. Jacobsen and *co*workers synthesized some chiral thioureas that are versatile, effective catalysts. A wide range of nucleophiles can be added to

electrophiles by thiourea catalysis. Strecker [48], hydrophosphorylation [49], nitro-Mannich [50] and Mannich [51] reactions are all possible. Hence, it should be noted that hydrogen bonding catalysis has a wide application area and it is a noteworthy area of organocatalysis.

Thiourea type catalysts can also be used in acyl Piclet–Spengler reaction [52]. Despite the imprecise mechanism of this activation, it provides the first access to a new type of reactions. Correspondingly, Mannich reactions onto acylated isoquinolines give the chiral products in high enantiomeric excesses, affording similar compounds. In Scheme 15, thiourea derived **16** was used as a catalyst [53].

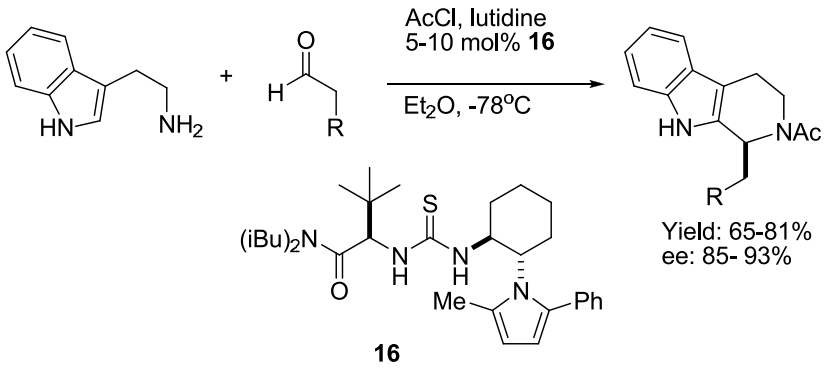

Scheme 15. Thiourea-catalyzed asymmetric reaction

Another application of thiourea catalysis is the Freidel-Crafts type reaction [54]. Electron-rich furan derivatives can be used for this reaction. 1,2-aza-Friedel-Crafts reaction catalyzed by a chiral phosphoric acid **17** is shown in Scheme 16. The present reaction has provided an atom-economical route to furan-2-ylamine derivatives with excellent enantioselectivity.

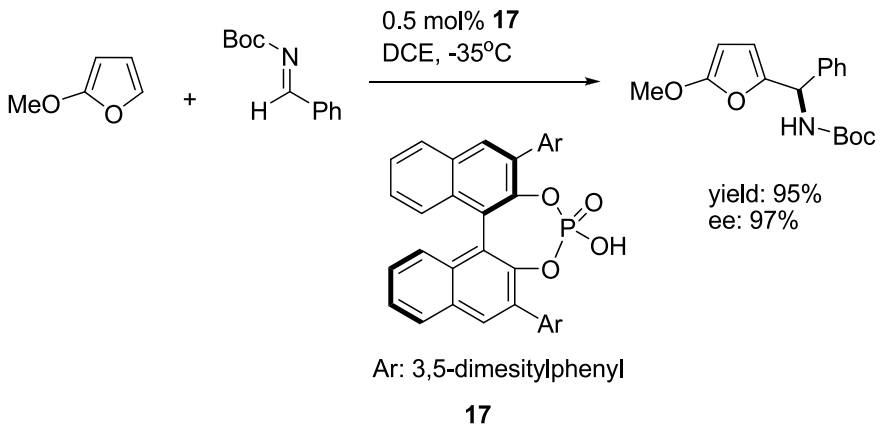

Scheme 16. Asymmetric Aza-Friedel−Crafts Alkylation of Furan

In recent times, List has developed a direct Pictet–Spengler reaction with aldehyde using compound **18** as a catalyst to form isoquinolines in high yields and enantiomeric excess (Scheme 17) [55].

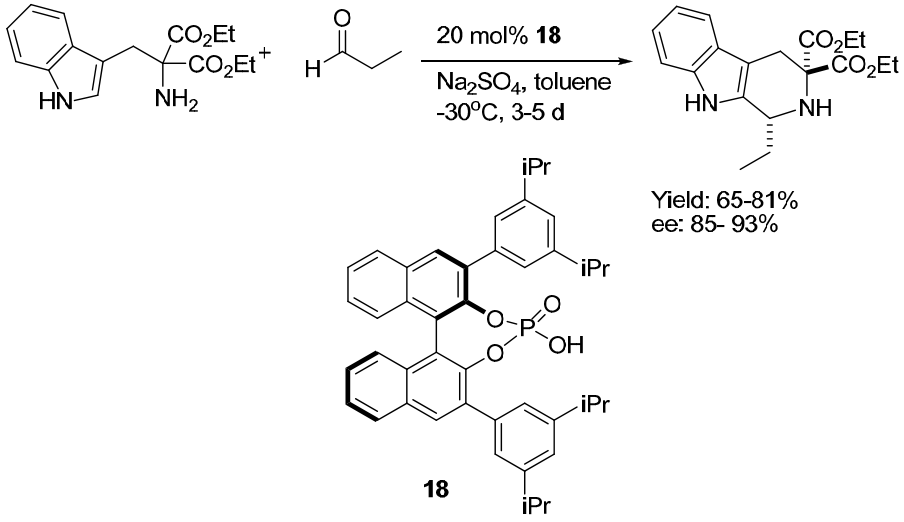

Scheme 17. Phosphoric acid-catalyzed Pictet-Spengler reaction

As a final point, an enantioselective reductive amination has been reported by several research groups. First study of the reduction of an imine with a Hantzch ester and catalytic phosphoric acid was done by Rueping [56]. List improves the method and performed a one-pot process from aldehyde to amine in enantiomeric excess up to 90% using **19** as a catalyst (Scheme 18) [57].

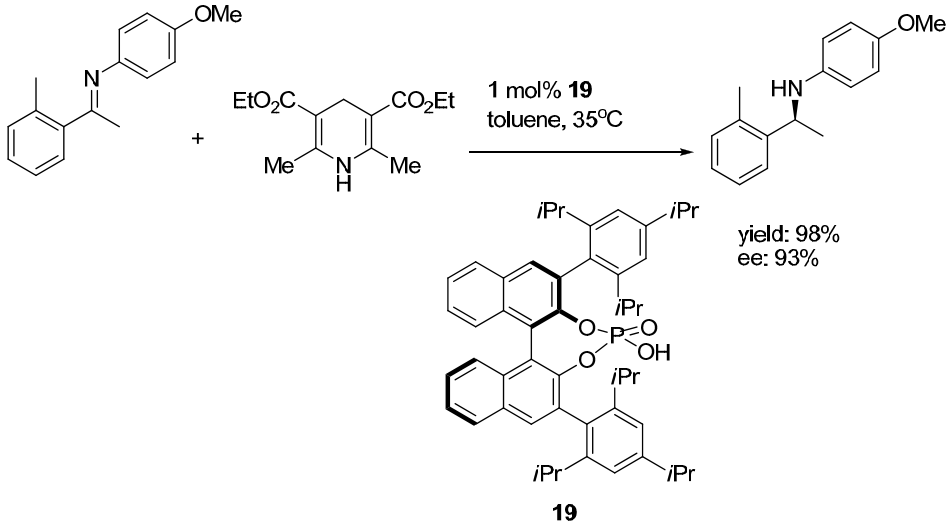

Scheme 18. Asymmetric transfer hydrogenation of imines

Another one-pot, direct reductive amination with broad substrate scope that enables the effective reductive amination of a range of methyl ketones and aryl amines was reported by MacMillan. Chiral phosphoric acid **20** was used in reductive amination of acetophenone (Scheme 19) [58].

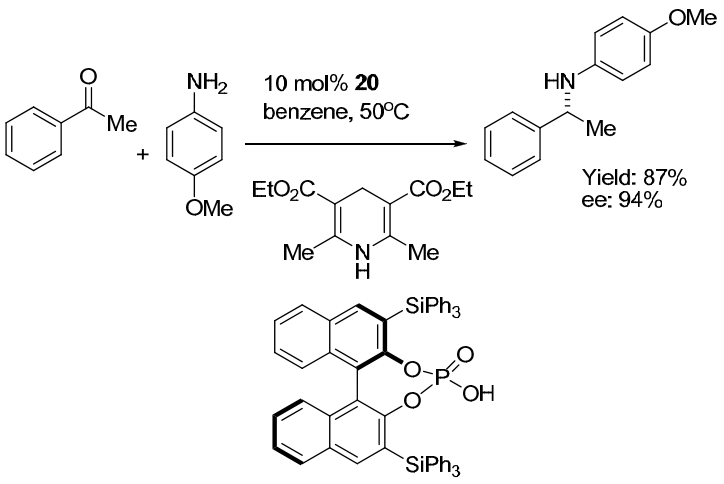

20

Scheme 19. Phosphoric acid-catalyzed reductive amination

1.4. Aim of the work

The objective is to synthesize novel organocatalysts that contain chiral camphor fused pyridine skeleton (Figure 10). Target six organocatalysts can be classified in three groups. The first group is named as nucleophilic and Lewis base type organocatalyst. Another group is proline amide derived organocatalysts that can be labeled as secondary amine catalysis via enamine formation. Finally, the last group is thiourea type organocatalysts as hydrogen bonding type catalysts.

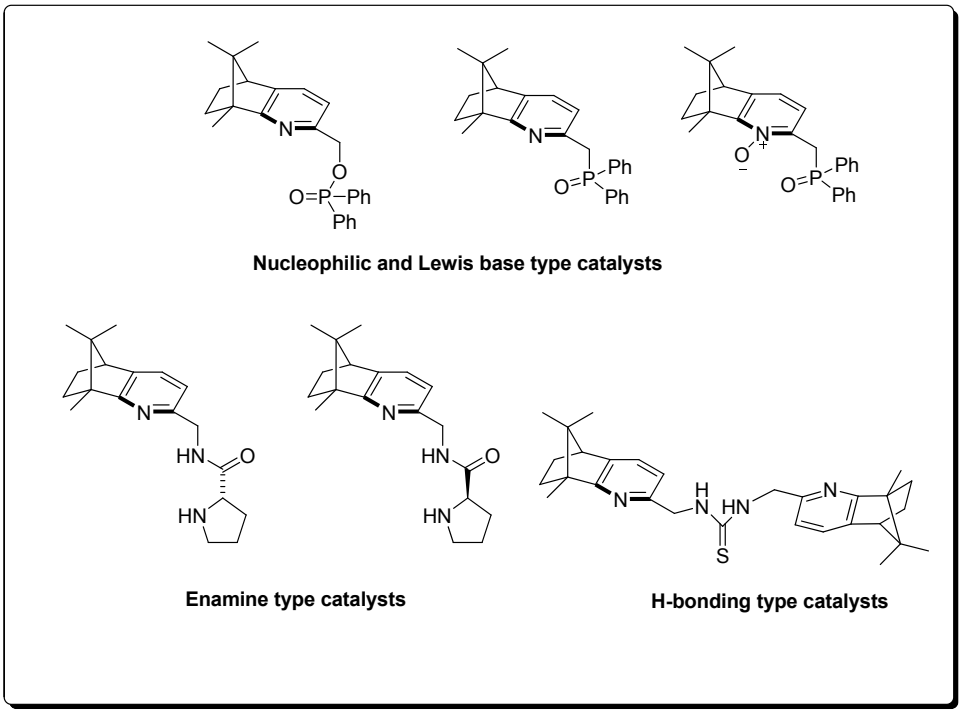

Figure 10. Target organocatalysts

Another part of the project is to test these novel catalysts in proper asymmetric transformations. The first group will be tested in asymmetric allylation of aldehyde using allyl trichlorosilane as an allylating reagent. The second group will also be tested in aldol. The final group will be tested in nitro-aldol and Baylis-Hillman reactions. Each asymmetric transformations that is applied is discussed in detail in results and discussion chapter.

CHAPTER 2

RESULTS AND DISCUSSIONS

2.1. Synthesis of camphor-fused pyridine ring

Chiral pyridines are used in many application areas of asymmetric organic synthesis, particularly as ligands in the preparation of chiral metal complexes [59, 60]. Since camphor-fused chiral auxiliaries are known to be especially effective [61], a number of pyridines fused to the camphor skeleton have been reported [62, 63]. Beside the use of camphor fused chiral pyridines as ligands or auxiliaries, they have been used as organocatalyst [64]. Here, we synthesized some novel camphor fused pyridine type organocatalysts.

In 2004, Tanyeli and *co*workers reported that the reaction of (+)-β-hydroxymethylenecamphor **21**, synthesized from *D*-camphor, with various enamines gives corresponding camphor based chiral pyridine derivatives in good yields [65]. In this approach, the first step involves the synthesis of (+)-β-hydroxymethylenecamphor **21** (Scheme 20). The chemical yield was improved up to 96% by adding ethyl formate dropwise and keeping the temperature at 0^{o}C throughout the addition process. All the spectroscopic data of compound **21** are in accordance with the literature [65].

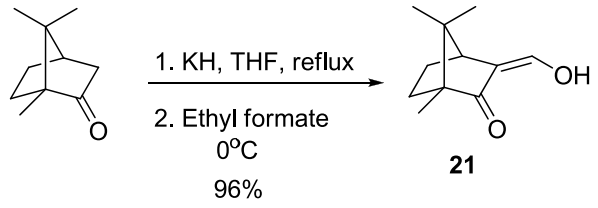

Scheme 20. Synthesis of **21**

The second step is the annulation of compound **21** with the enamine, (*Z*)-4-aminopent-3-en-2-one (Fluoral-P) **22**, synthesized by the literature procedure [66] (Scheme21).

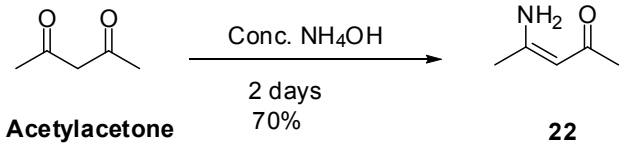

Scheme 21. Synthesis of (*Z*)-4-aminopent-3-en-2-one, **22**

Annulation reaction was carried out in a sealed tube at 170°C (Scheme 22) and the deacetylated product **23** was isolated in 55% chemical yield. Tanyeli and *co*workers proposed the following mechanism for annulations and deacetylation [64] (Figure 11).

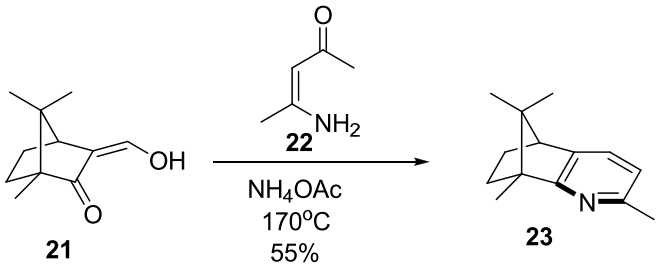

Scheme 22. Synthesis of camphor- based pyridine, **23**

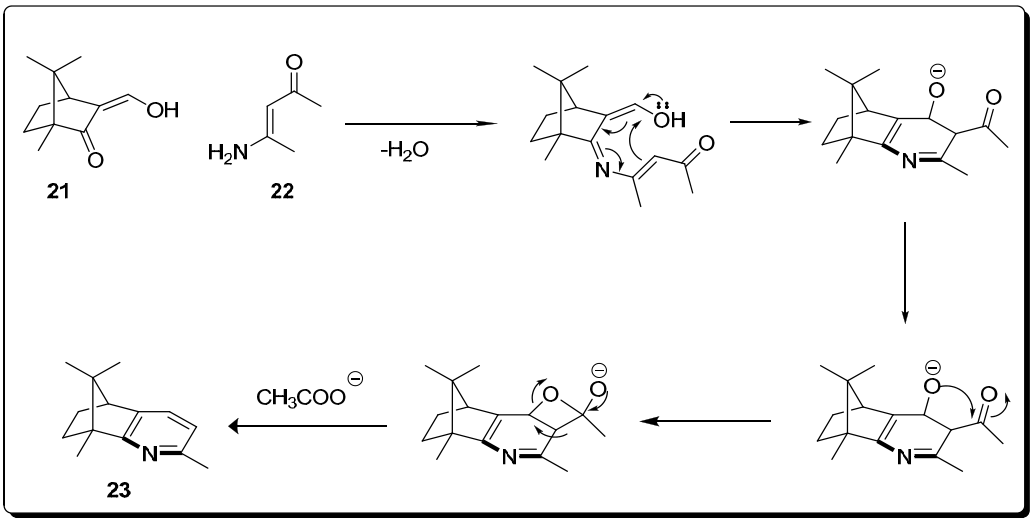

Figure 11. Mechanism of annulation and deacetylation reaction

2.2. Functionalization of camphor fused pyridine via Boekelhide Rearrangement

The key step of our synthetic route is the activation of methyl group connected to pyridine ring via shifting oxygen from nitrogen to carbon. This reaction is also named as Boekelheide rearrangement since 1953. Boekelheide stated that compound **25** is synthesized via a reaction of 2-picoline-N-oxide **24** with acetic anhydride (Scheme 23) [67]. In this study, mechanism of the reaction was also discussed. Although the first step, acetylation of N-oxide from oxygen atom is clear, the subsequent steps of the mechanism are not so clear. It was reported that the reaction proceeded through a cyclic or ionic mechanism [67]. This would lead us to functionalize camphor fused chiral pyridine skeleton from the second position of pyridine ring.

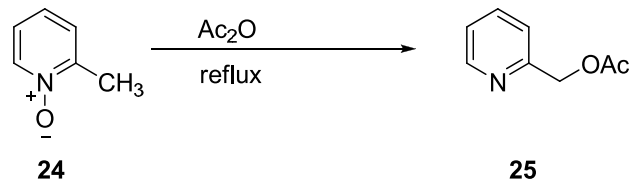

Scheme 23. Boekelheide rearrangement

The first step is converting camphor fused chiral pyridine, **23** into its *N*-oxide, **26** (Scheme 24). Furthermore, Boekelheide rearrangement could be applied to *N*-oxide, **26.**

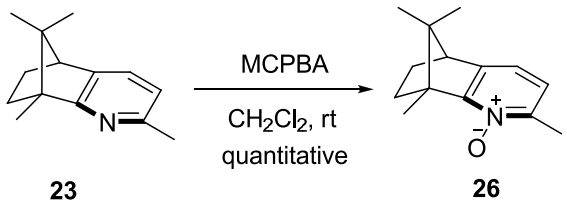

Scheme 24. Synthesis of *N*-oxide, **26**

After synthesizing *N*-oxide **26**, it was transformed into 2-hydroxymethylene pyridine, **27**. However, in order to make oxygen shift, several methods from the recent literature were applied. These attempts are summarized in scheme 25. All three experiments were resulted in very low chemical yield. As a first attempt, trifluoroacetic anhydride (TFAA) was used at room temperature [68]. Since the yield was quite low, 1,2-dichloroethane was used as a solvent due to its high boiling point. It was expected that the chemical yield could be increased by increasing temperature. However, this expectations failed by second attempt. As a third attempt, triflic anhydride was used due to its better leaving group property.

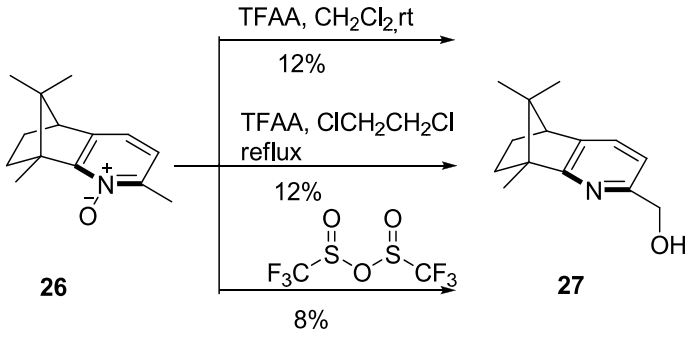

Scheme 25. Boekelheide rearrangement with different reagent

Finally, original Boekelheide procedure was applied using acetic anhydride. Since the product is acetylated, basic hydrolysis was made to get corresponding pyridinyl alcohol, **27** in quite high chemical yield (Scheme 26).

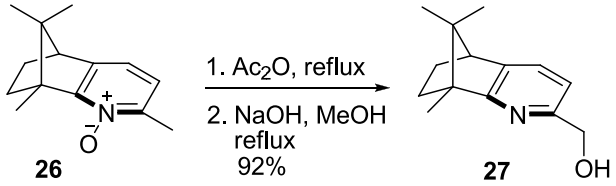

Scheme 26. Synthesis of 2-hydroxymethylene pyridine, **27**

Characterization of the *N*-oxide, **26** was easily done by NMR spectroscopy. The ^{1}H-NMR spectrum of camphor fused pyridine, **23** (Figure A3) reveals that there are four different singlets with the same integration value belonging to characteristic three methyl protons of camphor skeleton and methyl protons connected to pyridine ring. Methyl protons connected to pyridine ring appeared at 2.44 ppm and pyridine (aromatic) protons resonate at 6.73 ppm and 7.14 ppm as doublets with the equal coupling constants, *J*= 7.2 Hz. Since the electron density of

the pyridine ring was increased as a result of *N*-oxide, aromatic signals appeared in higher field as it is expected. In the ^{1}H-NMR spectrum of *N*-oxide **26** (Figure A5), methyl protons connected to pyridine shifted to 2.37 ppm and one of the aromatic proton shifted to 6.89 ppm from 7.14 ppm. In ^{13}C-NMR, one pyridine carbon appeared 170.2 ppm for compound **23** (Figure A4), whereas it was observed at 153.8 ppm for *N*-oxide **26** (Figure A6).

In our synthetic strategy, pyridinyl alcohol **27** was transformed to target organocatalysts by applying traditional methods. Therefore, the structure elucidation of key product **27** without any doubt was crucial. In ^{1}H-NMR of *N*-oxide **26**, four singlets that belong to methyl group, appear between 0.62 ppm and 2.37 ppm. However, the methyl group attached to second position of pyridine ring for compound **26** at 2.37 ppm was disappeared and two new singlets at 4.70 and a broad peak at 4.51 ppm, belonging to methylene protons and hydroxyl proton of hydroxylmethylene group, respectively (Figure A8). In the ^{13}C-NMR spectrum of pyridinyl alcohol **27** (Figure A9), the signal of methyl carbon attached to pyridine ring at 20.1 ppm for *N*-oxide **26** was disappeared and new methylene carbon at 64.3 ppm was observed. The high resolution mass spectrum of the product **27** was given in figure 12. The HRMS result of **27** ($C_{14}H_{19}NO$) was found for $[M+H]^{+}$: 218.1537 and the calculated value for $[M+H]^{+}$: 218.1545.

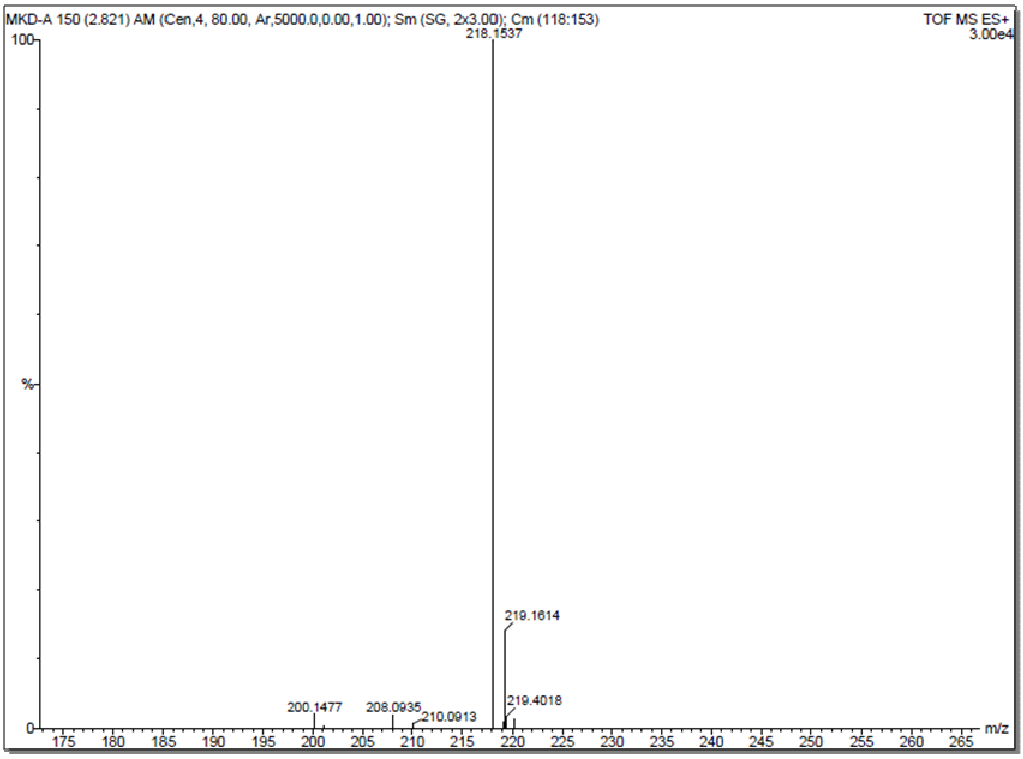

Figure 12. HRMS spectrum of isolated product **27**

2.3. Synthesis of nucleophilic and Lewis base type organocatalysts

Various *N*- or *P*-oxides and *N,N'*- or *P,P'*-dioxides, which are able to activate trichlorosilanes and catalyze a number of asymmetric transformation reactions i.e. allylation, propargylation, aldol condensation, ring opening of epoxides, etc. [64]. The allylation of aldehydes is usually the first choice reaction to test the catalytic properties and enantioselectivities of a new organocatalyst. Herein, we report a new and simple route to the synthesis of *P*-oxide and *P,N*-dioxide using two different ways: (*i*) direct phosphorylation of alcohol, (*ii*) tosylation of pyridinyl alcohol and subsequent nucleophilic substitution of tosylate with diphenylphosphide. The first way to synthesize *P*-oxide is the direct phosphorylation of previously synthesized alcohol **27** via diphenylphosphine chloride with a base (Scheme 27). Since our molecule phosphinate **29** is the

oxidized form of the phosphinooxy **28**, inert atmosphere condition was not necessary. In other words, the *P*-oxide **29** was obtained by air-oxidation.

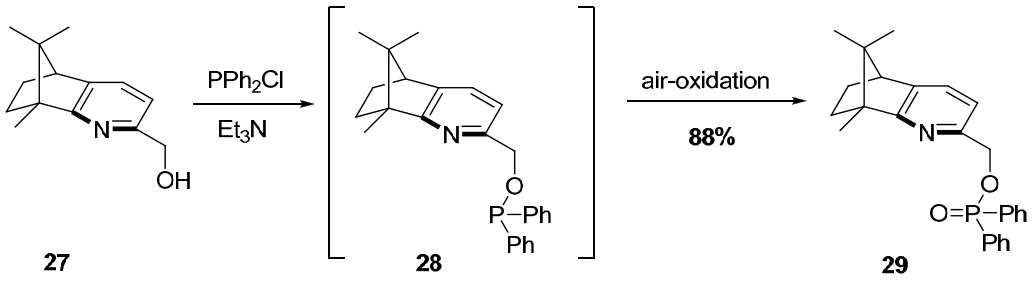

Scheme 27. Synthesis of catalyst **29**

Another synthetic way to synthesize *P*-oxide and *P,N*-dioxide involves tosylation of pyridinyl alcohol **27** and subsequent nucleophilic substitution with diphenylphosphide (Scheme 28).

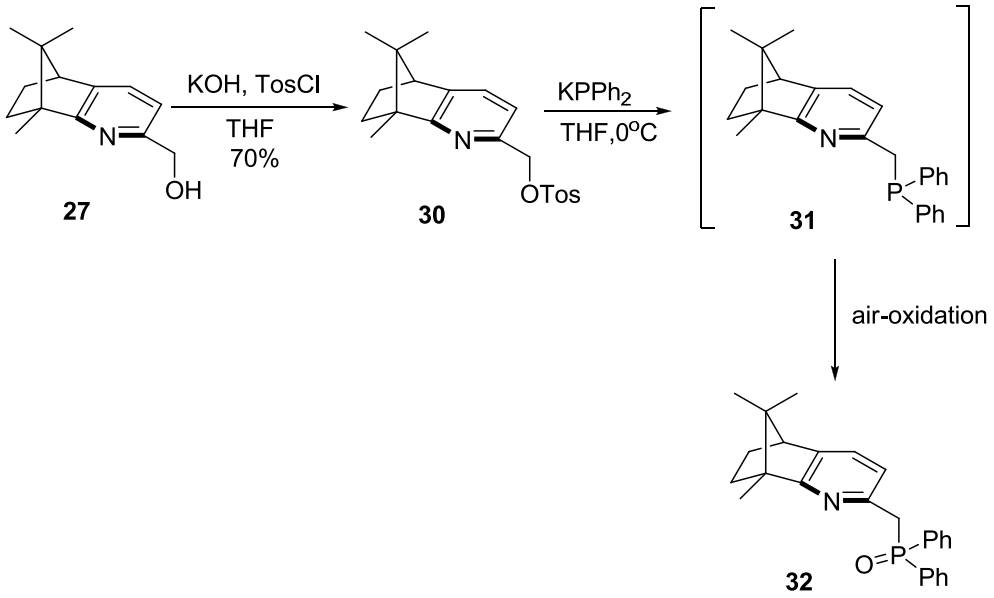

Scheme 28. Synthesis of organocatalyst **32**

Finally, *P*-oxide **32** was transformed into a new type of nucleophilic and Lewis base organocatalyst *P,N*-dioxide **33** with MCPBA in DCM at room temperature (Scheme 29).

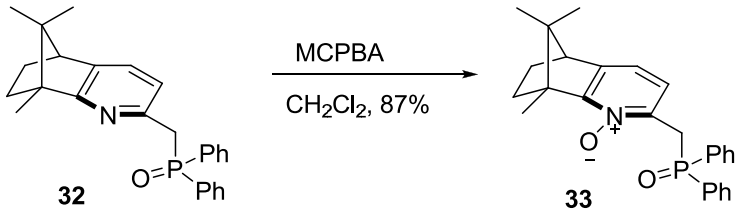

Scheme 29. Synthesis of *P,N*-dioxide, **33**

Structure elucidation of the phosphinate **29** was done by comparing ^{1}H-NMR and ^{13}C-NMR spectra of pyridinyl alcohol **27**. In this type of compound, the most valuable information is obtained from the aromatic protons in terms of the number of the different protons and carbons, their chemical shifts and relative integration values. Another valuable finding is the disappearance of hydroxyl proton signal in ^{1}H-NMR spectrum. Catalyst **29** reveals twelve protons in the aromatic region (Figure A15). Two of them belong to pyridine unit and the rest belongs to phenyl units of diphenylphosphinate group. Another significant observation was shifting of CH_2 protons from 4.70 ppm to 5.05 ppm. In the ^{13}C-NMR, ten additional carbon signals were seen in the aromatic region due to coupling of carbon atoms and phosphorous. Carbon signal of methylene also shifted from 64.3 ppm to 67.4 ppm as a doublet having a *J* value of 6 Hz (Figure A16).

The tosylate **30** was also characterized by spectroscopic methods. The ^{1}H-NMR spectrum of **30** showed that two set of doublets (*J*= 8 Hz) at 7.73 ppm and 7.22 ppm as belonging to the aromatic protons of tosyl unit. The methyl protons of tosyl unit gave a singlet at 2.33 ppm (Figure A17). Another difference in ^{1}H-NMR spectra was the shift of CH_2 protons, connected to the pyridine ring, from 4.70 ppm to 5.02 ppm. The ^{13}C-NMR spectrum of **30** is also helpful to characterize the

product. The additional signals at 127.0, 127.2, 128.7, 132.4 and 21 ppm correspond to aromatic carbons and methyl carbon of tosyl unit, respectively (Figure A18).

The ^{1}H-NMR spectrum of camphor fused 2-((diphenylphosphoryl)methyl) pyridine **32** revealed additional ten aromatic protons between 7.00 ppm and 7.51 ppm (Figure A20). The other evidence for the phosphorylation was the shift of CH_2 protons from 5.02 ppm to 3.57 ppm. In ^{13}C-NMR spectrum ten additional aromatic carbon signals are observed in aromatic region (Figure A21). These spectrospcopic data are just to prove phosphorylation reaction. HRMS result gave us sufficient information about whether the product is oxidized or not. HRMS result of the compound **32** as 402.1987 is in accordance with the calculated mass 402.1977.

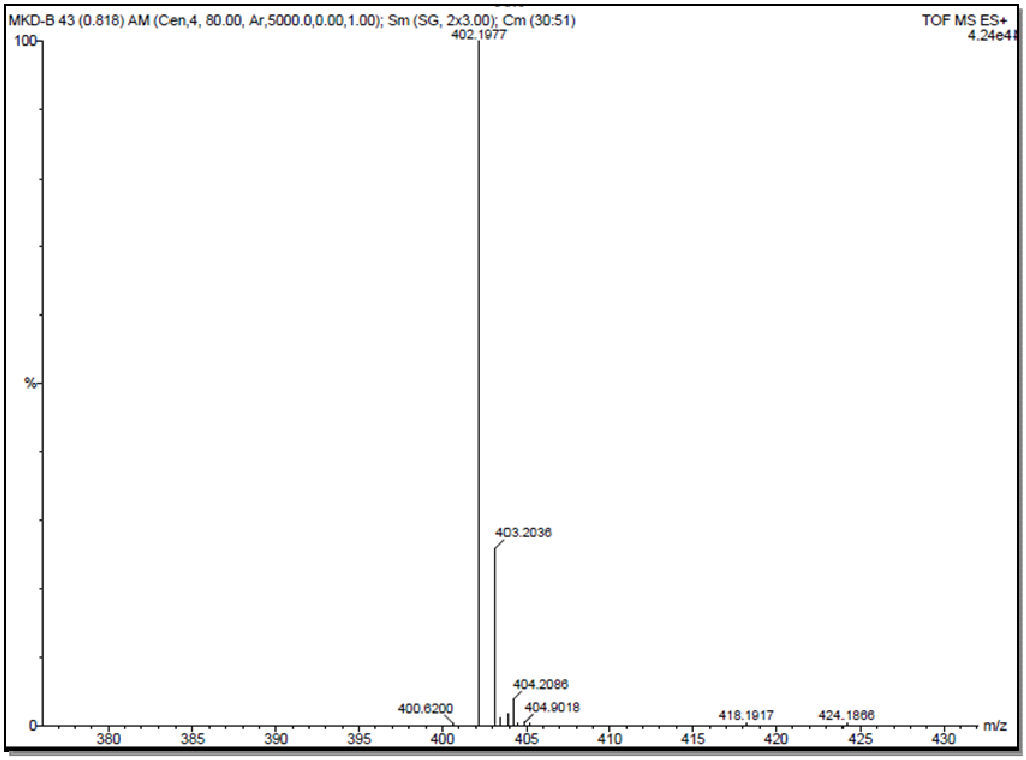

Figure 13. HRMS spectrum of catalyst **32**

Structure elucidation of the *P,N*-dioxide **33** was done by comparing ^{1}H-NMR spectrum of compound **32**. Conversion of pyridine to pyridine oxide changed the electron density of the molecule **32** and in the ^{1}H-NMR of *P*-oxide **32**, aromatic protons of pyridine ring resonated at 6.75 ppm and 6.84 ppm and the protons of CH_2 attached pyridine ring were observed at 3.54 ppm. On the other hand, in the^{1}H-NMR of *P,N*-dioxide **33** (Figure A22), one of the aromatic proton shifted from 6.75 ppm to 7.36 ppm and the other aromatic signal remained same at 6.85 ppm. The methylenic protons also shifted to 4.05 ppm and 4.35 ppm.

2.4. Synthesis of proline amide type organocatalysts

As it was discussed in the introduction chapter, the use of proline as an organocatalyst has opened a new era in asymmetric synthesis. After the reinvestigation of proline, scientists developed proline-derived organocatalysts [69]. In order to synthesize target proline amide type organocatalysts, tosylated pyridinyl alcohol **30** was firstly converted to pyridinyl amine **35** in two steps: (*i*) azide formation and (*ii*) reduction of azide (Scheme 30).

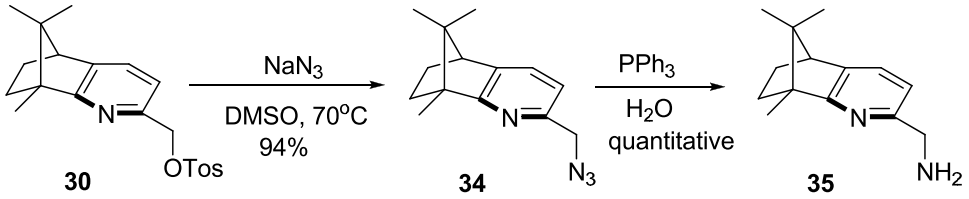

Scheme 30. Synthesis of pyridinyl amine, **35**

The target *L*-proline amide derivative **38** was synthesized via DCC coupling of pyridinyl amine **35** with *N*-Boc-*L*-proline (Scheme 31). *L*-proline had to be protected to prevent self-coupling reaction. It was protected with di-tert-butyl dicarbonate [70] in 92% chemical yield.

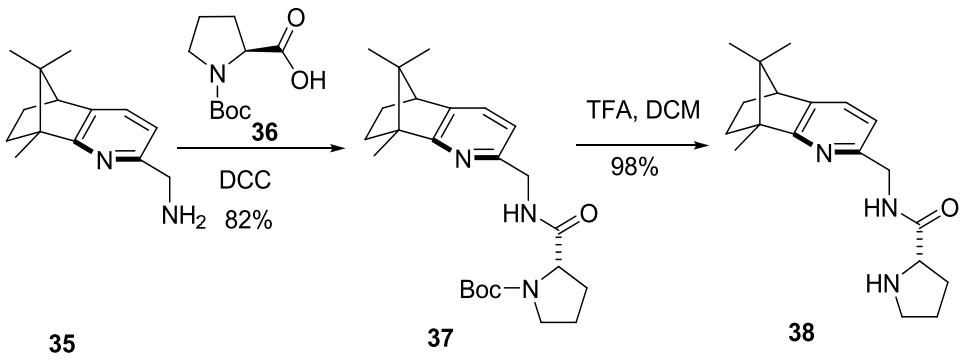

Scheme 31. Synthesis of *L*-proline amide, **38**

The structure of azide **34** was elucidated by comparing ^{1}H-NMR and ^{13}C-NMR spectra of tosylated alcohol **30**. The protons of methylene group attached to pyridine ring shifted to high field from 5.02 ppm to 4.40 ppm due to relatively low electron withdrawing property of azide, and four aromatic protons and the methyl signal of tosyl unit were disappeared (Figure A24). In ^{13}C-NMR, aromatic carbons and methyl carbon signals of tosyl unit also disappeared (Figure A25). In the GC-MS spectrum, molecular peak of azide 242.1 was observed (Figure A26).

In the ^{1}H-NMR of the pyridinyl amine **35**, a broad singlet at 1.80 ppm with an integral value of two protons indicated the reduction of azide **34** to pyridinyl amine **35**. The signal of methylene unit connected to NH_2 group shifted to 3.82 ppm from 4.40 ppm (Figure A27). In the ^{13}C-NMR, same methylene carbon shifted from 41.0 ppm to 47.8 ppm due to more electron withdrawing ability of amine group (Figure A28).

Characterization of *L*-proline amide **38** was done by ^{1}H-NMR and ^{13}C-NMR spectroscopy. In the ^{1}H-NMR, the most characteristic signal was the amide proton NH which resonated at 8.35 ppm (Figure A29). The carbon of the amide group was seen at 174.9 ppm in the ^{13}C-NMR spectrum of compound **38** (Figure A30).

It is well-known that when two different chiral units are combined to form a new chiral compound, this combination may cause matching and/or mismatching property in asymmetric synthesis. In order to check this property, it should be essential to introduce oppositely configurated *D*-proline (Scheme 32).

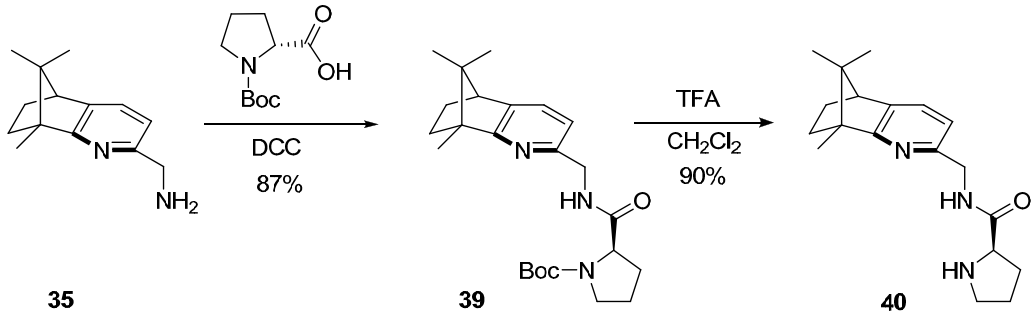

Scheme 32. Synthesis of *D*-proline amide, **40**

2.5. Synthesis of thiourea-derived organocatalysts

Organocatalysts containing thiourea functional group have been widely used in many application areas in asymmetric synthesis due to their double-hydrogen bonding interaction [71]. Most common use involves the asymmetric synthesis with the compounds having carbonyl and nitro groups. As it was mentioned in the introduction chapter, thiourea type organocatalysts can be classified as hydrogen-bonding catalysts.

Two novel thiourea type chiral organocatalysts were developed. Pyridinyl amine **35** was chosen as a proper starting compound to synthesize the thiourea type C_2-symmetric organocatalyst **41** (Scheme 33). Previously synthesized 2-aminomethylene pyridine **35** was reacted with carbon disulfide and DCC.

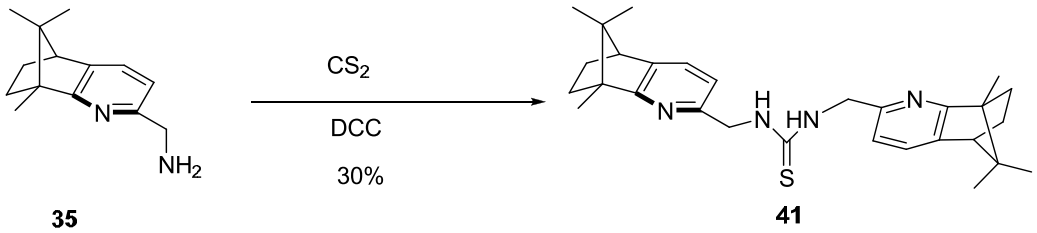

Scheme 33. Synthesis of C_2-symmetric organocatalyst, **41**

C_2-symmetric thiourea **41** was characterized by comparing ^{1}H-NMR, ^{13}C-NMR spectra and GC-MS of starting amine **35**. Disappearance of NH_2 protons and formation of characteristic carbon signal of thiourea unit at 193.4 ppm are the evidence for the formation of the product **41** (Figure A33). The mass spectroscopy of the compound **41** is shown below (Figure 14). Although the molecular peak was not observed in the spectrum, two fragmented mass, 258.1 and 215.0 were observed in the spectrum

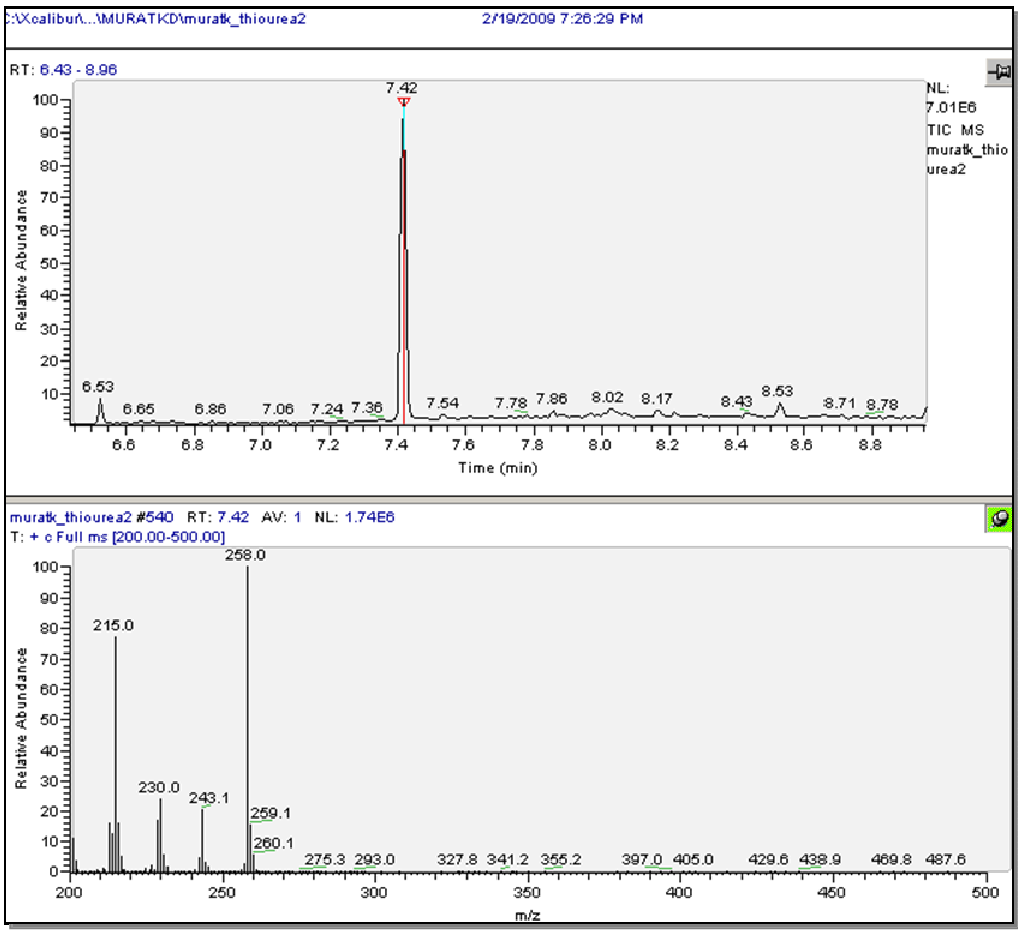

Figure 14. GC-MS spectrum of compound **41**

2.6. Application of chiral organocatalyst in asymmetric reactions

2.6.1. Asymmetric allylation reaction of aldehyde

Chiral pyridine-based *N*-oxides have emerged in the last few years as powerful Lewis basic catalysts for asymmetric allylation transformations with good to excellent enantioselectivities and with catalyst loading that is unusually low in the organocatalyst realm [72]. Consequently, catalytic effectiveness of the synthesized nucleophilic and Lewis base type organocatalysts **29**, **32** and **33** (Figure 15) were tested in the asymmetric allylation reaction of aldehydes.

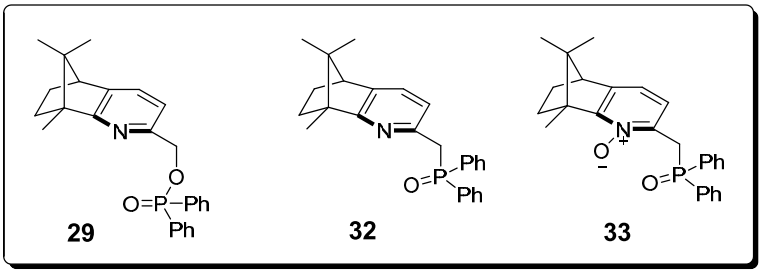

Figure 15. Nucleophilic organocatalysts **29**, **32** and **33**

p-Nitrobenzaldehyde and allyltrichlorosilane were chosen as a model substrate and as an allylating reagent, respectively. It is important to use stochiometric amount of DIPEA (Scheme 35)

.

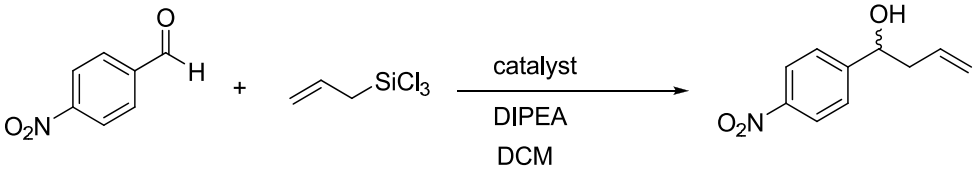

Scheme 34. Asymmetric allylation of 4-nitrobenzaldehyde

In these conditions, all three catalysts were tested and the results are summarized in Table 1. All allylation reactions was carried out at room temperature and obtained yields were very low. The product was synthesized almost as a racemic mixture.

Table 1. Results of asymmetric allylation reaction

Entry	Catalyst	Yield(%)[a]	Ee(%)[b]
1	**29**	14	0
2	**32**	24	1
3	**33**	30	1

[a] Isolated yields were calculated after column chromatography.

[b] Enantiomeric ratios were determined by HPLC.

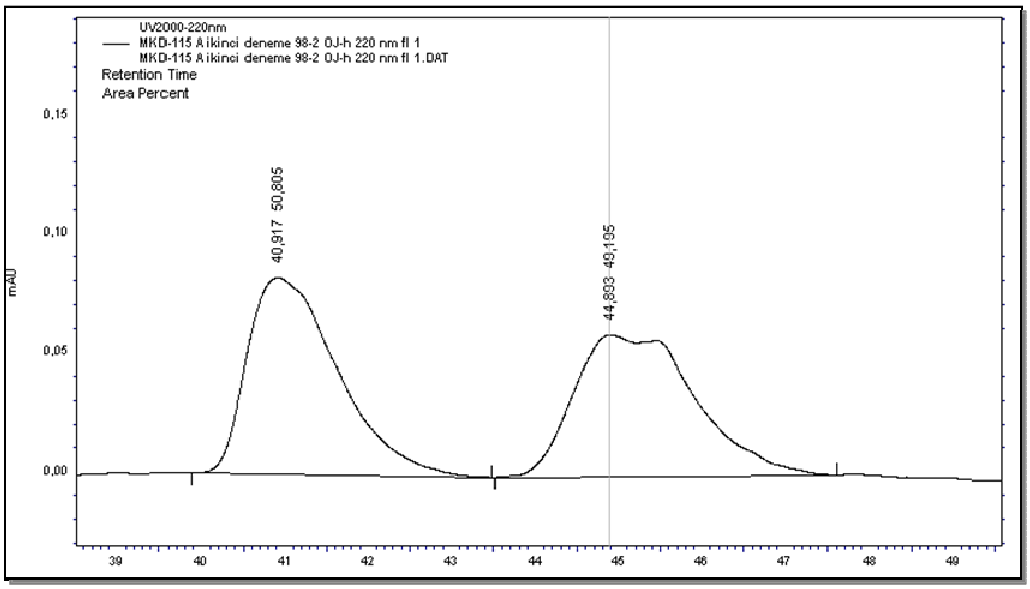

Figure 16. HPLC chromatogram of allylated product using catalyst **33**

The general proposed transition state of catalysts is shown in Figure 17. Since *P*-oxide coordinates to silicon atom from one side, for catalysts **29** and **32** transition "A" can be proposed for this asymmetric transformation.

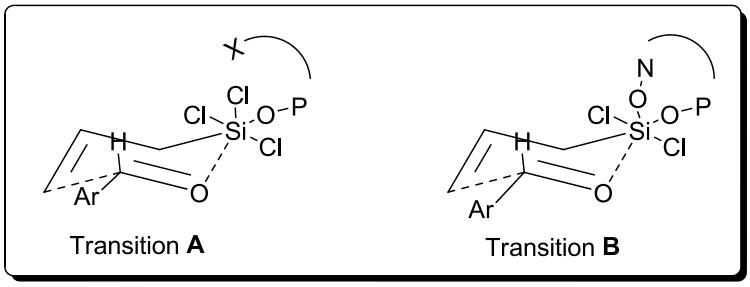

Figure 17. Proposed transition states of allylation reaction

Different from the proposed transition state for catalysts **29** and **32**, catalyst *P,N*-dioxide **33** binds to silicon using two sides of molecule that is shown as transition "B" in Figure 17.

2.6.2. Enantioselective aldol reaction

Proline-derived organocatalysts have been tested in many asymmetric reactions. More detailed information about this subject is given in the introduction part. Direct aldol reaction was chosen for testing catalytic effecttiveness of compound **38** and **40** (Figure 18). As mentioned before, these two catalysts are diastereomer of each other and the purpose of synthesizing both diastereomer was to discuss the matching or mismatching properties of proline and camphor unit.

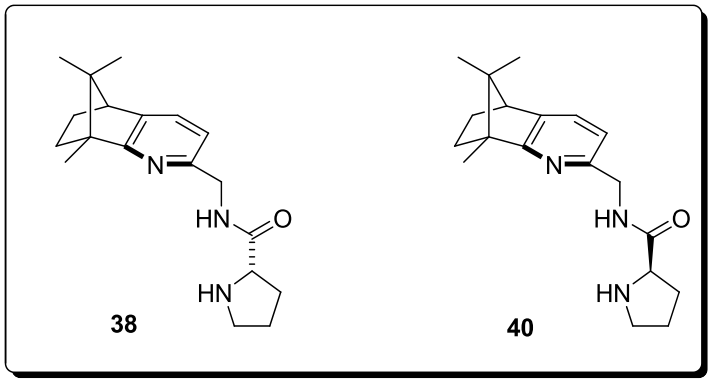

Figure 18. Proline amide catalysts **38** and **40**

As a substrate, 4-nitrobenzaldehyde was chosen. Water and acetic acid were used as solvent and additive, respectively. General reaction is shown below (Scheme 36).

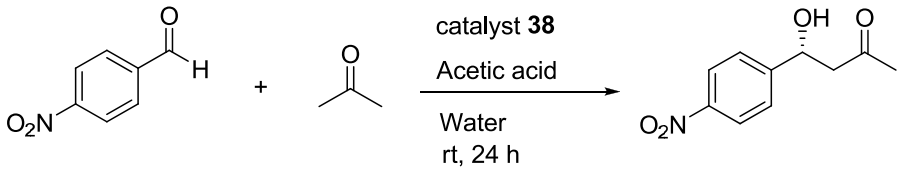

Scheme 35. Asymmetric aldol reaction using catalyst **38**

Firstly, catalyst **38** was tested because *L*-proline used in the synthesis of catalyst is cheaper than the other enantiomer. After giving this decision, five different conditions were applied for the first screening of the reaction conditions (Table 2).

Table 2. Results of asymmetric aldol reaction using *L*-proline amide, **38**

Entry	Cat. (mol%)	Solvent	HAc (mol%)	Yield (%)[a]	Enantiomeric excess (%)[b]
1	10%	-	-	10	24
2	10%	-	10%	60	12
3	10%	Water	-	30	25
4	10%	Water	10%	86	30
5	5%	Water	5%	50	33

[a] Isolated yields were calculated after column chromatography.

[b] Enantiomeric ratios were determined by HPLC analysis using a chiral column. The major product has *R* configuration.

L-proline amide **38** was tested 10 mol% loading without any additive to observe a catalytic activity of **38**. Since acetone also acts as solvent, no need to use another solvent. The isolated yield was 10% and the enantiomeric excess was observed as 24% (Entry 1). Acetic acid addition increases the reaction rate and the chemical yield but the e.e. value decreased to 12% (Entry 2). After that, aceton-water mixture was chosen as a solvent system without any additive. The yield was 30% and e.e. was 25% (Entry 3). Adding acetic acid and water resulted in quite high yield (86%) and the enantiomeric excess also increased to 30% (Entry 4). In order to observe the effect of catalyst amount, 5 mol% catalyst was used under the same conditions with Entry 4. Suprisingly, decreasing catalyst amount from 10 mol% to 5 mol% increases e.e. value slightly (Entry 5).

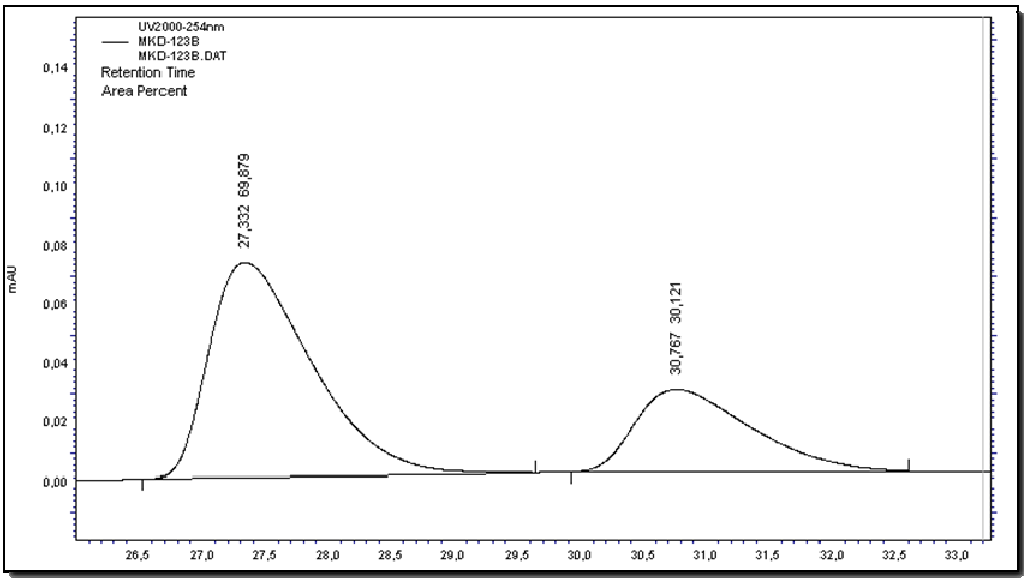

Figure 19. HPLC chromatogram of aldol product using catalyst **38**

After getting first results, acid screening was done to understand acid effect. In all reactions, same conditions were applied with the entry 4 from table 2, except the type of acid. The best result of the experiments was obtained by the use of *p*-toluenesulfonic acid. The yield and ee are 28% and 39% respectively.

Table 3. Effect of acid for aldol reaction

Entry	Acid Additive	Yield (%)[a]	Ee (%)[b]
1	HCl	60	26
2	TFA	6	22
3	PTSA	24	0
4	*p*-toluenesulfonic acid	28	39

[a] Isolated yields were calculated after column chromatography.

[b] Enantiomeric ratios were determined by HPLC analysis using a chiral column. The major product has *R* configuration.

From Table 2 and Table 3, acetic acid is the appropriate additive, although *p*-toluenesulfonic acid gave the highest ee, but low yield. The next step was decreasing temperature in order to increase selectivity. When the reaction was done at 0^{o}C, the selectivity increased from 30% to 40% (Table 4).

Table 4. Effect of temperature for aldol reaction[a]

Entry	Temp.(^{o}C)	HAc (mol%)	Yield (%)[b]	Ee (%)[c]
1	25	10	86	30
2	0	10	85	40
3	0	20	94	40

[a] The reaction was carried out using 10 mol% catalyst **38**.

[b] Isolated yields were calculated after column chromatography.

[c] Enantiomeric ratios were determined by HPLC analysis using a chiral column. The major product has *R* configuration.

CHAPTER 3

CONCLUSION

In conclusion, starting from easily available natural (+)-camphor, six organocatalysts containing camphor based chiral pyridine were successfully synthesized. These organocatalysts can be classified into three different groups. **29**, **32**, and **33** are nucleophilic and Lewis base type catalysts, **38** and **40** are enamine type catalysts, **41** is the hydrogen bonding type catalyst. Nucleophilic and Lewis base type organocatalysts were tested in allylation of aldehydes via allyltrichlorosilane. The selectivity for this type of reaction is very low. *L*-proline amide **38** and *D*-proline amide **40** were also tested in direct aldol reaction between acetone and *p*-nitrobenzaldehyde in aqueous medium. The yields were quite high and the enantioselectivities were obtained up to 40%.

As a furher work, conditions of allylation reaction will be optimized in order to get better results. Up to now, we have just applied once for each catalyst. Catalysts **29**, **32**, and **33** will also be tested in other asymmetric transformation reactions. Higher ee values for aldol reaction will be obtained by further screening of temperature, and substrates. Since we did not test thiourea type organocatalyst **41**, we cannot make any comment about its catalytic activity. However, according to literature, it is known that thiourea type organocatalysts can give good selectivity in aza-Henry, nitro-Michael reactions, etc.

CHAPTER 4

EXPERIMENTAL

Following instruments and materials were used for the purification and characterization of products during the study.

NMR spectra were recorded on a Bruker DPX 400 spectrometer. Chemical shifts are expressed in ppm. downfield from tetramethylsilane, which is used as internal standard; the ^{1}H-NMR data are presented in the order value of the signal, peak multiplicity (abbreviations are as follows: s, singlet; d, doublet; t, triplet; q, quartet; m, multiplet; br, broad) and coupling constants in Hertz integrated number of protons.^{13}C-NMR spectra were measured at 100 MHz and the chemical shifts were reported relative to $CDCl_3$ triplet centered at 77.0 ppm.

Optical rotations were measured in a 1 dm cell using a Rudolph Research Analytical Autopol III, automatic polarimeter at specified temperatures.

HPLC measurements were performed with ThermoFinnigan Spectra System instrument. Separations were carried out on Chiralcel OJ-H analytical column (250 x 4.60 mm) with hexane/2-propyl alcohol as eluent.

Flash column chromatography was employed using thick-walled glass columns with a flash grade silicagel (Merck Silica Gel 60, particle size: 0.040-0.063 mm, 230-400 mesh ASTM). Reactions were monitored by thin layer chromatography using pre-coated silica gel plates (Merck Silica Gel PF-254), visualized with UV-light, polymolybden phosphoric acid in methanol, ninhydrin and anisaldehyde. The relative portions of solvents are in volume:volume ratio used in column chromatography as eluent.

4.1. Synthesis of (+)-*β*-hydroxymethylenecamphor, 21

To a stirred solution of KH (5 g, 125 mmol) in 300 mL of freshly distilled THF, (+)-camphor (15 g, 100 mmol) was added and the mixture is stirred in reflux. After an hour, the mixture was cooled down to 0°C in an icebath. The THF solution (50 mL) of ethyl formate (10 mL, 130mmol) was added dropwise within 30 minutes and the following mixture was allowed stirring for ten h at room temperature. At the work-up stage, 50 mL of water was added dropwise to the mixture and the aqueous layer was washed with ether to remove unreacted camphor. Combined aqueous layer was acidified using 6 M HCl until pH reaches to 3-4. Acidic solution was extracted with ether (2x100 mL). Finally combined organic phase was dried over $MgSO_4$, and evaporated in *vacuo* to yield (+)-*β*-hydroxymethylenecamphor **21** in 96% yield as a pale yellow solid.

4.2. Synthesis of (*Z*)-4-aminopent-3-en-2-one (Fluoral-P), 22

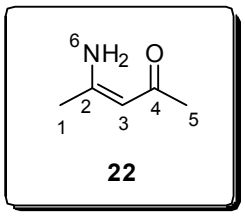

22

When 250 mL of concentrated ammonium hydroxide was added to 0.5 moles of acetylacetone (51 mL), a solid immediately formed in a mildly exothermic reaction. The reaction mixture was allowed to stand for 2 days and then dissolved in chloroform and washed twice with water. The chloroform was dried over $MgSO_4$, filtered, and evaporated in *vacuo* to afford a yellow oily solid. The crude product was purified by flash column chromatography on silica gel using mixtures of EtOAc and hexane as eluent at ratio of 1:1. This is a pale yellow solid **22** (34.6 g, 70% yield). Mp: 37-43 °C, lit. [73] 38°C; ^{1}H-NMR: δ 1.83 (s, 3H, H_5), 1.94 (s, 3H, H_1), 4.94 (s, 1H, H_3), 5.35 (br, 1H, H_6), 9.61 (br, 1H, H_6'); ^{13}C-NMR: δ 22.1 (C_1), 29.1 (C_5), 95.6 (C_3), 161.3 (C_2), 196.5 (C_4).

4.3. Synthesis of camphor fused pyridine, (+)-23

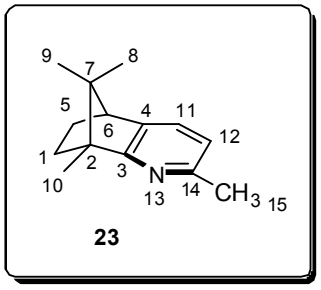

23

To a mixture of (+)-β-hydroxymethylenecamphor (8 g, 44 mmole) and enamine **22** (13.3 g, 134 mmole) in a sealed tube ammonium acetate (400 mg, 5.1 mmole) was added and the tube was sealed. Then it was heated for 20 h in a sand bath at 170 °C. The tube was opened and the crude material was chromotographed on silica gel using ethyl acetate/hexane (1:5) as eluent. The yellow oily product **23** was obtained 55% yield. $[\alpha]^{20}_{D}$ = +25.4 (*c*, 2.0, cyclohexane); ^{1}H-NMR: δ 0.47 (s, 3H, H_8), 0.90 (s, 3H, H_9), 0.99-1.05 (m, 1H, H_1-*endo*), 1.08-1.16 (m, 1H, H_5-*endo*), 1.24 (s, 3H, H_{10}), 1.73-1.79 (m, 1H, H_1-*exo*), 1.97-2.04 (m, 1H, H_5-*exo*), 2.44 (s, 3H, H_{15}), 2.71 (d, *J*=4.0 Hz, 1H, H_6), 6.73 (d, *J*=7.4 Hz, 1H, H_{12}), 7.14 (d, *J*=7.4 Hz, 1H, H_{11}); ^{13}C-NMR: δ 10.8 (C_{10}), 19.6 (C_9), 20.3 (C_8), 24.8 (C_{15}), 26.6 (C_5), 32.1(C_1), 51.6 (C_6), 54.4 (C_7), 57.1 (C_2), 119.9 (C_{12}), 128.6 (C_{11}), 138.3 (C_4), 154.4 (C_{14}), 170.2 (C_3); HRMS calc. for $C_{14}H_{20}N$ $[M+H]^+$: 202.1596, found $[M+H]^+$: 202.1607.

4.4. Synthesis of *N*-oxide, 26

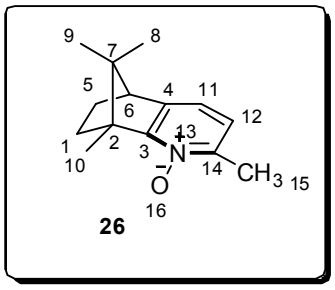

26

To a solution of camphor fused pyridine **23** (2.40 g, 12.0 mmol) in 100 mL CH_2Cl_2, MCPBA with a purity of 70% (5.80 g, 23.5 mmol) was added at room temperature. The mixture was stirred at same temperature about 4 h. When the reaction completed, saturated Na_2CO_3 solution was added until pH was 8-9. Then, the aqueous phase was extracted with CH_2Cl_2 (3 x 50 mL). Organic phase was dried over anhydrous $MgSO_4$ and evaporated. Impurities were removed by a short column filled with silica gel and eluting with $CHCl_3$:MeOH:NH_3 (95:4:1) and 2.59 g N-oxide **24** was isolated in quantitative yield as a yellow liquid. $[\alpha]^{24}_{D}$ = -30.22 (*c*, 2.0, CH_2Cl_2); ^{1}H-NMR: δ 0.62 (s, 3H, H_8), 0.85 (s, 3H, H_9), 1.01-1.04 (m,

1H, H_1-*endo*), 1.40-1.46 (m, 1H, H_5-*endo*), 1.58 (s, 3H, H_{10}), 1.74-1.80 (m, 1H, H_1-*exo*), 1.98-2.05 (m, 1H, H_5-*exo*), 2.37 (s, 3H, H_{15}), 2.73 (d, *J*=4.0 Hz, 1H, H_6), 6.84 (d, *J*=7.2 Hz, 1H, H_{11}), 6.89 (d, *J*=7.2 Hz, 1H, H_{12}); ^{13}C-NMR: δ 12.3 (C_{10}), 17.3 (C_{15}), 18.5 (C_8), 20.0 (C_8), 26.0 (C_5), 31.0 (C_1), 51.4 (C_6), 55.0 (C_7), 57.0(C_2), 118.8 (C_{12}), 123.0 (C_{11}), 143.5 (C_4), 146.7 (C_{14}), 153.8 (C_3).

4.5. Synthesis of pyridinyl alcohol, 27

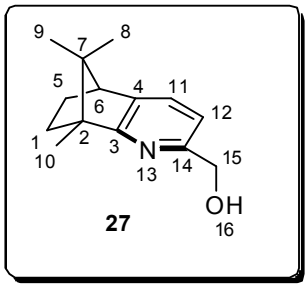

To a solution of N-oxide **24** (1.98 g, 9.1 mmol) in 10 mL toluene 100 mL two-necked reaction flask, 10 mL acetic acid was added. The reaction mixture was refluxed for 2 h. Monitored by TLC, after all starting material was consumed, the reaction was quenched with 40 mL ice-water and concentrated NaOH was added in small portions in a water-ice bath until pH was 9-10. The crude acetylated product was dissolved in 30 mL methanol and refluxed for 75 minutes. Hydrolysis of acetylated product was monitored by TLC in EtOAc/Hexane (1:1). After reaction completed, the mixture was extracted with Et_2O (3 x 75 mL). Solvent was dried over $MgSO_4$ and then concentrated under reduced pressure. The residue was purified by silica gel chromatography in a column (silica gel; EtOAc:Hexanes, 1:1). After removing the solvent, the alcohol product **7** was isolated in 92% yield as a white solid. $[\alpha]^{24}_D$ = +23.16 (*c*, 1.0, CH_2Cl_2); mp: 94-97^{o}C; ^{1}H-NMR: δ 0.53 (s, 3H, H_8), 0.98 (s, 3H, H_9), 1.06-1.18 (m, 2H, H_1-*endo* and H_5-endo), 1.30 (s, 3H, H_{10}), 1.82-1.88 (m, 1H, H_1-exo), 2.07-2.13 (m, 1H, H_5-*exo*), 2.83 (d, *J*= 3.6 Hz, 1H, H_6), 4.51 (br, 1H, H_{16}), 4.70 (d, *J*= 4.4 Hz, 2H, H_{15}), 6.92 (d, *J*=7.2 Hz, 1H, H_{12}), 7.32 (d, *J*=7.2 Hz, 1H, H_{11}); ^{13}C-NMR: δ 10.3 (C_{10}), 19.2 (C_9), 20.0 (C_8), 26.1 (C_5), 31.6 (C_1), 51.3 (C_6), 54.1 (C_7), 57.0 (C_2), 64.3 (C_{15}), 117.4 (C_{12}), 128.5 (C_{11}), 139.7 (C_4), 155.1 (C_{14}), 169.3 (C_3); HRMS calc. for $C_{14}H_{19}NO$ $[M+H]^+$: 218.1545,found $[M+H]^+$: 218.1537.

4.6. Synthesis of phosphinate, 29

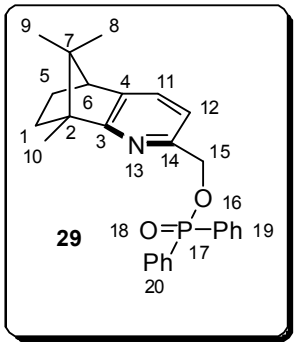

To a solution of camphor fused pyridin-2-yl methanol **27** (200 mg, 0.92 mmol) in THF containing three equivalent of triethylamine (0.36 mL, 3.76 mmol) was added 0.19 mL of PPh_2Cl (224 mg, 1,01 mmol) at -78 °C. The solution was stirred for 2 h from -78 °C to room temperature, and stirred additional 12 h to oxidize by air. All volatiles were removed under reduced pressure. The residue was dissolved in diethyl ether to precipitate triethylammonium chloride. After filtration, the solvents were removed under reduced pressure and compound **29** was isolated as a pale yellow oil. Yield: 367 mg, 88%. $[\alpha]^{31}_{D}$ =+5.53 (*c*, 4.0, $CHCl_3$); ^{1}H-NMR: δ 0.44 (s, 3H, H_8), 0.90 (s, 3H, H_9), 0.98-1.13 (m, 2H, H_1-*endo* and H_5-endo), 1,20 (s, 3H, H_{10}), 1.73-1.80 (m, 1H, H_1-*exo*), 1.98-2.02 (m, 1H, H_5-*exo*), 2.74 (d, J_{HH}=4 Hz, 1H, H_6), 5.05 (d, J_{PH}=8.0 Hz, 2H, H_{15}), 7.10 (d, J_{HH}=7.2 Hz, 1H, H_{12}), 7.24 (d, J_{HH}=7.2 Hz, 1H, H_{11}), 7.32-7.44 (m, 6H, H_{19}'s and H_{20}'s), 7.76-7.82 (m, 4H, H_{19}'s and H_{20}'s); ^{13}C-NMR: δ 10.3 (C_{10}), 19.2 (C_9), 20.0 (C_8), 26.0 (C_5), 31.6 (C_1), 51.3 (C_1), 54.0 (C_6), 56.8 (C_7), 64.3 (C_2), 67.4 (d, J_{PC}=6.0 Hz, C_{15}), 118.7 (C_{12}), 128.3 (C_{Ph}), 128.4 (C_{Ph}), 128.5 (C_{Ph}), 130.9 (C_{Ph}), 131.8 (2C, C_{Ph}), 131.9(2C, C_{Ph}), 132.0 (C_{Ph}), 132.3 (C_{Ph}), 140.3 (C_{11}), 152.0 (C_4), 152.1 (C_{14}), 169.9(C_3).

4.7. Synthesis of tosylate, 30

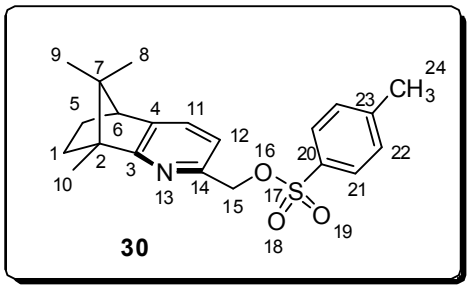

To a solution of camphor fused pyridin-2-yl methanol **27** (1.14 g, 5.25 mmol) in THF (25 mL) was added KOH (470 mg, 8.4 mmol) followed by *p*-toluenesulfonyl chloride (1.3 g, 6.83 mmol) at 0^{o}C. The reaction mixture was allowed to warm to room temperature with stirring. After stirred for 12 h at room temperature, the

reaction was filtered through Celite, and the solvent was removed *in vacuo*. The residue was purified by chromatography (silica gel, ethyl acetate: hexane (1:3)) to afford 1.95 g of tosylate **30** (70% yield) as a white solid. mp: 44-47°C; $[\alpha]^{24}_{D}$ = +15.4 (*c*, 1.0, CH_2Cl_2); ^{1}H-NMR: δ 0.39 (s, 3H, H_8), 0.88 (s, 3H, H_9), 0.93-1.05 (m, 2H, H_1-*endo* and H_5-endo), 1.14 (s, 3H, H_{10}), 1.71-1.77 (m, 1H, H_1-*exo*), 1.97-2.03 (m, 1H, H_5-*exo*), 2.34 (s, 3H, H_{24}), 2.72 (d, *J*= 4.0 Hz, 1H, H_6), 5.02 (s, 2H, H_{15}), 6.96 (d, *J*=7.6 Hz, 1H, H_{12}), 7.21 (m, 3H, H_{11}, H_{22} and $H_{22'}$), 7.72 (d, *J*=8.0 Hz, 2H, H_{21} and $H_{21'}$); ^{13}C-NMR: δ 9.2 (C_{10}), 18.1 (C_{24}), 18.8 (C_9), 20.6 (C_8), 24.9 (C_5), 30.4 (C_1), 50.2 (C_6), 53.0 (C_7), 55.8 (C_2), 71.6 (C_{15}), 118.2 (C_{12}), 127.0 ($2C_{21}$),127.2 (C_{11}), 128.6 ($2C_{22}$), 132.4 (C_{23}), 139.9 (C_4), 143.4 (C_{24}), 148.2 (C_{14}), 169.1 (C_3).

4.8. Synthesis of *P*-oxide, 32

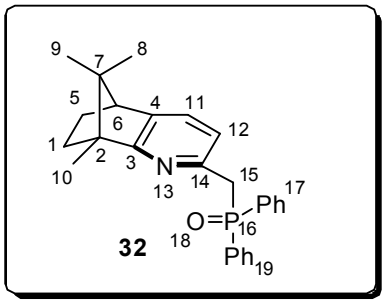

32

A solution of potassium diphenylphosphide in 0.5 M THF (12 mL, 6 mmol) was added to a solution of tosylate **30** (1.35 g, 3.63 mmol) in 25 mL THF at 0°C. It was allowed to warm and stirred twelve h at room temperature. The reaction mixture was filtered through celite and washed with toluene.A filtrate was evaporated and purified by column chromatograpy on silica gel, (EtOAc:Hexane: 6:1) to afford product **32** as a yellow oil in 65% yield. ^{1}H-NMR: δ 0.00 (s, 3H, H_8), 0.56 (s, 3H, H_9), 0.63-0.64 (m, 2H, H_1-*endo* and H_5-endo), 0.78 (s, 3H, H_{10}), 1.37-1.42 (m, 1H, H_1-*exo*), 1.64-1.69 (m, 1H, H_5-*exo*), 2.37 (d, J_{HH} = 3.6 Hz, 1H, H_6), 3.51 (d, J_{PH} = 12.0 Hz, 1H, H_{15}), 3.58 (d, J_{PH} = 14.0 Hz, 1H, $H_{15'}$), 6.74 (d, J_{HH} = 8.0 Hz, 1H, H_{12}), 6.84 (d, J_{HH} = 8.0 Hz, 1H, H_{11}), 6.95-7.15 (m, 6H, H_{Ph}), 7.31-7.51 (m, 4H, H_{Ph}); ^{13}C-NMR: δ 10.1 (C_{10}), 19.0 (C_9), 19.7 (C_8), 25.8 (d, J_{PC} = 0.9 Hz, C_5), 31.2 (C_1), 40.3 (d, J_{PC} = 65.0 Hz, C_{15}), 50.9 (C_7), 53.7 (C_2), 56.5 (C_6), 121.5 (d, J_{PC} = 5.0 Hz, C_{12}), 127.8 (C_{Ph}), 127.9 (C_{Ph}), 128.0 (C_{Ph}), 128.2 (C_{Ph}), 128.6 (d, J_{PC} = 10.0 Hz, C_{Ph}), 130.4 (d, J_{PC} = 12.0

Hz, C_{Ph}), 131.0 (C_{Ph}), 131.2 (d, J_{PC} = 4.0 Hz, C_{Ph}), 132.3 (C_{11}), 138.6 (d, J_{PC} = 2.0 Hz, C_4), 147.4 (d, J_{PC} = 8.0 Hz, C_{14}), 169.3 (C_3).

4.9. Synthesis of *P,N*-dioxide, 33

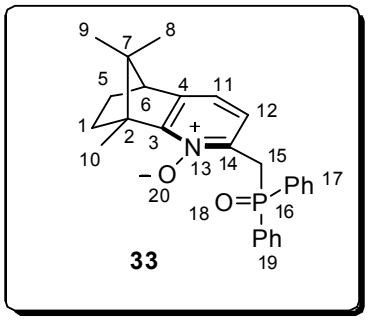

33

To a solution of *P*-oxide **32** (200 mg, 0.5 mmol) in 25 mL CH_2Cl_2, MCPBA with 70% purity (148 mg, 0.6 mmol) was added. The reaction mixture was stirred at room temperature. After reaction completed, it was quenched with saturated Na_2CO_3 until pH was reached 9-10, and extracted with DCM (2x25 mL). Organic phase was dried over $MgSO_4$, filtrated and concentrated *in vacuo*. Crude product was purified with flash chromatography to obtain a yellow oil substance, **33** (87% yield). $[\alpha]^{31}_D$ = -39.76(*c*, 1.0, $CHCl_3$); ^{1}H-NMR: δ 0.39 (s, 3H, H_8), 0.81 (s, 3H, H_9), 0.87-0.94 (m, 1H, H_1-*endo*), 1.18-1.24 (m, 1H, H_5-*endo*), 1.45 (s, 3H, H_{10}), 1.68-1.74 (m, 1H, H_1-*exo*), 1.93-2.00 (m, 1H, H_5-*exo*), 2.66 (d, J_{HH} = 3.6 Hz, 1H, H_6), 4.05 (m, 1H, H_{15}), 4.35 (m, 1H, $H_{15'}$), 6.85 (d, J_{HH} = 7.6 Hz, 1H, H_{12}), 7.28-7.45 (m, 7H, H_{11} and H_{Ph}), 7.78-7.83 (m, 4H, H_{Ph}); ^{13}C-NMR: δ 12.3 (C_{10}), 18.5 (C_9), 20.0 (C_8), 25.6 (C_3), 31.1(d, J_{PC} = 66.0 Hz, C_{15}), 51.4 (C_7), 55.1 (C_2), 57.0 (C_6), 119.3 (C_{12}), 124.4 (C_{11}), 127.8 (C_{Ph}), 128.0 (C_{Ph}), 128.1 (C_{Ph}), 128.3 (C_{Ph}), 129.5 (d, J_{PC} = 50.0 Hz, C_{Ph}), 130.8 (C_{Ph}), 130.9 (C_{Ph}), 131.0 (C_{Ph}), 131.7 (C_{Ph}), 141.7 (d, J_{PC} = 6.5 Hz, C_{14}), 144.4 (C_4), 153.9 (C_3).

4.10. Synthesis of azide, 34

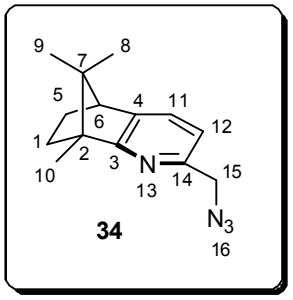

34

To a 50 mL-flask 1.69 g of tosylate **30** (4.52 mmol)was added and it was dissolved in 15 mL dried DMSO in argon atmosphere. Sodium azide (0.5 g, 7.70 mmol) was added at room temperature. The reaction mixture was heated to 70°C and stirred at this temperature about 12 h. 15 mL of water was added and the mixture was extracted with ether (2x50 mL). Combined organic phase was dried over $MgSO_4$, filtrated and concentrated *in vacuo*. The crude product was purified by column chromatography using silica gel (EtOAc:Hexane, 1:3) to afford compound **34** as a colorless oil (1.03 g, 94% yield). $[\alpha]^{25}_D$ = +6.08 (*c*, 1.11, CH_2Cl_2); ^{1}H-NMR: δ 0.54 (s, 3H, H_8), 1.00 (s, 3H, H_9), 1.11-1.21 (m, 2H, H_1-*endo* and H_5-endo), 1.31 (s, 3H, H_{10}), 1.83-1.89 (m, 1H, H_1-*exo*), 2.08-2.16 (m, 1H, H_5-*exo*), 2.84 (d, J = 3.6 Hz, 1H, H_6), 4.40 (s, 2H, H_{15}), 6.98 (d, J = 7.6 Hz, 1H, H_{12}), 7.34 (d, J = 7.2 Hz, 1H, H_{11}); ^{13}C-NMR: δ 10.3 (C_{10}), 19.2 (C_9), 20.0 (C_8), 26.0 (C_5), 31.5 (C_1), 51.3 (C_{15}), 54.1 (C_7), 55.7 (C_2), 56.9 (C_6), 118.9 (C_{12}), 128.4 (C_{11}), 140.4 (C_4), 151.5 (C_{14}), 170.6 (C_3).

4.11. Synthesis of 2-(aminomethylene) pyridine, 35

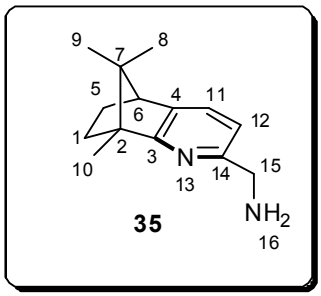

35

To a solution of azide **34** (300 mg, 1.24 mmol) in 20 mL THF, triphenyl phosphine dissolved in 2 mL water was added. The mixture was stirred overnight at room temperature. The reaction mixture was treated with 2 N HCl (5 mL) and washed with ether (3x10 mL). Aqueous phase was neutralized with 3 N NaOH solution and then extracted with DCM (3x20 mL). The organic phase was dried over $MgSO_4$, filtrated, concentrated under reduced pressure to afford amine **35** as a yellow oil (270 mg, 100% yield). $[\alpha]^{25}_D$ = +10.4 (*c*, 1.0, CH_2Cl_2); ^{1}H-NMR: δ 0.46 (s, 3H, H_8), 0.91 (s, 3H, H_9), 1.00-1.15 (m, 2H, H_1-*endo* and H_5-endo), 1.23 (s, 3H,

H_{10}), 1.73-1.84 (m, 3H, H_1-*exo* and H_{16}), 1.98-2.08 (m, 1H, H_5-*exo*), 2.73 (d, J = 3.6 Hz, 1H, H_6), 3.82 (s, 2H, H_{15}), 6.83 (d, J_{HH} = 7.2 Hz, 1H, H_{12}), 7.20 (d, J_{HH} = 7.2 Hz, 1H, H_{11}); ^{13}C-NMR: δ 10.4 (C_{10}), 19.2 (C_9), 20.0 (C_8), 26.1 (C_5), 31.7 (C_1), 47.8 (C_{15}), 51.2 (C_7), 54.0 (C_2), 56.7 (C_6), 117.6 (C_{12}), 128.1 (C_{11}), 139.0 (C_4), 157.8 (C_{14}), 169.8 (C_3).

4.12. Synthesis of (*S*)-1-(tert-butoxycarbonyl)pyrrolidine-2-carboxylic acid, 36

Triethylamine (8.3 mL, 0.6 mol) was added to an ice-cold suspension of (S)-proline (5.0 g, 0.045mol) in 100 mL of DCM. Next, di-tert-butyl dicarbonate (13.1 g, 0.065 mol) in DCM (10 mL) was added over 10 minutes, and the mixture was stirred at 0^{o}C for 2.5 h. The reaction was discontinued by addition of saturated citric acid (25 mL), and the organic phase was washed with brine (2x25 mL) and water (50 mL). Removal of solvent *in vacuo* yielded crude product which was dissolved in hot EtOAc. Following addition of hexane (200 mL) compound **36** was crystallized from the cooled solution to yield 8.6 g, 92%. Mp: 134^{o}C (lit.mp 134-136^{o}C).

4.13. Synthesis of *L*-proline amide, 38

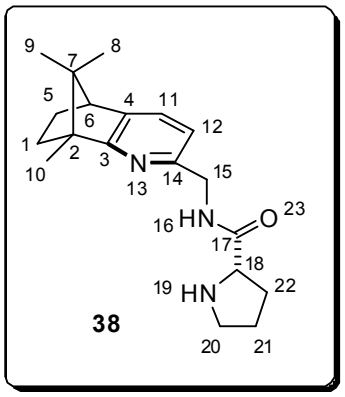

38

N-Boc-(S)-proline (360 mg, 1.7 mmol) and DCC (345 mg, 1.7 mmol) were dissolved in dry DCM (10 mL). The mixture was stirred at 0^{o}C for 30 minutes, and then amine **35** (300 mg, 1.4 mmol) dissolved in DCM (5 mL) was added dropwise at same temperature. It was stirred additional 2 h at room temperature. The resulting white suspension was filtered. The filtrate was washed with saturated $NaHCO_3$, concentrated under reduced pressure to afford *N*-Boc-protected-*L*-prolineamide **36** (474 mg, 82%). Without further purification of **36**, the crude

product was dissolved in DCM (5 mL). TFA (5 mL) was added at room temperature and stirred for 2 h. The solution was basified to pH 10 with 2 M KOH solution and extracted with chloroform (3x30 mL). Organic phases were combined, washed with brine and concentrated under reduced pressure to afford *L*-proline amide **38** as a white foaming solid (350 mg, 98% yield). $[\alpha]^{31}_{D}$ =-50.30 (*c*, 2.0, $CHCl_3$); ^{1}H-NMR: δ 0.47 (s, 3H, H_8), 0.93 (s, 3H, H_9), 1.00-1.13 (m, 2H, H_1-*endo* and H_5-endo), 1.23 (s, 3H, H_{10}), 1.60-1.72 (m, 2H, H_{21}), 1.75-1.81 (m, 1H, H_1-*exo*), 1.86-1.94 (m, 1H, H_5-*exo*), 2.00-2.12 (m, 2H, H_{22}), 2.25 (br, 1H, H_{19}), 2.74 (d, J = 3.6 Hz, 1H, H_6), 2.88-2.99 (m, 2H, H_{20}), 3.72 (dd, J = 4.8 Hz, J = 8.8 Hz, 1H, H_{18}), 4.42 (m, 2H, H_{15}), 6.82 (d, J = 7.2 Hz, 1H, H_{12}), 7.21 (d, J = 7.2 Hz, 1H, H_{11}), 8.35 (br, 1H, H_{16}); ^{13}C-NMR: δ 10.3 (C_{10}), 19.3 (C_9), 20.0 (C_8), 26.1 (C_5), 26.2 (C_{21}), 30.8 (C_{22}), 31.7 (C_1), 44.1 (C_{20}), 47.3 (C_{15}), 51.3 (C_7), 54.0 (C_2), 56.9 (C_6), 60.7 (C_{18}), 118.3 (C_{12}), 128.4 (C_{11}), 139.4 (C_4), 153.1 (C_{14}), 169.7 (C_3), 174.9 (C_{17}).

4.14. Synthesis of *D*-proline amide, 40

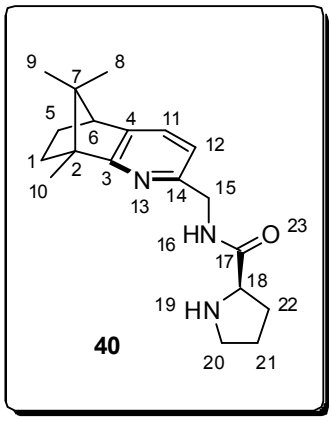

40

N-Boc-(*R*)-proline (180 mg, 0.85 mmol) and DCC (173 mg, 0.85 mmol) were dissolved in dry DCM (5 mL). The mixture was stirred at 0^{o}C for 30 minutes, and then amine **35** (150 mg, 0.70 mmol) dissolved in DCM (5 mL) was added dropwise at same temperature. It was stirred additional 2 h at room temperature. The resulting white suspension was filtered. The filtrate was washed with saturated $NaHCO_3$, concentrated under reduced pressure to afford *N*-Boc-protected-*D*-proline amide **39** (252 mg, 87%). The crude product was dissolved in DCM (5 mL). TFA (3 mL) was added at room temperature and stirred for 2 h. The solution was basified to pH 10 with 2 M KOH solution and extracted with chloroform (3x30 mL). Organic phases were combined, washed with brine and concentrated under reduced pressure to afford *D*-proline amide **40** as a white solid (172 mg, 90% yield). $[\alpha]^{31}_{D}$ =+17.0 (*c*, 2.0, $CHCl_3$); ^{1}H-NMR: δ 0.46 (s, 3H,

H_8), 0.92 (s, 3H, H_9), 1.00-1.15 (m, 2H, H_1-*endo* and H_5-endo), 1.23 (s, 3H, H_{10}), 1.59-1.72 (m, 2H, H_{21}), 1.72-1.82 (m, 1H, H_1-*exo*), 1.86-1.94 (m, 1H, H_5-*exo*), 2.00-2.10 (m, 2H, H_{22}), 2.16 (br, 1H, H_{19}), 2.74 (d, J = 4.0 Hz, 1H, H_6), 2.86-2.99 (m, 2H, H_{20}), 3.72 (dd, J = 5.2 Hz, J = 9.1Hz, 1H, H_{18}), 4.42 (d, J = 2.6 Hz, 1H, H_{15}), 4.43 (d, J = 2.8 Hz, 1H, $H_{15'}$), 6.83 (d, J = 7.2 Hz, 1H, H_{12}), 7.21 (d, J = 7.2 Hz, 1H, H_{11}), 8.36 (br, 1H, H_{16}); ^{13}C-NMR: δ 10.3 (C_{10}), 19.3 (C_9), 19.9 (C_8), 26.1 (C_5), 26.1 (C_{21}), 30.8 (C_{22}), 31.6 (C_1), 44.2 (C_{20}), 47.3 (C_{15}), 51.3 (C_7), 54.0 (C_2), 56.9 (C_6), 60.7 (C_{18}), 118.4 (C_{12}), 128.4 (C_{11}), 139.4 (C_4), 153.1 (C_{14}), 169.8 (C_3), 174.9 (C_{17}).

4.15. Synthesis of C_2-symmetric thiourea, 41

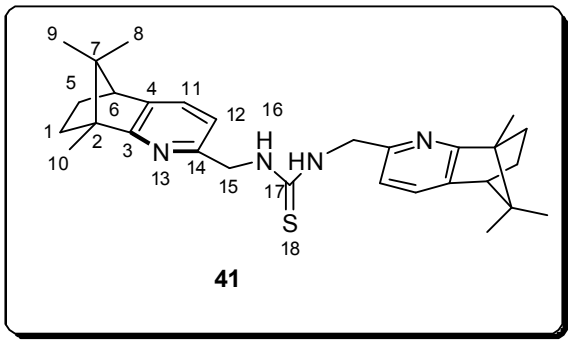

41

To a solution of amine **35** (300 mg, 1.39 mmol) in chloroform (8 mL), DMAP (425 mg, 3.48 mmol), DCC (144 mg, 0.70 mmol) and CS_2 (0.30 mL, 4.87 mmol) were added at -10^{o}C. The mixture was stirred for an hour, then refluxed for 16 h. Solvent was evaporated under reduced pressure. The crude product was purified by column chromatography (EtOAc:Hexane, 1:5) to afford compound **41** as a yellowish oil (200 mg, 30% yield). $[\alpha]^{31}_D$ =+6.90 (*c*, 1.0, $CHCl_3$);^{1}H-NMR: δ 0.46 (s, 3H, H_8), 0.92 (s, 3H, H_9), 1.01-1.14 (m, 2H, H_1-*endo* and H_5-endo), 1.22 (s, 3H, H_{10}), 1.77-1.83 (m, 1H, H_1-*exo*), 2.02-2.09 (m, 1H, H_5-*exo*), 2.78 (d, J= 4.0 Hz, 1H, H_6), 4.73 (s, 2H, H_{15}), 6.99 (d, J=7.2 Hz, 1H, H_{12}), 7.31 (d, J=7.2 Hz, 1H, H_{11}); ^{13}C-NMR: δ 10.3 (C_{10}), 19.2 (C_9), 20.0 (C_8), 26.0 (C_5), 31.6 (C_1), 50.3 (C_{15}), 51.3 (C_7), 54.2 (C_2), 57.0 (C_6), 117.6 (C_{12}), 128.6 (C_{11}), 140.6 (C_4), 149.8 (C_{14}), 170.6 (C_3), 193.4 (C_{17}).

4.16. General procedure for the allylation reaction

Allyltrichlorosilane (100 μL, 0.7 mmol) was added to a solution of the catalyst (10 mol %) in CH_2Cl_2, diisopropylethylamine (85 μL, 0.5 mmol), and *p*-nitrobenzaldehyde (75 mg, 0.5 mmol) under argon at the room temperature. The mixture was then stirred at this temperature until completion (by TLC monitoring) and then quenched with aqueous saturated $NaHCO_3$ (5 mL). The aqueous layer was extracted with CH_2Cl_2 (3x5 mL) and the combined organic layers were washed with brine, dried over MgSO4, and the solvent was removed in *vacuo*. The crude product was purified by flash column chromatography with a EtOAc/Hexanes 1:1 as eluent. HPLC analysis of 1-(4-nitrophenyl)but-3-en-1-ol: Chiralcel OJ-H at room temperature, *n*-hexane/2-propanol = 98:2, 1.0 mL/min, 220 nm, t_R= 41.5 min, t_S= 45.9 min.

4.17. General procedure for the aldol reaction

To a solution of catalyst (0.01 mmol) in water (1.0 mL), the respective acid (0.01 or 0.02 mmol) was added. *p*-Nitrobenzaldehyde (75 mg, 0.5 mmol) and acetone (2.0 mL) were added at room temperature. The reaction was stirred at this temperature for 24 h. The reaction was monitored by TLC and quenched with saturated ammonium chloride solution (5 mL) on completion and extracted with CH_2Cl_2 (2x10 mL). The organic layer was dried over anhydrous $MgSO_4$ and evaporated under reduced pressure to obtain crude product. Column chromatography of the crude on silica gel using mixture of ethyl acetate and hexane 1:2 as eluent, gave pure product. The enantiomeric excess of product was determined on HPLC using a Chiralcel OJ-H column and mixture of *n*-hexane and 2-propanol in ratio of 90:10 as eluents UV 254 nm, flow rate 1.0 mL/min. t_R=26.5min and t_S=29.7 min.

REFERENCES

1. Procter, G., *Asymmetric Synthesis*, Oxford Science Publications, New York, **1996,** 1.

2. Koskinen, A. *Asymmetric Synthesis of Natural Products*, John Wiley & Sons Inc., New York, **1998**, 28.

3. Walshe, J. M. "The story of penicillamine: a difficult birth". *Mov. Disord.* **2003,** *18*, 853.

4. Kruger, A.D. Current aspects of using ketamine in childhood. *Anaesthesiologie und Reanimation.* **1998**; *23*, 64.

5. Blaschke, G.; Kraft, H. P.; Markgraf, H. *Chem. Ber.* **1980**, *113*, 2318.

6. Katzung, B. G. *Basic & Clinical Pharmacology*, Prentice-Hall International Inc., **1995**, chapter 1.

7. Nicolaou, K. C.; Sorensen, E. J. *Classics in Total Synthesis* Wiley-VCH, Weinheim, **1996**, 344.

8. Dalko, P. I.; Moisan, L. "In the Golden Age of Organocatalysis", *Angew. Chem. Int. Ed.* **2004**, *43*, 5138.

9. von Liebig, J. *Ann. der Chem. Pharm.* **1860**, *113*, 246–247.

10. Pracejus, H.;Liebigs, J. *Ann. Chem*. **1960**, *634*, 9.

11. Langstrom, B.; Bergson, G. *Acta Chem. Scand*. **1973**, *27*, 3118.

12. Wynberg, H. *Top. Stereochem*., **1986**, *16*, 87.

13. Hajos, Z. G.; Parrish, D. R. *J. Org. Chem*. **1974**, *39*, 1615.

14. Eder, U.; Sauer, G.; Wiechert, R. *Angew. Chem. Int. Ed. Engl.* **1971**, *10*, 496.

15. Danishefsky, S. J.; Masters, J. J.; Young, W. B.; Link, J. T.; Snyder, L.B.; Magee, T. V.; Jung, D. K.; Isaacs, R. C. A.; Bornmann, W. G.; Alaimo, C. A.; Coburn, C. A.; DiGrandi, M .J. *J. Am. Chem. Soc*. **1996**, *118*, 2843.

16. Iyer, M. S.; Gigstad, K. M.; Namdev, N. D.; Lipton, M. *J. Am. Chem. Soc*. **1996**, *118*, 4910.

17. Dolling, U. H.; Davis, P.; Grabowski, E.J.J. *J. Am. Chem. Soc*. **1987**,*106*, 446.

18. Berkessel, A.; Gröger, H. *Asymmetric Organocatalysis, From Biomimetic Concepts to Applications in Asymmetric Synthesis*. VCH, Weinheim, **2005**, 21.

19. List, B.; Castello, C. *Synlett* **2001**, 1687.

20. Pan, S. C.; List, B. *Ernst Schering Foundation Symposium Proceedings*, **2008**, 1.

21. Gaunt, M. J.; Johansson, C. C.C.; McNally, A.; Vo, N. T. *Drug Discovery Today* **2007**, *12*, 8.

22. Hoang, L.; Bahmanyar, S.; Houk, K. N.; List, B. *J. Am. Chem. Soc*. **2003**, *125*, 16.

23. Merino, P.; Tejero, T. *Angew. Chem. Int. Ed*. **2004**, *43*, 2995.

24. List, B. *J. Am. Chem. Soc*. **2002**, *124*, 5656.

25. Ibrahim, I.; Togni, A. *Chem. Commun*. **2004**, 1147.

26. Marigo, M.; Fielenbach, D.; Braunton, A.; Kjaersgaard, A.; Joergensen, K. A. *Angew. Chem. Int. Ed.* **2005**, *44*, 3703.

27. Ahrendt, K. A.; Borths C. J.; MacMillan, D. W. C. *J. Am. Chem. Soc*., **2000**, *122*, 4243.

28. Kunz, R. K.; MacMillan, D. W. C. *J. Am. Chem. Soc*., **2005**, *127*, 3240.

29. Maringo, M.; Franze´n, J.; Poulsen, T. B.; Zhuang W.; Jørgensen, K. A. *J. Am. Chem. Soc.*, **2005**, *127*, 6964.

30. Prieto, A.; Halland N.; Jørgensen, K. A. *Org. Lett*., **2005**, *7*, 3897.

31. Huang, Y.; Walji, A. M.; Larsen, C. H.; MacMillan, D. W. C. *J. Am. Chem. Soc*., **2005**, *127*, 15051.

32. Lygo, B.; Andrews, B. I. *Acc. Chem. Res*. **2004**, *37*, 518.

33. Helder, R.; Hummelen, J. C.; Laane, R. W. P. M.; Wiering, J. S.; Wynberg, H. *Tetrahedron Lett.* **1976**, *17*, 1831.

34. Lygo, B.; Wainwright, P. G. *Tetrahedron Lett*. **1998**, *39*, 1599.

35. Corey, E. J.; Zhang, F. Y. *Org. Lett*. **1999**, *1*, 1287.

36. Zhang, F. Y.; Corey, E. *J. Org. Lett*. **2004**, *6*, 3397.

37. Fini, F.; Herrera, R. P.; Pettersen, D. P.; Ricci, A.; Sgarzani, V. *Adv. Synth. Catal.* **2006**, *348*, 2043.

38. Murugan, E.; Siva, *A. Synthesis* **2005**, 2022.

39. France, S.; Guerin, D. J.; Miller, S. J.; Lectka, T. *Chem. Rev*. **2003**, *103*, 2985.

40. Basavaiah, D.; Rao, A. J.; Satyanarayana, T. *Chem. Rev*. **2003**, *103*, 811.

41. Shi, M.; Xu, Y. M. *Angew. Chem. Int. Ed.* **2002**, *41*, 4507.

42. Read de Alaniz, J.; Rovis, T. *J. Am. Chem. Soc*. **2005**, *127*, 6284.

43. Pihko, P. *Angew. Chem. Int. Ed. Engl.* **2004**, *43*, 2062.

44. Bolm, C.; Rantanen, T.; Schiffers, I.; Zani, L. *Angew. Chem. Int. Ed. Engl.* **2005** , *44*, 1758.

45. Huang, Y.; Unni, A. K.; Thadani, A. N.; Rawal, V. H. *Nature* **2003**, *424*, 146.

46. McDougal, N. T.; Schaus, S. E. *J. Am. Chem. Soc*. **2003**, 125, 12094.

47. Matsui, K.; Takizawa, S.; Sasai, H.. *J. Am. Chem. Soc*. **2005**, *127*, 3680.

48. Vachal, P.; Jacobsen, E. N. *J. Am. Chem. Soc.* **2002**, *124*, 10012.

49. Joly, G.D.; Jacobsen, E. N. *J. Am. Chem. Soc.* **2004**, *126*, 4102.

50. Yoon, T.P.; Jacobsen, E. N. *Angew. Chem. Int. Ed.* **2005**, *44*, 466.

51. Wenzel, A.G.; Jacobsen, E. N. *J. Am. Chem. Soc*. **2002**, *124*, 12964.

52. Taylor, M.S.; Jacobsen, E. N. *J. Am. Chem. Soc*. **2004**, *126*, 10558.

53. Taylor, M. S.; Tokunaga, N.; Jacobsen, E. N. *Angew. Chem. Int. Ed. Engl.* **2005**, *44*, 6700.

54. Uraguchi, D.; Sorimachi, K.; Terada, M. *J. Am. Chem. Soc*. **2004**, *126*, 11804.

55. Seayad, J.; Seayad, A. M.; List, B. *J. Am. Chem. Soc.* **2006**, *128*, 1086.

56. Ruepig, M.; Sugiono, E.; Azap, C.; Theissmann, T.; Bolte, M. *Org. Lett*. **2005**, *7*, 3781.

57. Hoffman, S. *Angew. Chem. Int. Ed. Engl*. **2005**, *44*, 7424.

58. Storer, R.I.; Carrera, D. E.; Ni, Y.; MacMillan, D. W. C. *J. Am. Chem. Soc*. **2005**, *128*, 84.

59. Fache, F.; Schulz, E.; Tommasino, M. L.; Lemaire, M. *Chem. Rev.* **2000**, *100*, 2159.

60. Chelucci, G.; Thummel, R. P. *Chem. Rev.* **2002**, *102*, 3129.

61. Oppolzer, W. *Tetrahedron*, **1987**, *43,* 1969

62. Chelucci, G.; Gladiali, S.; Marchetti, M. *J. Heterocycl. Chem.* **1988,** *25*, 1761.

63. Strekowski, L.; Wydra, R. L.; Cegla, M. T.; Czarny, A.; Harden, D. B.; Patterson, *S.* E.; Battiste, M. A.; Coxon, J. M. *J. Org. Chem.* **1990,** *55***,** 4777.

64. For review on usage of pyridine-N-oxides, see: Chelucci, G.; Murineddu, G.; Pinna, G. A. *Tetrahedron: Asymmetry* **2004**, 15, 1373.

65. Tanyeli, C.; Akhmedov, İ. M.; Işık, M. *Tetrahedron Lett.* **2004**, *45*, 5799.

66. Miller, A. *J. Org. Chem*. **1984**, *49*, 4072.

67. Boekelheide, V. C.; Linn, W. J. *J. Am. Chem. Soc*. 1954, *76*, 1286.

68. Kaiser, S.; Smidt, S. P.; Pfaltz, A. *Angew. Chem. Int. Ed*. **2006**, *45,* 5194 – 5197.

69. Tang, Z.; Yang, Z.; Chen, X.; Cun, L.; Mi, A.; Jiang, Y.; Gong, L. *J. Am. Chem. Soc*. **2005**, *127*, 9285.

70. Pettit, G.; Singh, S. B.; Herald, D. L.; Lloyd-Williams, P.; Kantoci, D.; Burkett, D. D.; Barkoczy, J.; Hogan, F.; Terah, R.; Wardlaw, T. R. *J. Org. Chem.* **1994**, *59*, 6287.

71. Cao, L. C.; Ye, M. C.; Sun, X. L.; Tang, Y. *Org. Lett.*, **2006**, *8*, 2901.

72. Malkov, A. V.; Westwater, M. M.; Gutnov, A.; Ramirez-Lopez, P.; Friscourt, F.; Kadlcikova, A.; Hodacovac, J.; Rankovic, Z.; Kotora, M.; Kocovsky, P. *Tetrahedron* **2008**, 64, 11335.

73. Acetylacetoneamine is commercially available from Aldrich Company.

APPENDIX A

SUPPORTING INFORMATION

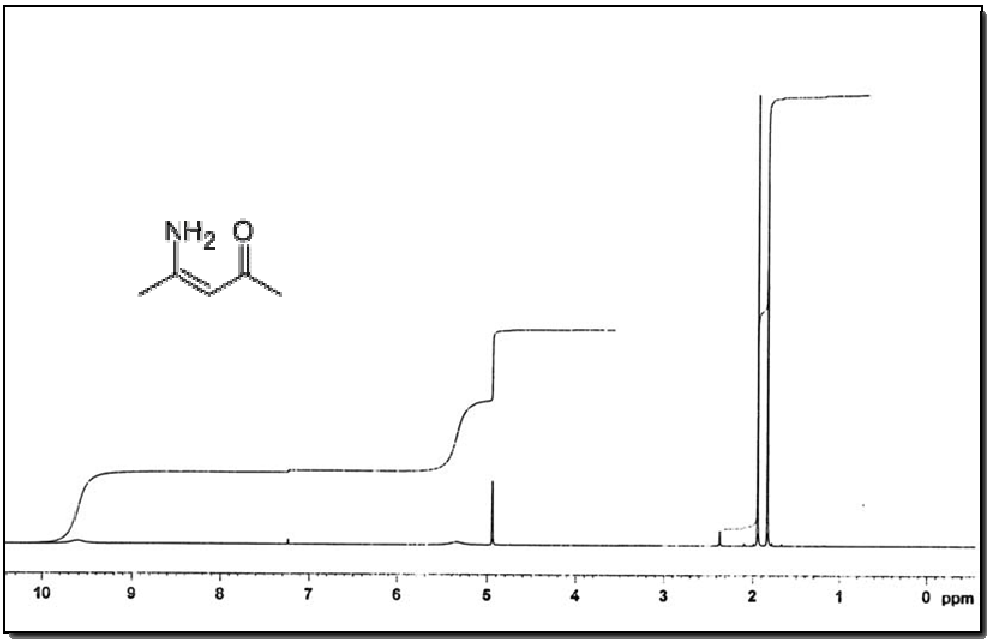

Figure A1. ^{1}H-NMR spectrum of (*Z*)-4-aminopent-3-en-2-one, **22**

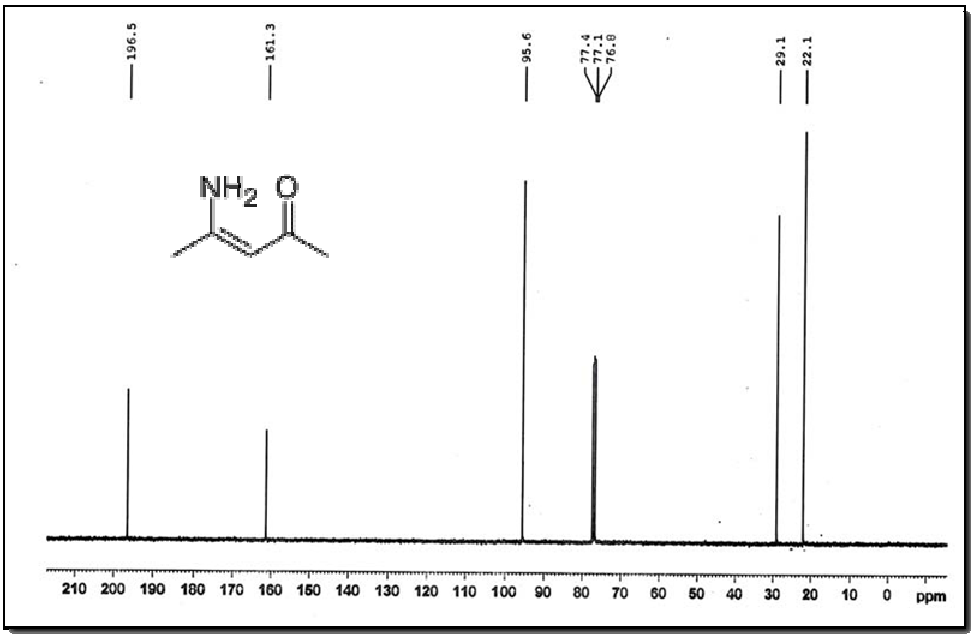

Figure A2. ^{13}C-NMR spectrum of (*Z*)-4-aminopent-3-en-2-one, **22**

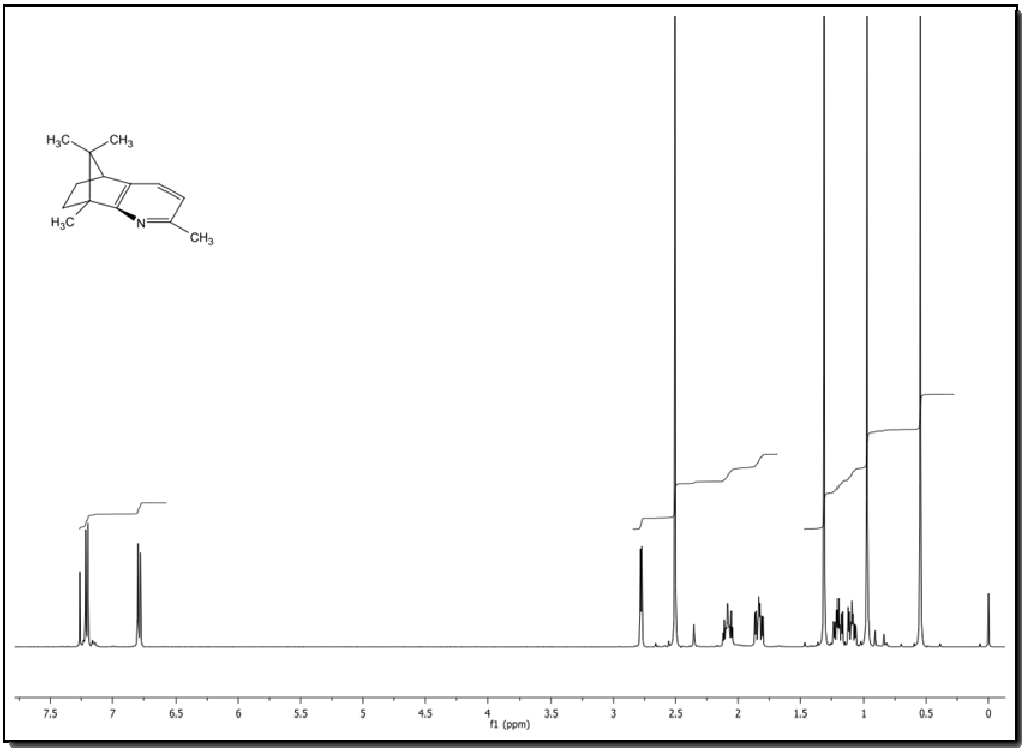

Figure A3. ^{1}H-NMR spectrum of camphor fused pyridine, **23**

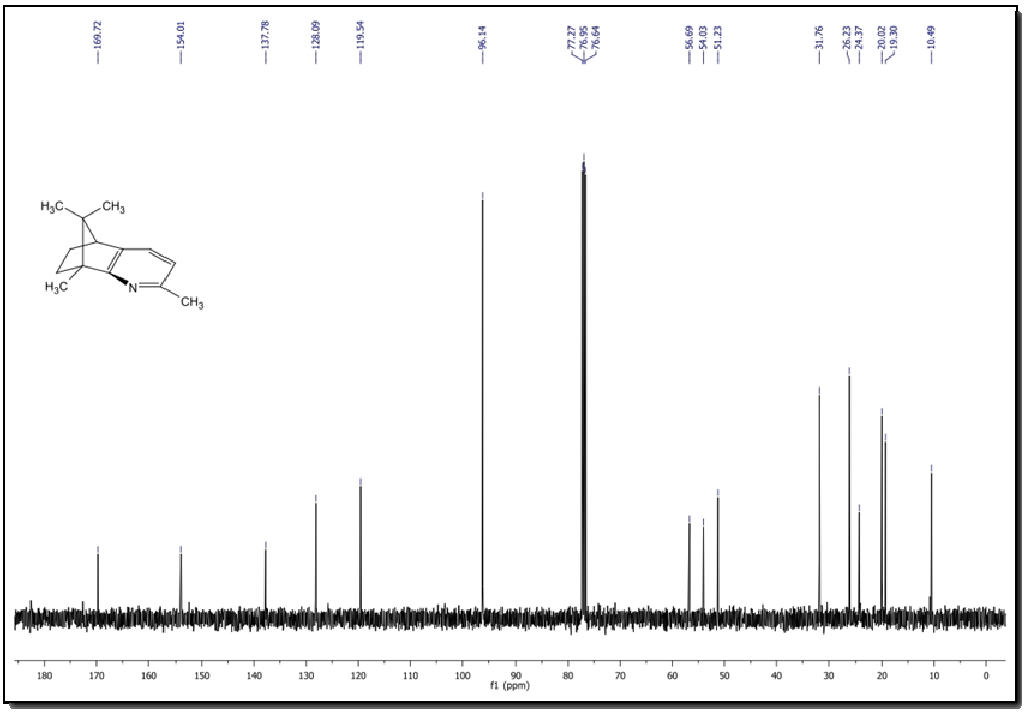

Figure A4. ^{13}C-NMR spectrum of camphor fused pyridine, **23**

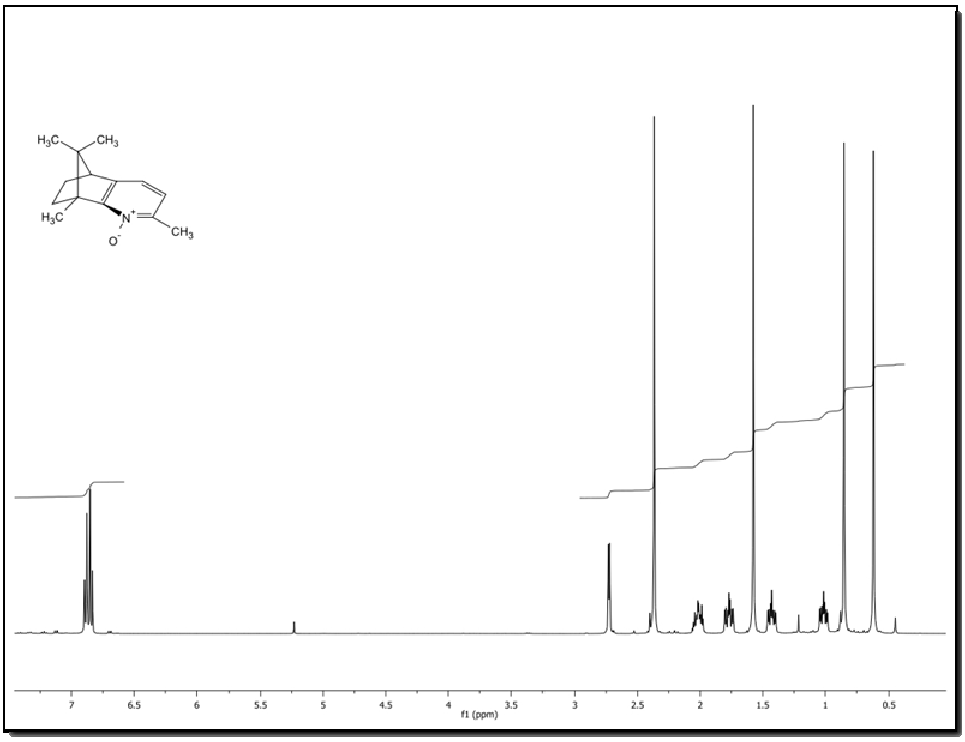

Figure A5. ^{1}H-NMR spectrum of *N*-oxide, **26**

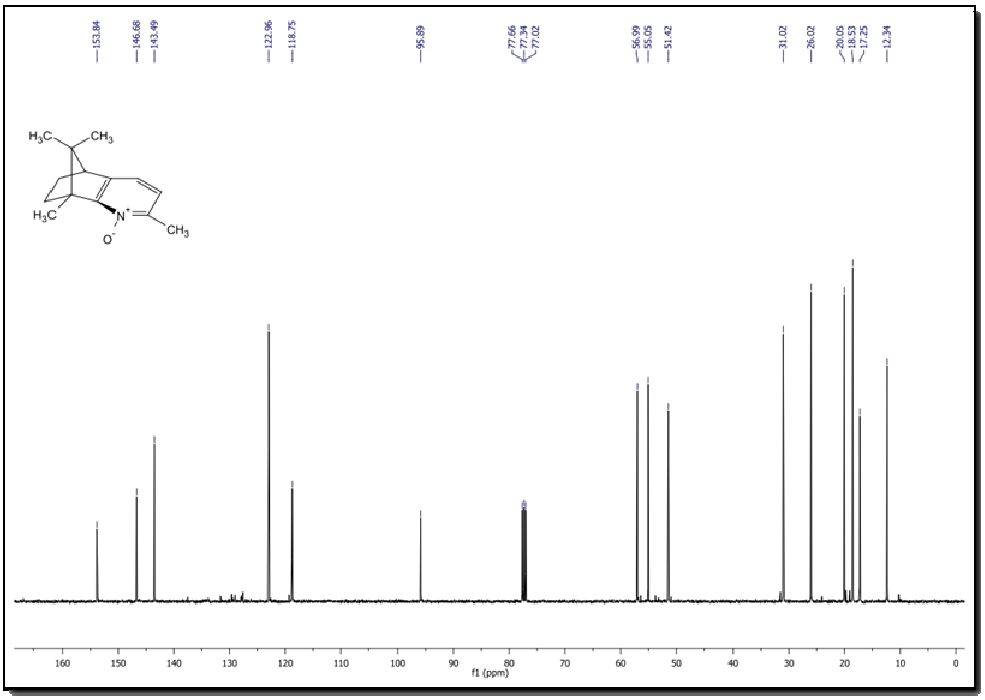

Figure A6. ^{13}C-NMR spectrum of *N*-oxide, **26**

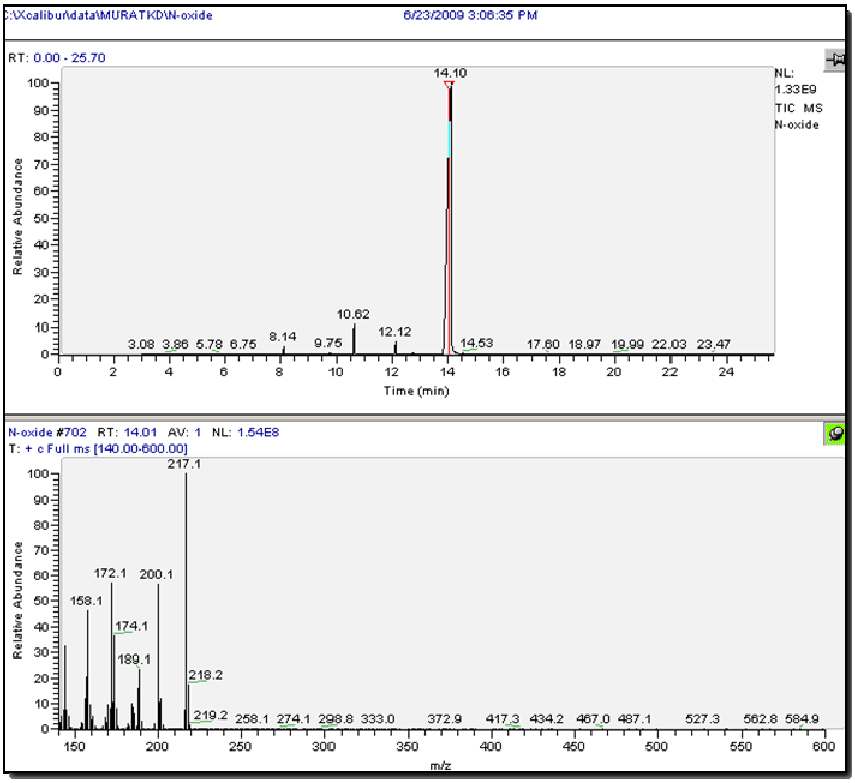

Figure A7. GC-MS spectrum of *N*-oxide, **26**

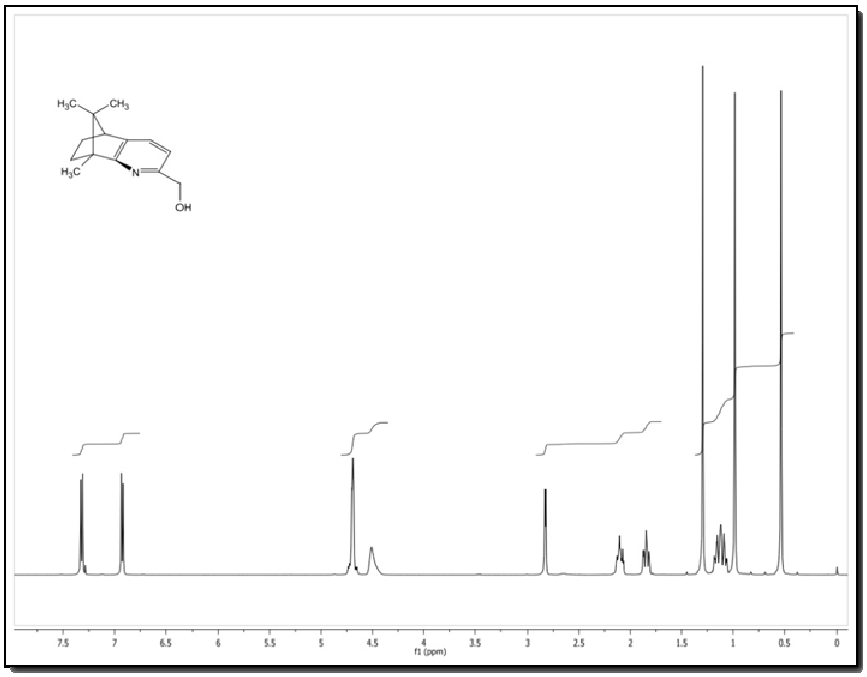

Figure A8. ^{1}H-NMR spectrum of 2-hydroxymethylene pyridine, **27**

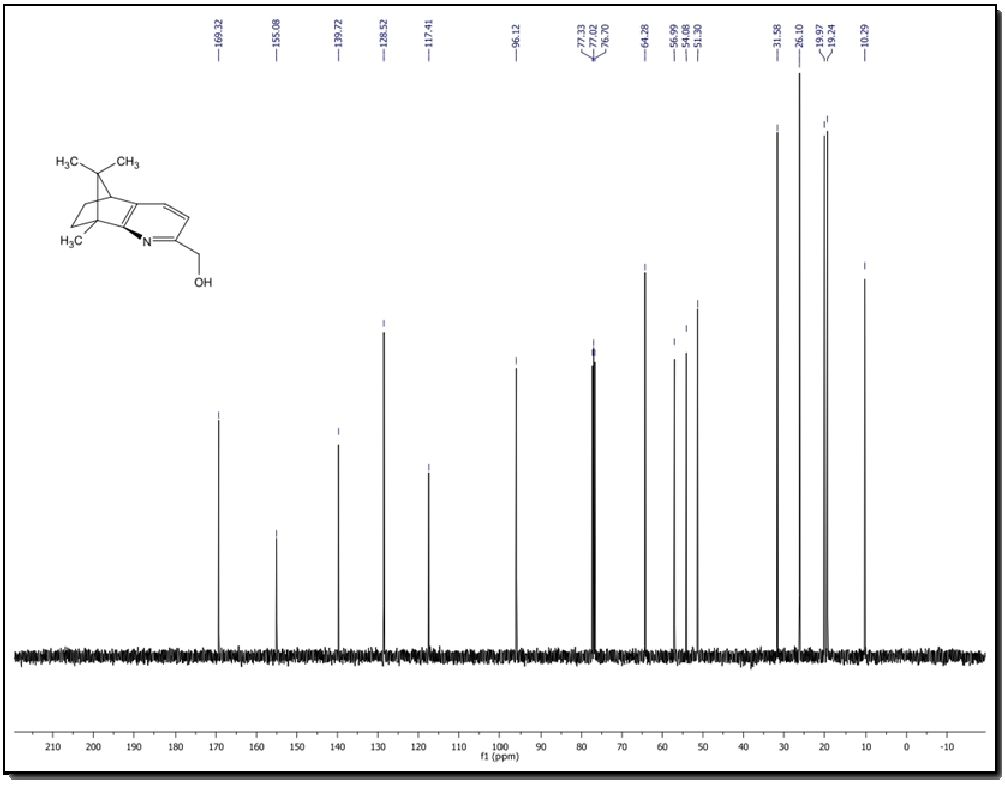

Figure A9. ^{13}C-NMR spectrum of 2-hydroxymethylene pyridine, **27**

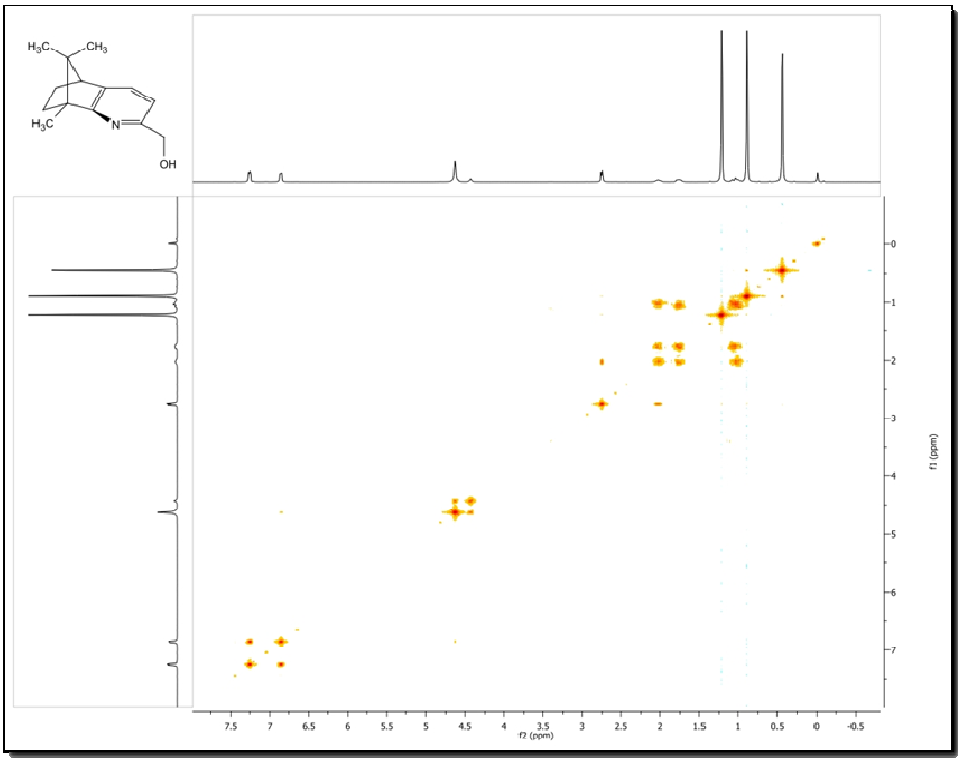

Figure A10. COSY spectrum of 2-hydroxymethylene pyridine, **27**

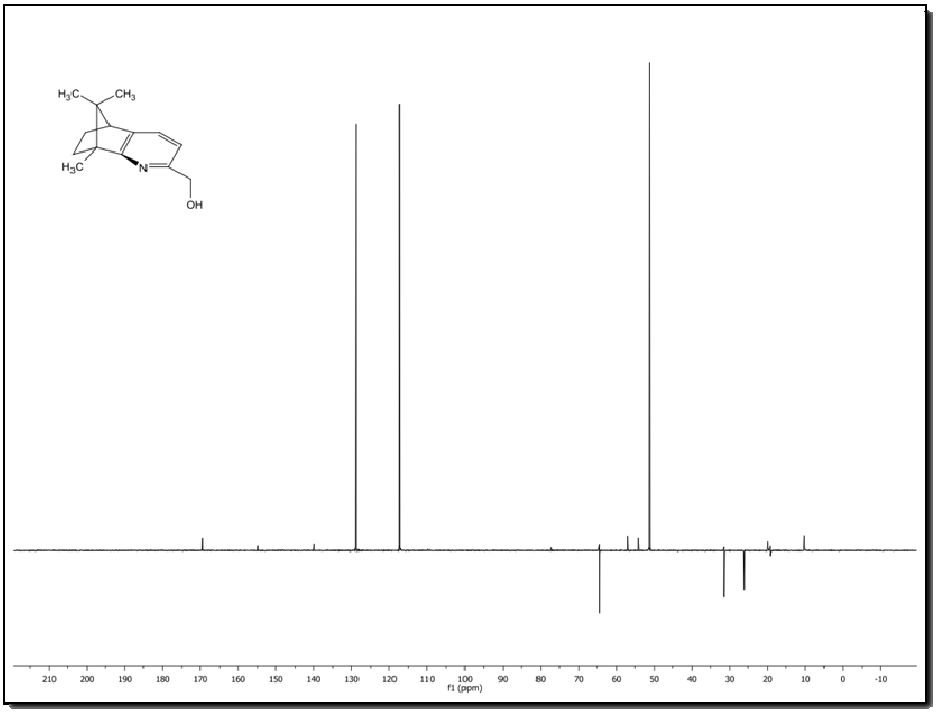

Figure A11. DEPT-90 spectrum of 2-hydroxymethylene pyridine, **27**

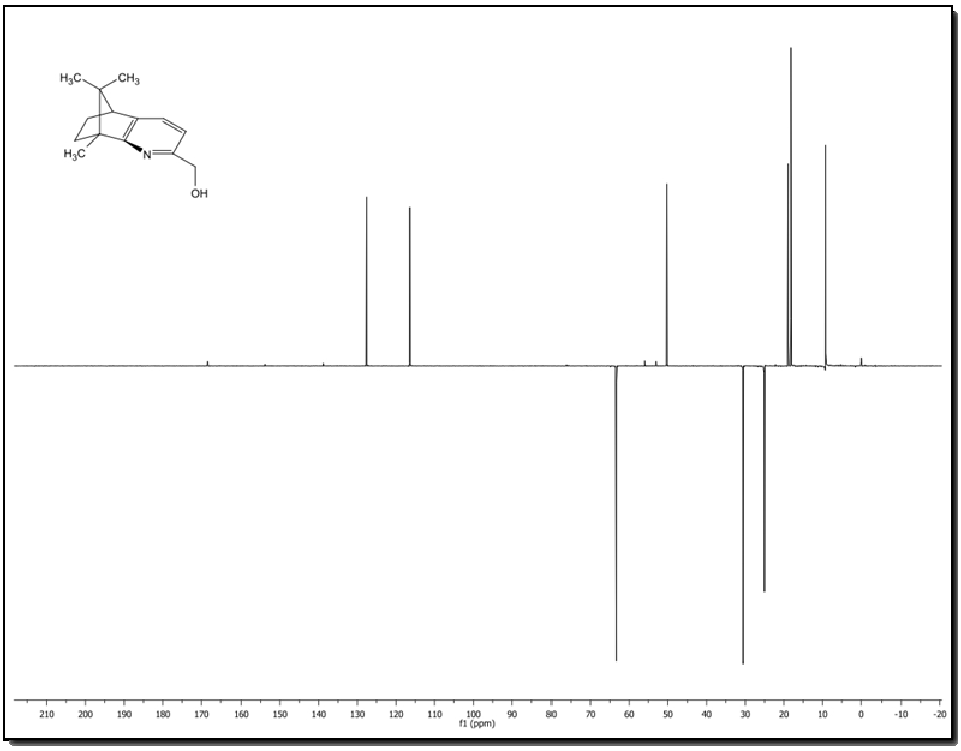

Figure A12. DEPT-135 spectrum of 2-hydroxymethylene pyridine, **27**

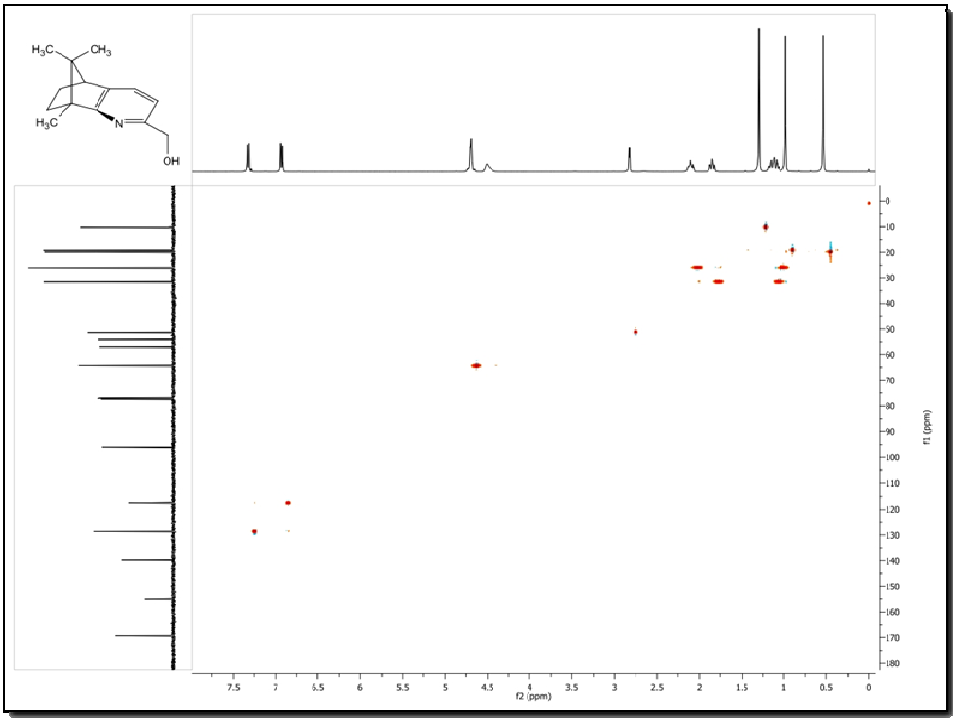

Figure A13. HSQC spectrum of 2-hydroxymethylene pyridine, **27**

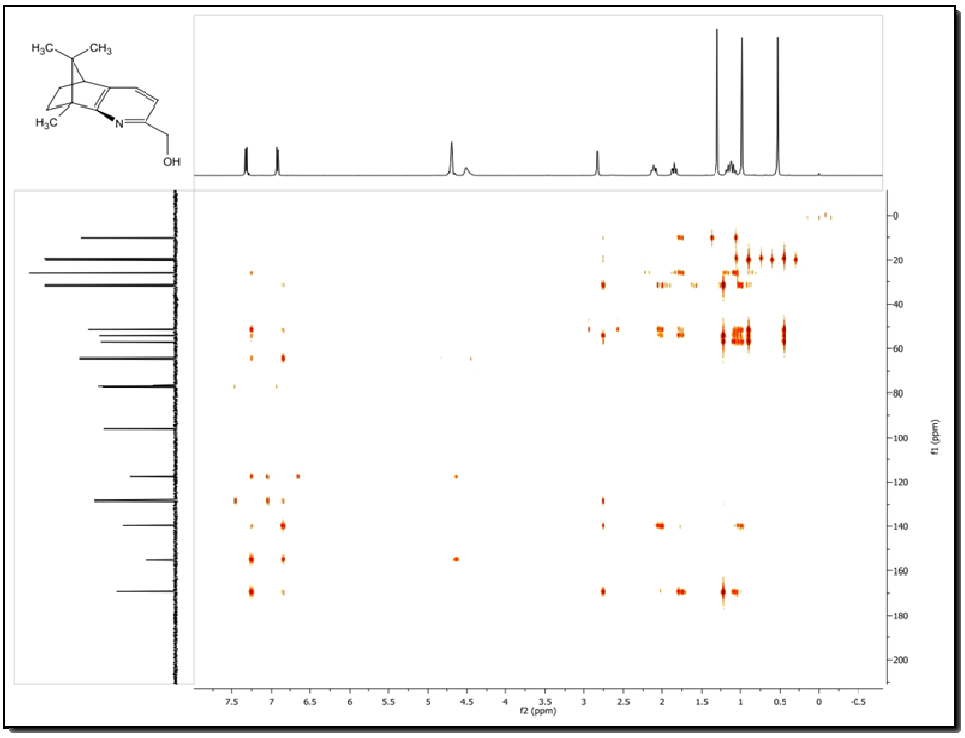

Figure A14. HMBC spectrum of 2-hydroxymethylene pyridine, **27**

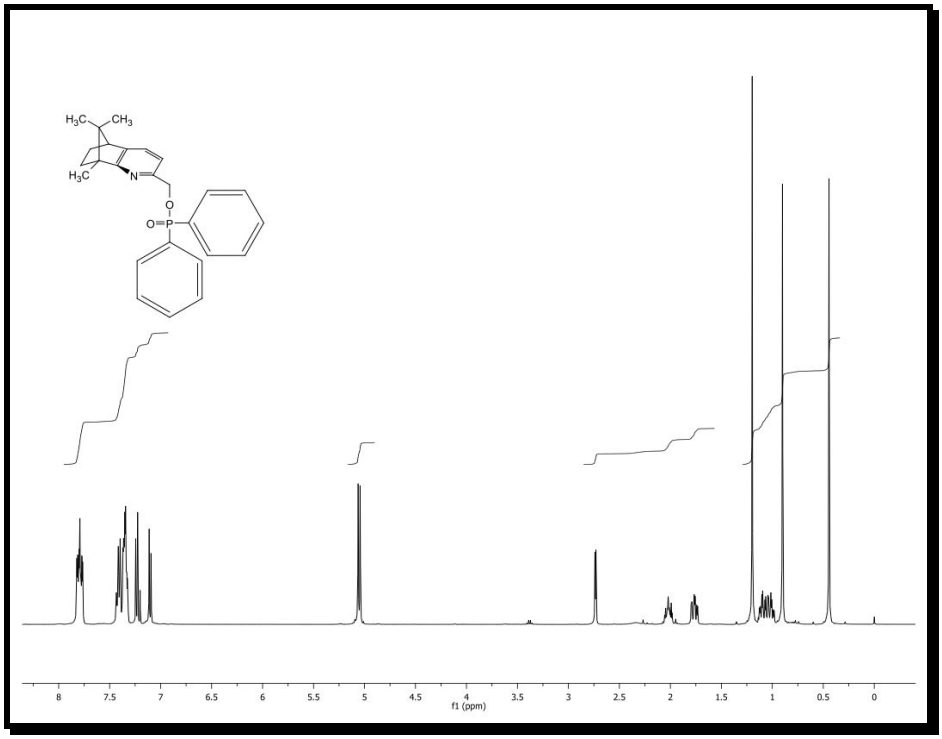

Figure A15. ^{1}H-NMR spectrum of compound **29**

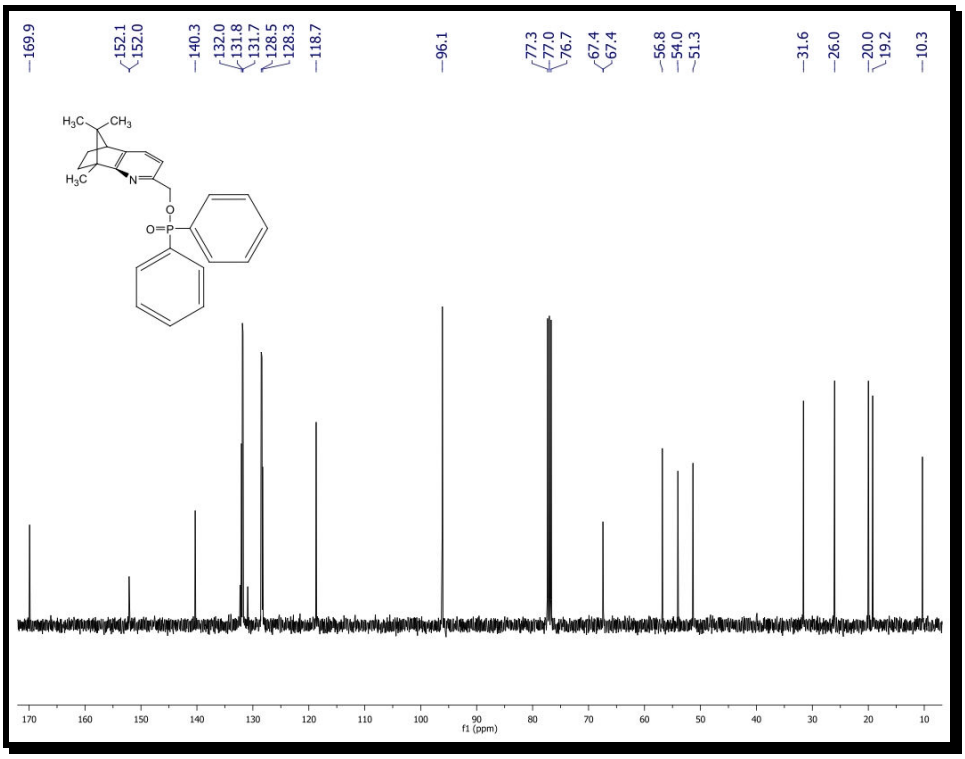

Figure A16. ^{13}C-NMR spectrum of compound **29**

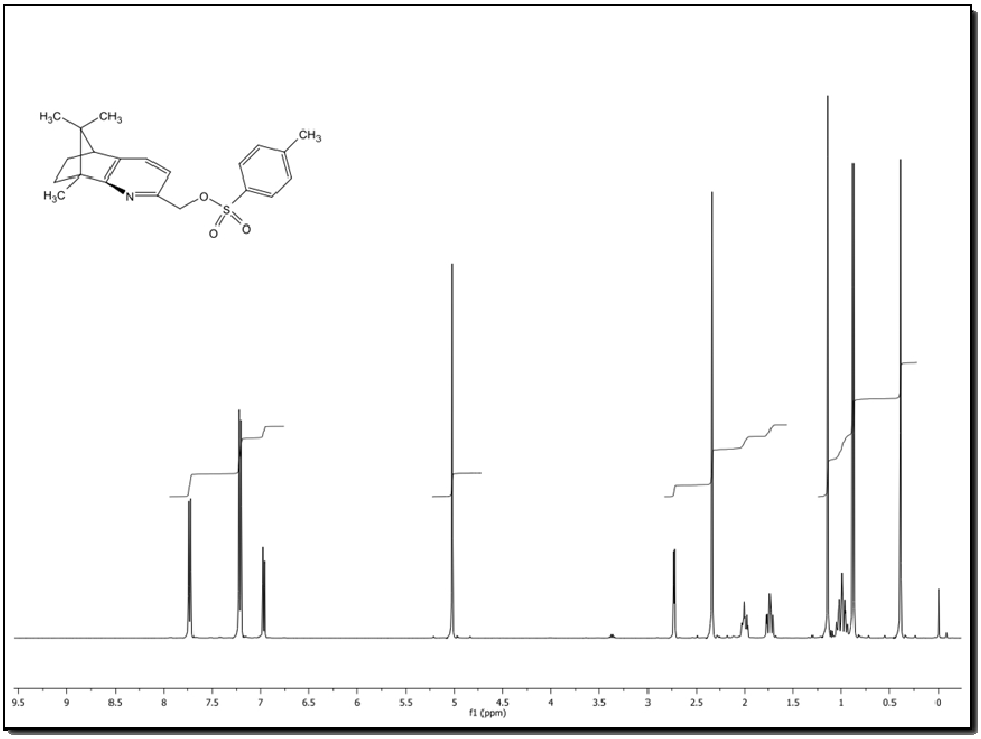

Figure A17. ^{1}H-NMR spectrum of tosylate, **30**

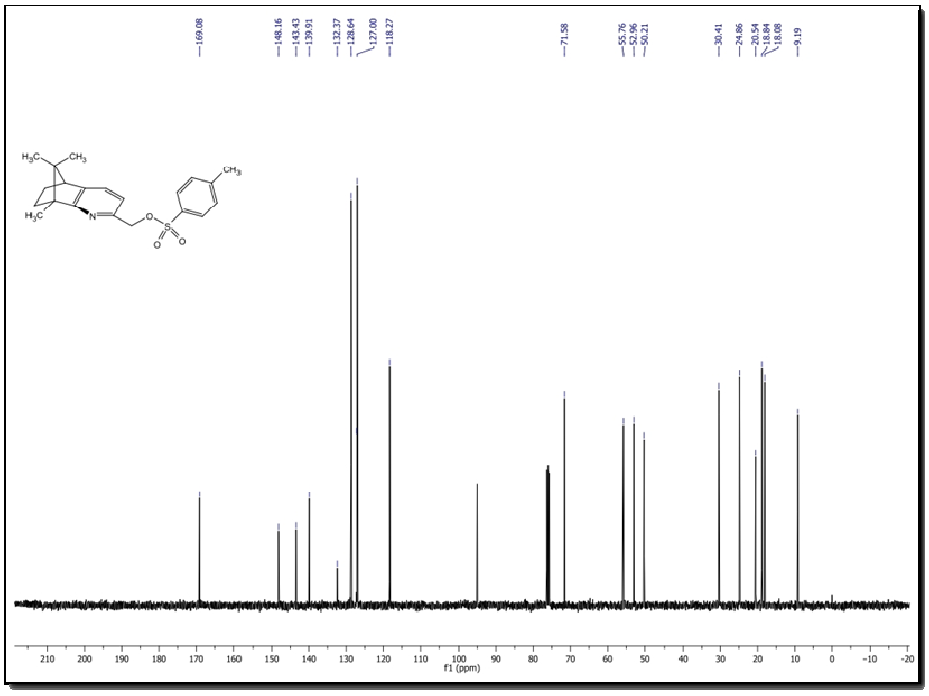

Figure A18. ^{13}C-NMR spectrum of tosylate, **30**

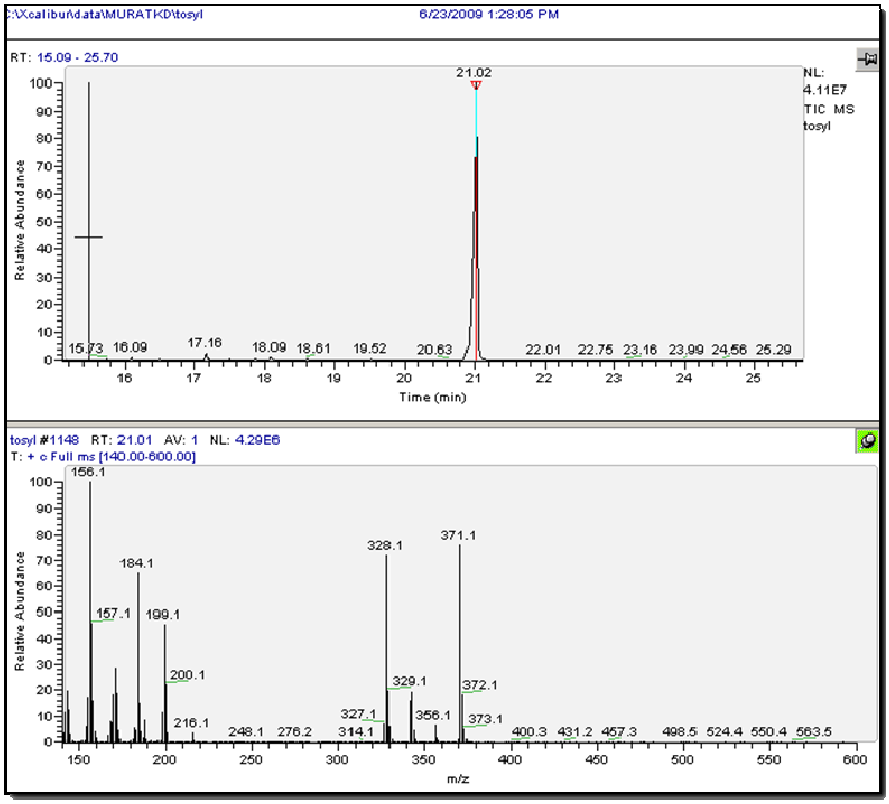

Figure A19. GC-MS spectrum of tosylate, **30**

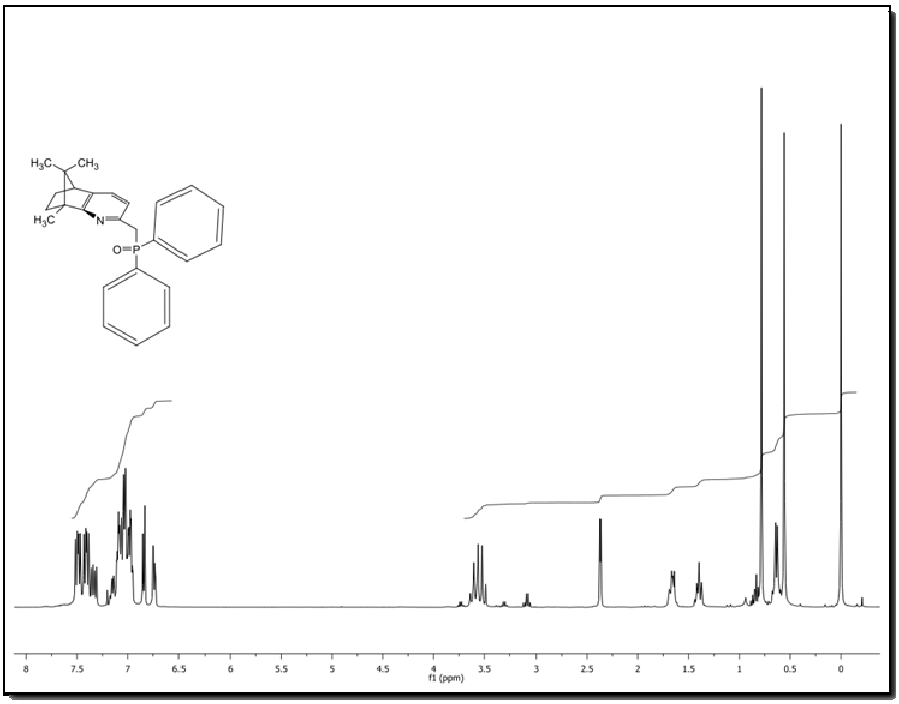

Figure A20. ^{1}H-NMR spectrum of compound **32**

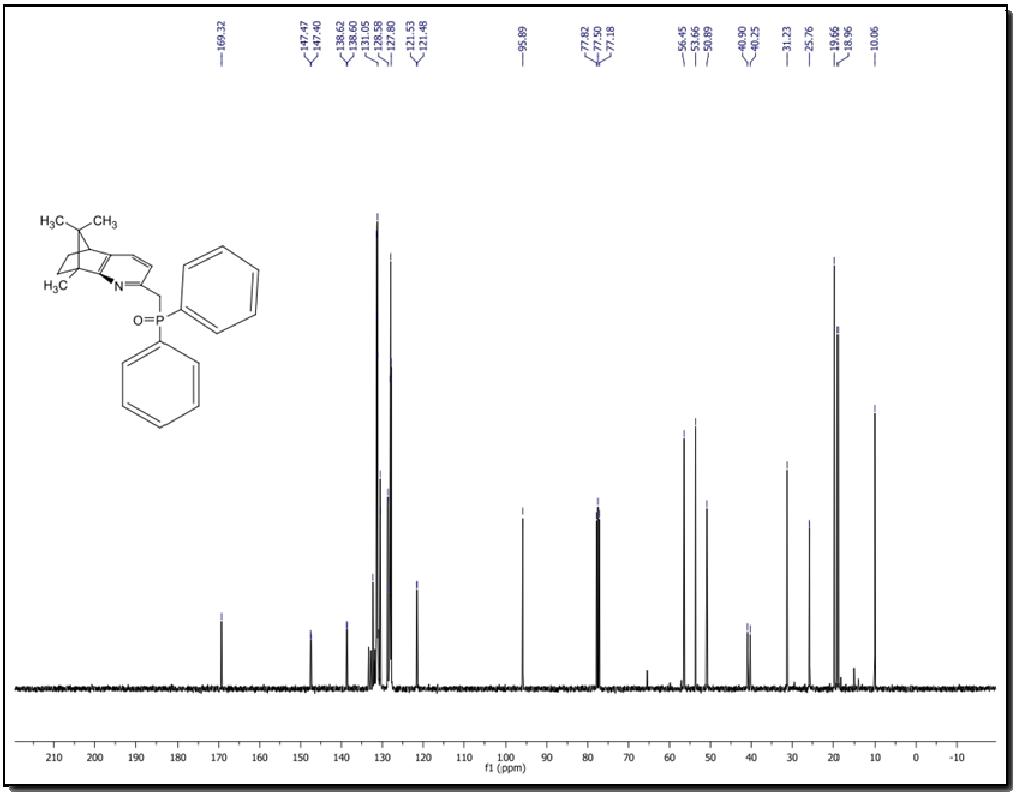

Figure A21. ^{13}C-NMR spectrum of compound **32**

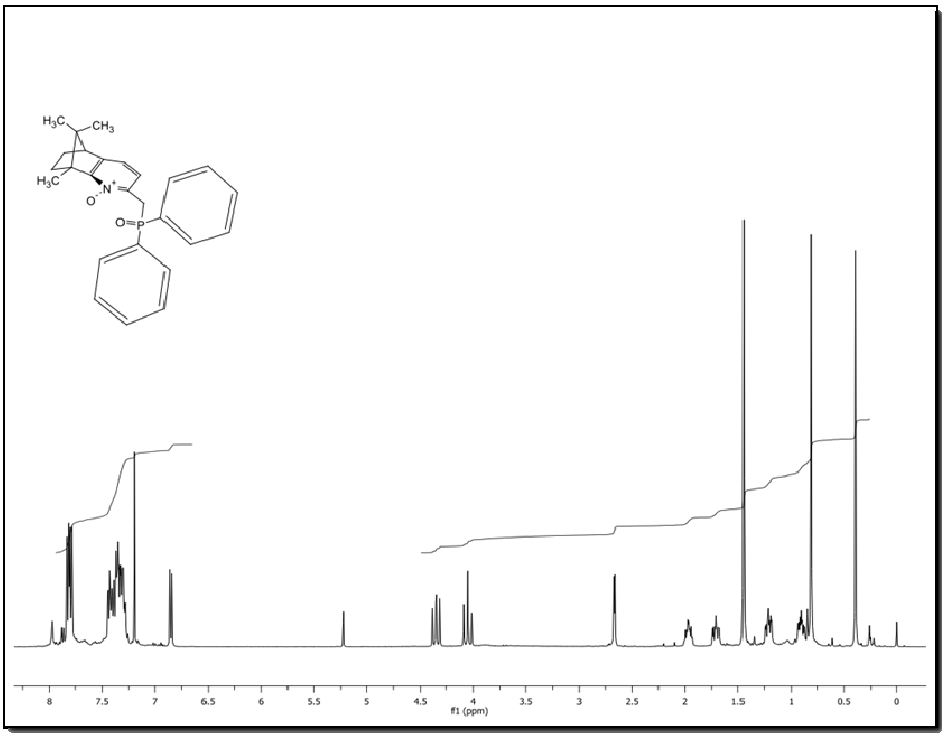

Figure A22. ^{1}H-NMR spectrum of *P,N*-dioxide, **33**

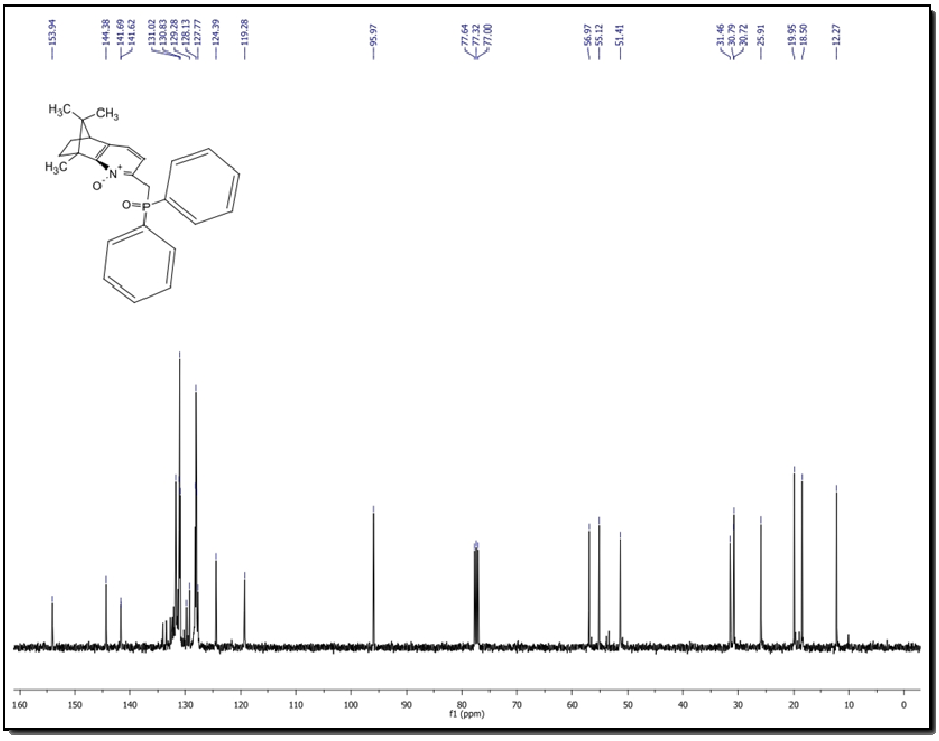

Figure A23. ^{13}C-NMR spectrum of *P,N*-dioxide, **33**

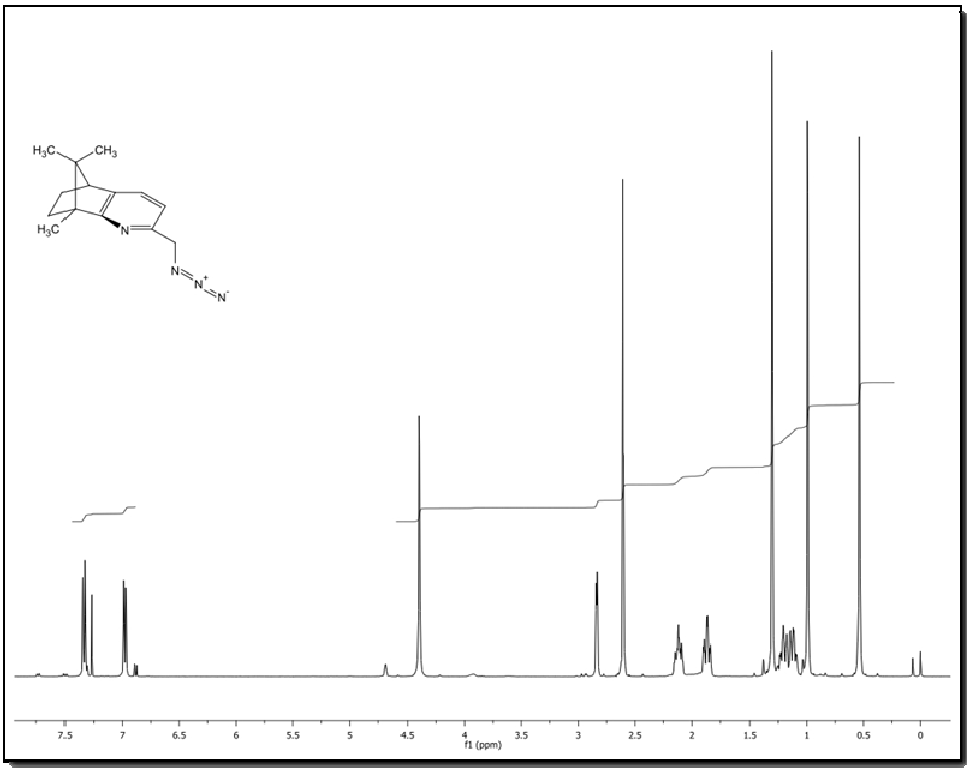

Figure A24. ^{1}H-NMR spectrum of azide, **34**

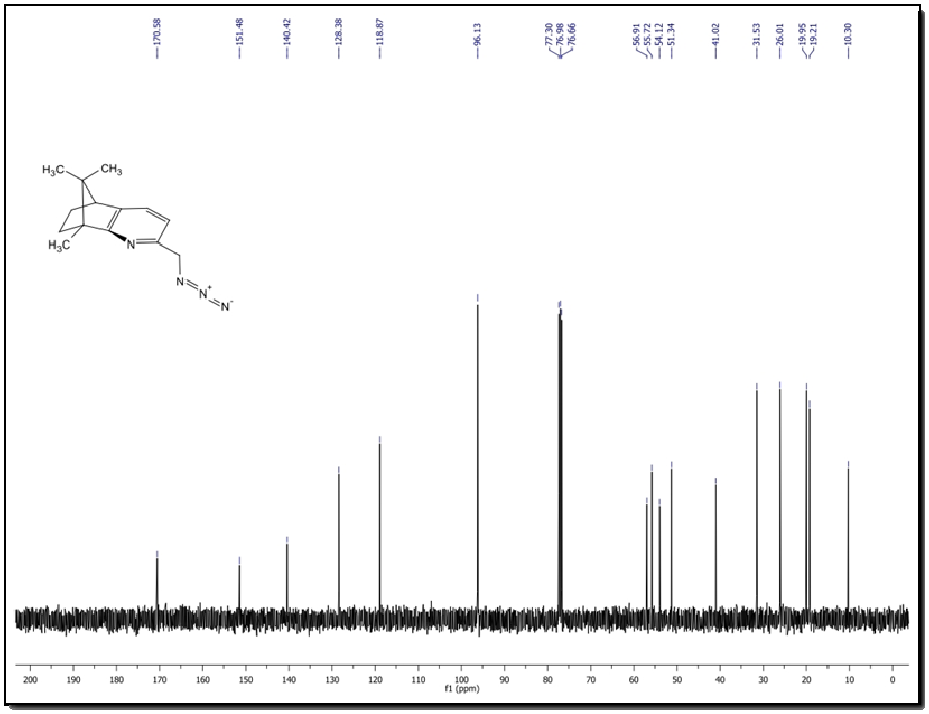

Figure A25. ^{13}C-NMR spectrum of azide, **34**

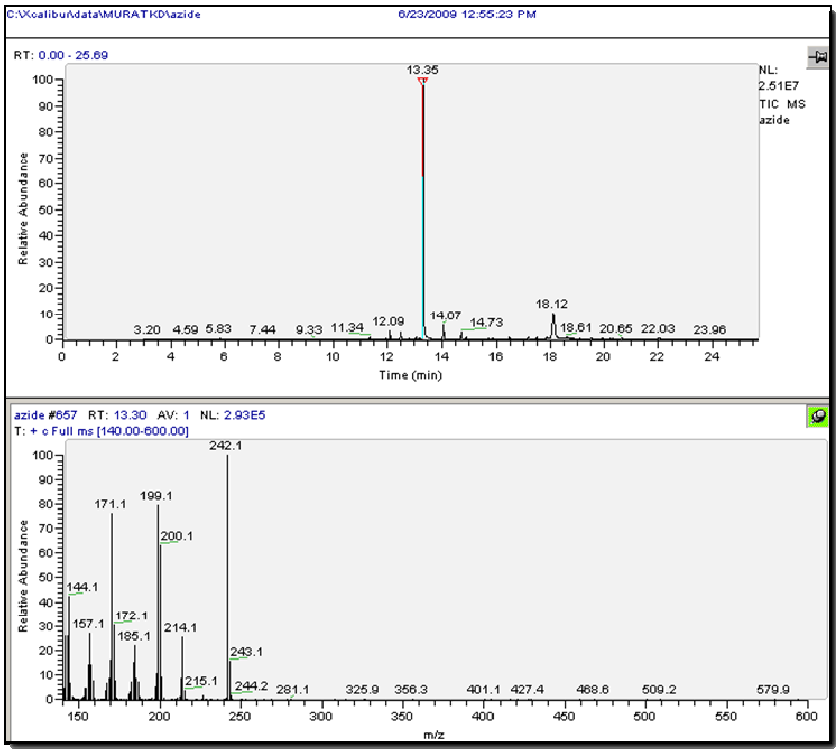

Figure A26. GC-MS spectrum of azide **34**

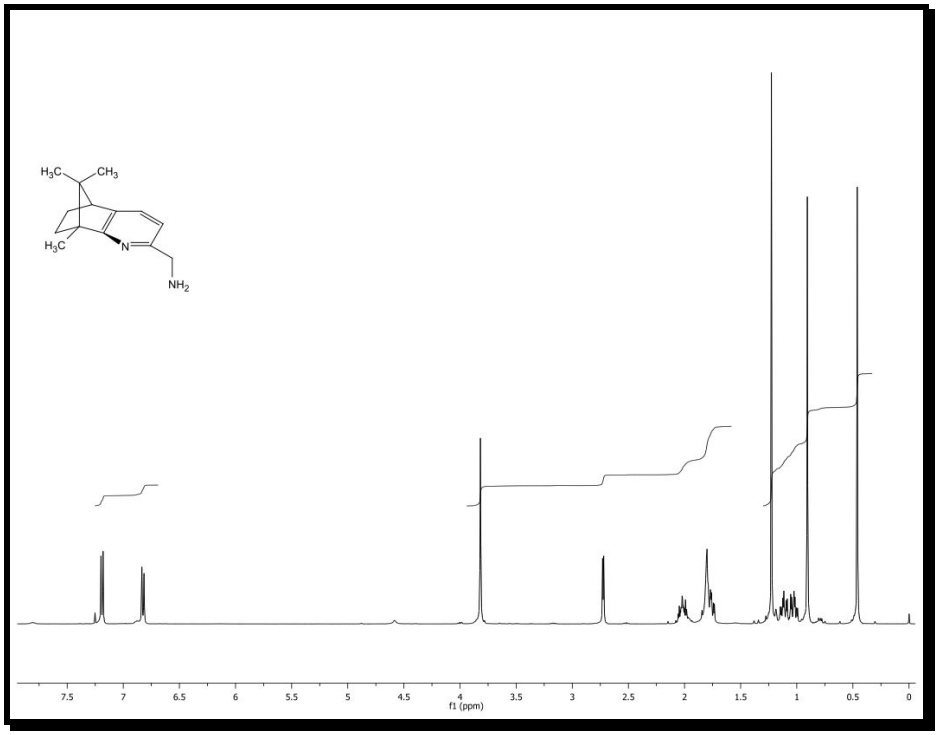

Figure A27. ^{1}H-NMR spectrum of amine, **35**

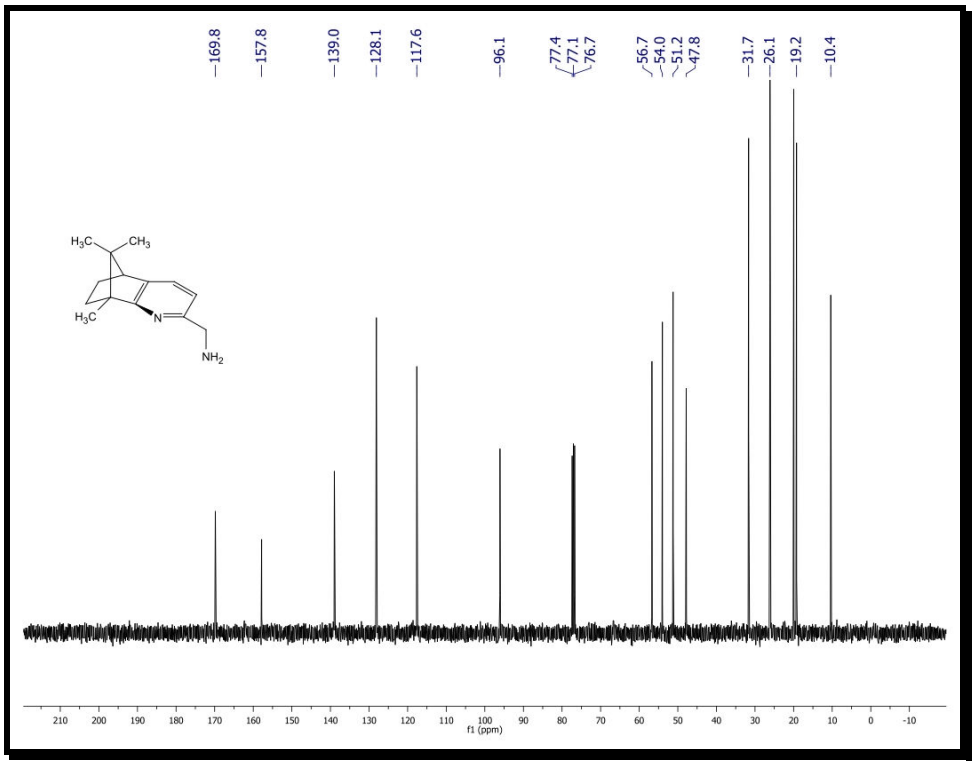

Figure A28. ^{13}C-NMR spectrum of amine, **35**

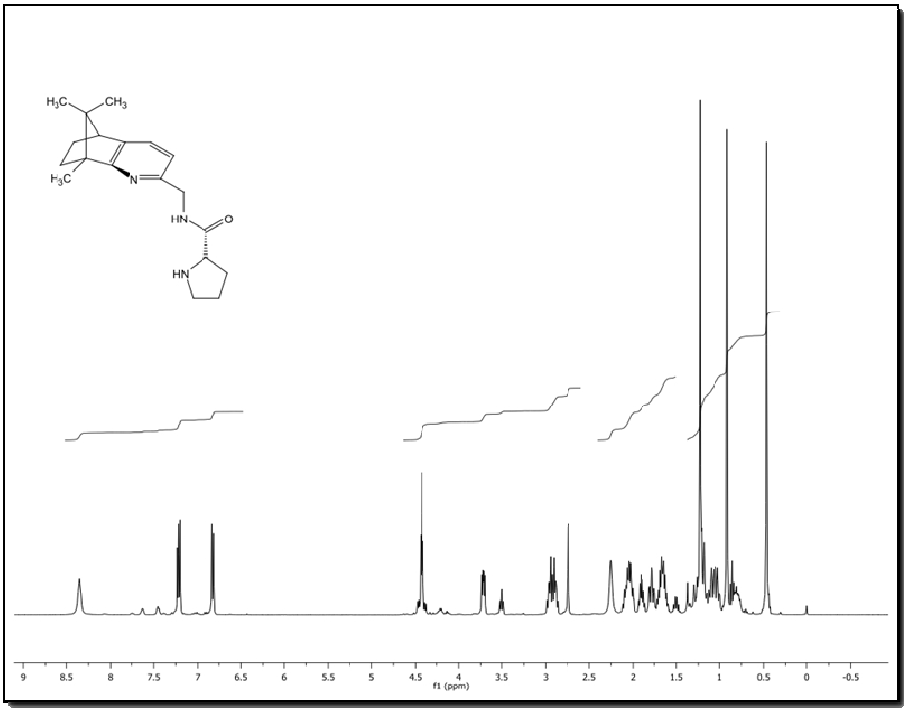

Figure A29. ^{1}H-NMR spectrum of compound **38**

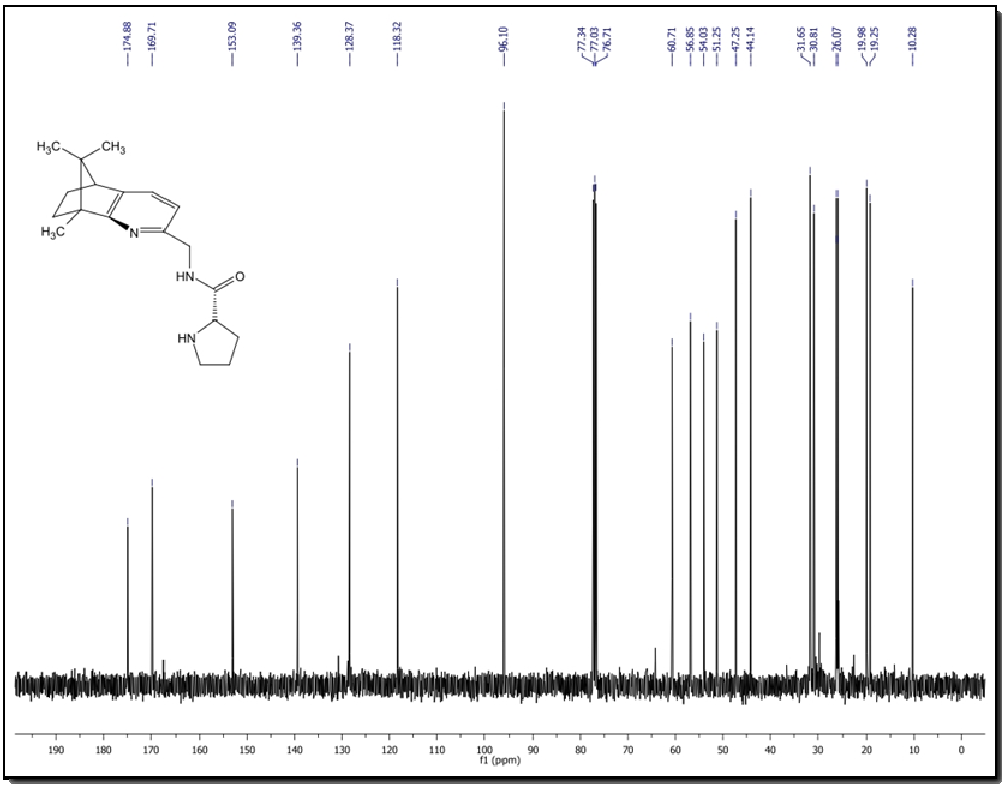

Figure A30. ^{13}C-NMR spectrum of compound **38**

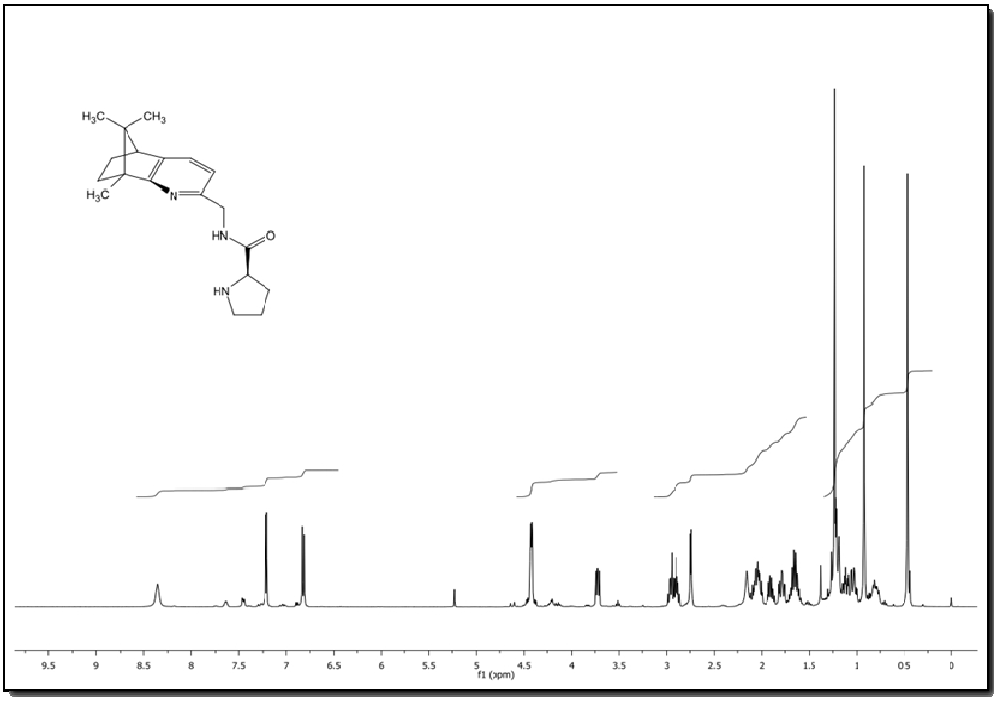

Figure A31. ^{1}H-NMR spectrum of compound **40**

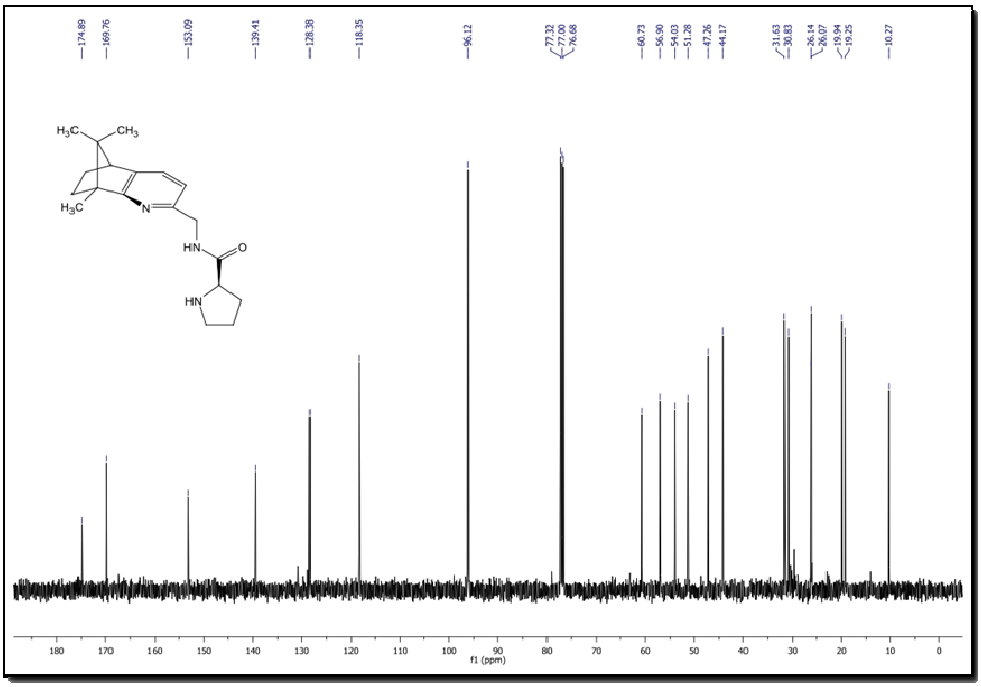

Figure A32. ^{13}C-NMR spectrum of compound **40**

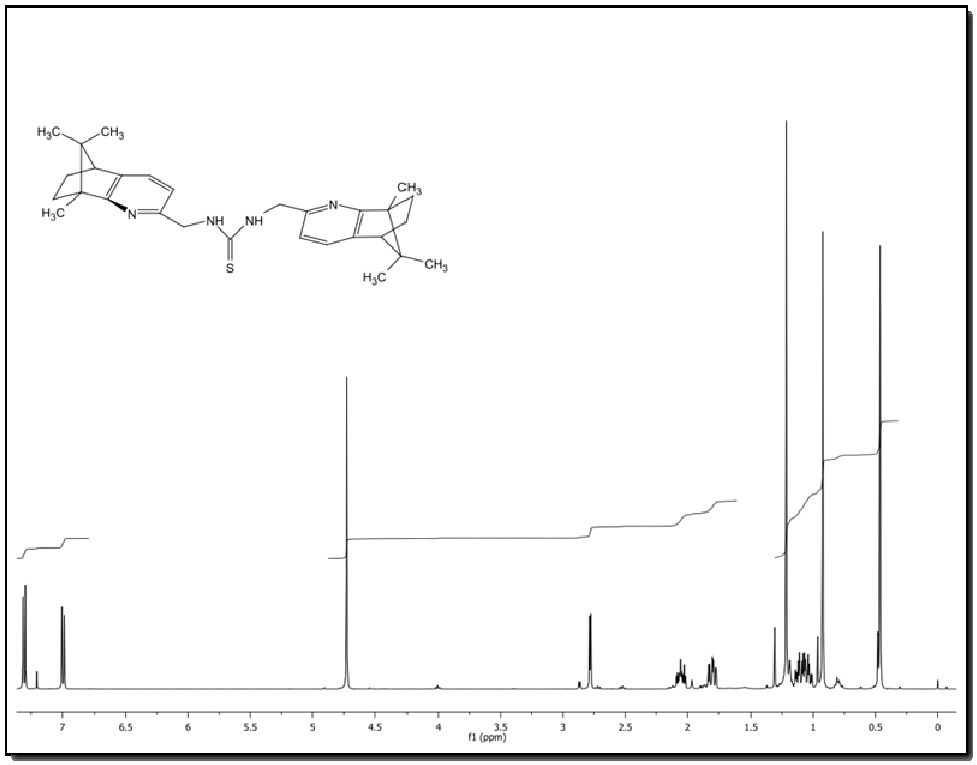

Figure A33. ^{1}H-NMR spectrum of compound **41**

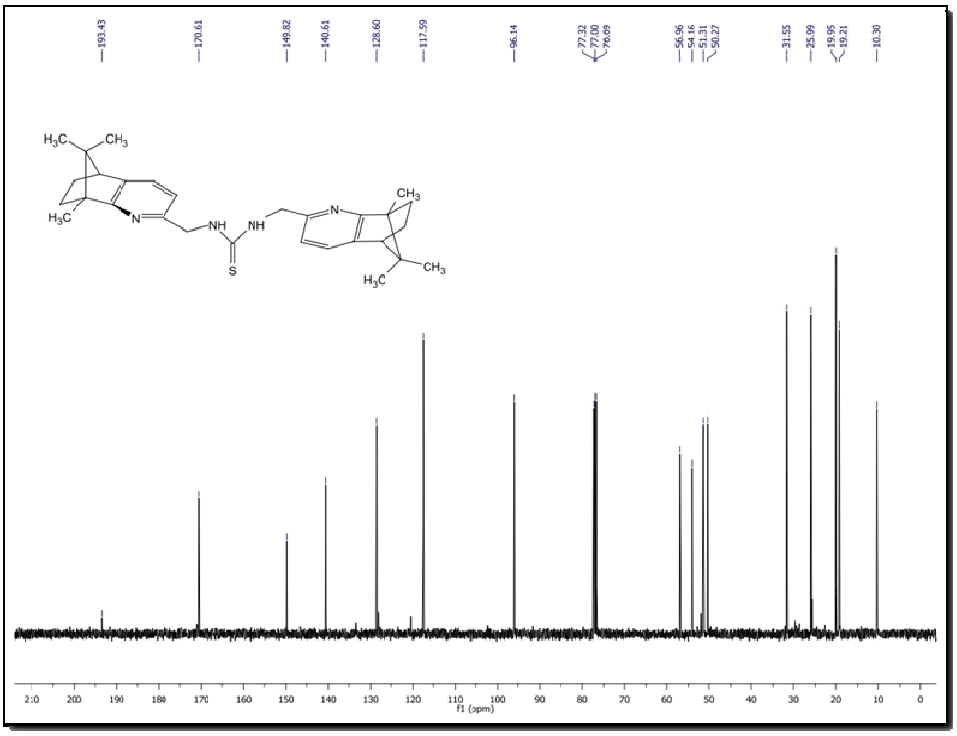

Figure A34. ^{13}C-NMR spectrum of compound **41**

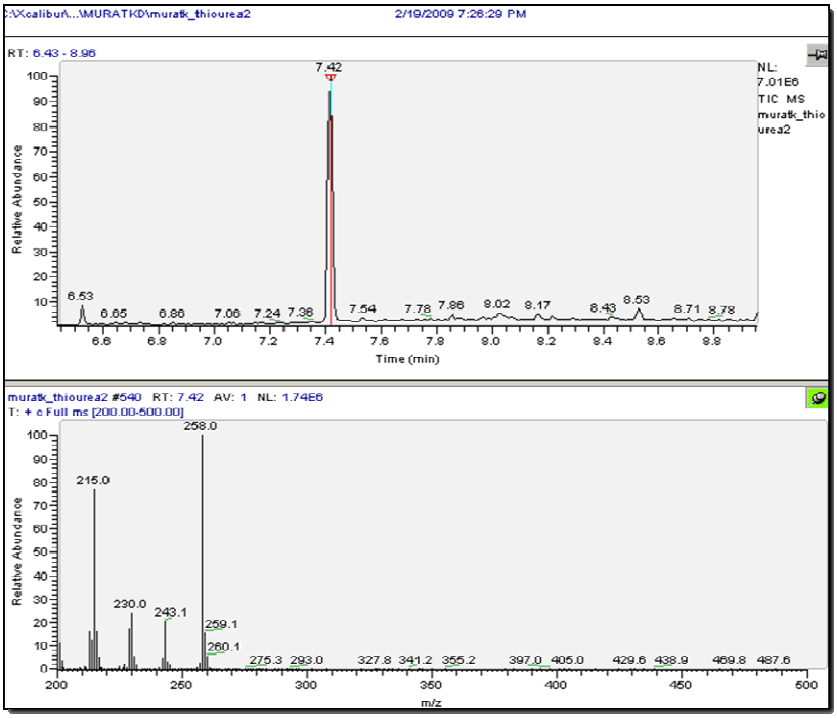

Figure A35. GC-MS spectrum of compound **41**

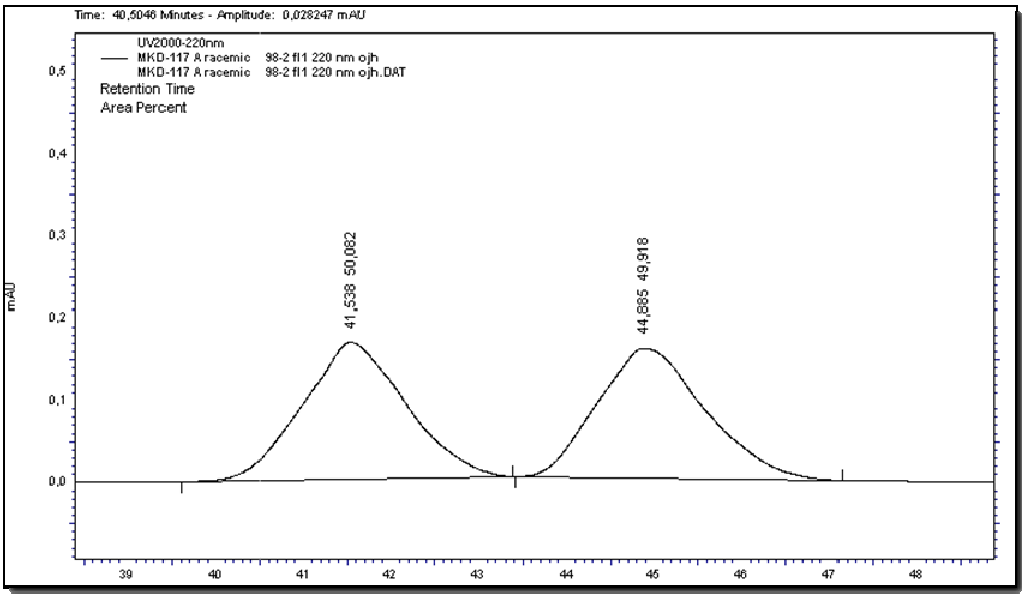

Figure A36. HPLC chromatogramof racemic 1-(4-nitrophenyl)but-3-en-1-ol

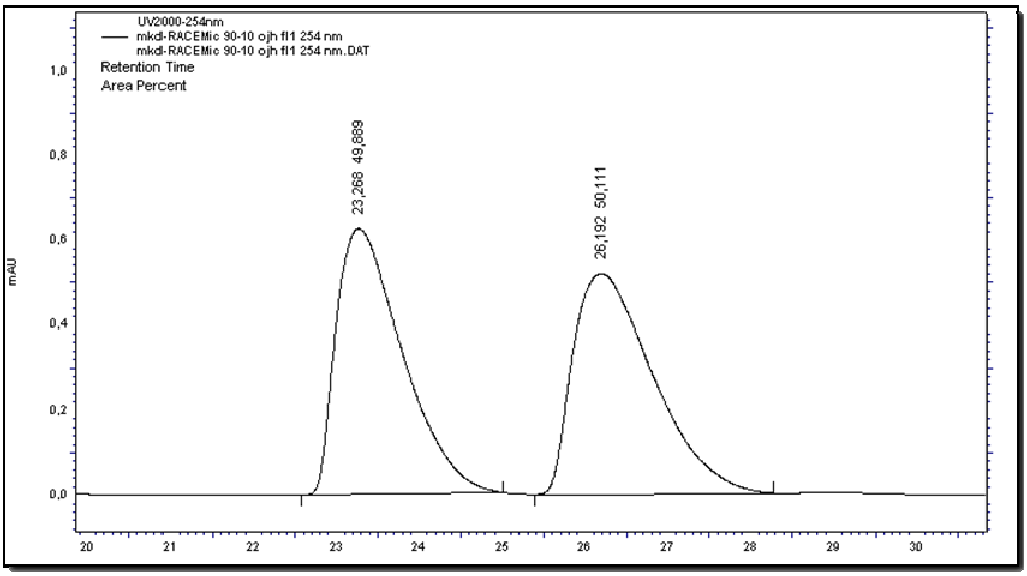

Figure A37. HPLC chromatogram of racemic 4-hydroxy-4-(4-nitrophenyl) butan-2-one